DISSERTATION

PHOSPHORUS DYNAMICS DURING GROWTH AND MATURATION PERIODS OF A BROWN ALGA *SARGASSUM MACROCARPUM*

September 2020

SOKA UNIVERSITY

GRADUATE SCHOOL OF ENGINEERING

MASAHIRO OHTAKE

PHOSPHORUS DYNAMICS DURING GROWTH AND MATURATION PERIODS OF A BROWN ALGA *SARGASSUM MACROCARPUM*

SEPTEMBER 2020

MASAHIRO OHTAKE

SOKA UNIVERSITY

Author:	Masahiro Ohtake
Title	Phosphorus dynamics during growth and maturation periods of a brown alga *Sargassum macrocarpum*
Department:	Environmental Engineering for Symbiosis
Faculty:	Engineering
Degree:	Ph. D.
Convocation:	September 2020

We certify that we read this dissertation and that, in our opinion, it is satisfactory in scope and quality as a dissertation for the degree of Doctor of Philosophy in Engineering.

September 2020

DISSERTATION COMMITTEE

Prof. Dr. Tatsuki Toda

Prof. Dr. Ken Furuya

Prof. Dr. Victor S. Kuwahara

Assoc. Prof. Dr. Gregory N. Nishihara

Contents

ACKNOWLEDGEMENT

I would like to express my deepest appreciation to my supervisor, Prof. Dr. Tatsuki Toda, and my co-supervisors, Prof. Dr. Ken Furuya, Prof. Dr. Victor S. Kuwahara, Assoc. Prof. Gregory N. Nishihara, for investing time and effort in the critical review of this thesis.

I gratefully acknowledge the support provided by Dr. Hiroyuki Takano, Dr. Takashi Kamiya, Dr. Kazuki Tamura and Dr. Tsuyoshi Aketo, Taiheiyo Cement Central Research Laboratory, Mr. Noriaki Morishita, Mr. Ichirou Oshiki and Mr. Kazushige Inoue, Taiheiyo Cement Corporation, and mayor Mr. Etsuo Egami, deputy mayor Mr. Nobuaki Ishida, Mr. Takeshi Iga, Mr. Rikuto Ehama, Shin-Kamigoto-cho town office, for their ongoing collaboration with our laboratory this study.

This study was carried out within a verification experiment commissioned by Shin-Kamigoto-cho town office, and was partly supported by collaborative research grant from Taiheiyo Cement Corporation to Prof. Tatsuki Toda. The part of this study also received the grant from Grant-in-Aid for Young Scientists (B) to Dr. Kenji Tsuchiya (grant No. 15K21449) and Grant-in-Aid for Scientific Research (C) to Assoc. Prof. Gregory N. Nishihara (grant No. 17KT0149), and a Sasakawa Grant for Science Fellows (grant No. 2018-7045) to Dr. Masahiro Ohtake.

I am grateful to Dr. Prof. Tomohiko Kikuchi and Dr. Prof. Shinji Shimode, Yokohama National University, and Dr. Makio Honda, the Japan Agency for Marine-Earth Science and Technology (JAMSTEC), for their cooperation. I thank the staff members, the Institute for East China Sea Research (ECSER) at Nagasaki University, local fishery association at Arikawa, Shin-kamigoto, Nagasaki, for their

support in performing the experiments.

During the long-term research visit in Shin-kamigoto, Nagasaki, the immeasurable improvements both of this study and livelihood was thanks to Mr. Kenjiro Hinode, Dr. Yukio Inoue, Mr. Koichi Ohsaki, Mr. Dominic F.C. Belleza, Ms. Hoshimi Kamisaki, Ms. Mizuki Tsunogai and many students from Nagasaki University, and Mr. Shigeo Nakamura, Ms. Sachiko Nakamura and local people. I am deeply grateful to Dr. Kenji Tsuchiya, the National Institute for Environmental Science (NIES), Dr. Youta Sugai, the Atmosphere and Ocean Research Institute (AORI) at the University of Tokyo, Dr. Masatoshi Kishi, Dr. Noriaki Natori, Dr. Minamo Hirahara, Dr. Yoshiki Takayama and my colleagues, Soka University, for not only giving me technical advice to improve my study but also sharing golden memories during study life.

I am full of gratitude to my family, Toshihiro Ohtake, Sanae Ohtake, Mitsutoshi Ohtake, Hiromi Ohtake, Kazuya Ohtake, for raising me up until today. I dedicate this thesis to the founder of Soka University, Dr. Daisaku Ikeda and Mrs. Kaneko Ikeda, for his endless expectation and encouragement throughout my life.

ABSTRACT

In order to clarify the external and internal availability of phosphorus in a canopy-forming seaweed along with their life cycle, monthly cultivations and field observations were conducted during growth and maturation periods of the brown alga *Sargassum macrocarpum*. This alga is one of the most major canopy-forming brown algae in Japanese coastal waters, and was found in the coastal area of the northern Goto Islands, characterized as a seasonally-oligotrophic region. This doctoral thesis aimed to reveal the physiological mechanisms of adaptation to phosphorus depletion.

Recently, site-specific phosphorus depletion in coastal waters has been caused by improved coastal management with decrease in anthropogenic phosphorus input. Consequently, seaweed beds composed of canopy-forming algae have concurrently changed over long-term periods. Although seaweed beds play an important role in supporting biodiversity in coastal ecosystems, declines in seaweed coverage have been observed due to inadequate nutrient uptake compared to the demand of seaweeds. Inherently, temperate seaweeds temporally undergo phosphorus limitation during seasonal phosphorus depletion periods. During these periods, they can maintain growth by using phosphorus in tissues after exposure to phosphorus-enriched conditions. Perennial brown seaweeds have high storage capacity dependant on low growth rate, suggesting that they can endure long-term nutrient limitation.

Canopy-forming brown alga *S. macrocarpum* is known as the major Fucales species found from temperate to sub-tropical regions of Japan. The annual variation of uptake and growth-related demand for phosphorus and the storage capacity under phosphorus-depleted environment has yet to be clarified. Thus, the aim of this study

was to understand the adaptation strategy of *S. macrocarpum* to the oligotrophic coastal environment conditions during the life cycle between growth and maturation.

In this doctoral thesis, the phosphorus dynamics during growth and maturation of *S. macrocarpum* were examined as follows: (1) annual variations of *in situ* uptake rate and growth-related demand for phosphorus (Study 1), and (2) storage capacities for phosphorus (Study 2). In Study 1, monthly investigations to estimate variations of phosphorus-uptake and -demand were conducted from December 2017 to January 2019. To evaluate nutrient-uptake characteristics, algal individuals were incubated for up to 6 hrs under multiple concentrations of nutrients. The photosynthetic rates were subsequently measured as oxygen production for up to 60 min under dark and multiple-light conditions. Seasonal phosphorus demands were estimated by multiplying the photosynthetic-based growth rates by the phosphorus-tissue content.

The *in situ* uptake rate for phosphorus seasonally changed along with the variation of ambient phosphate concentration and was relatively low (~0.2 μmol P g^{-1}DW d^{-1}) from spring to autumn and high (~0.4 to 1.7 μmol P g^{-1}DW d^{-1}) in winter. The *in situ* demand for phosphorus increased from the lowest (0.12 μmol P g^{-1}DW d^{-1}) in December 2017 to a single peak in March 2018 (1.02 μmol P g^{-1}DW d^{-1}), and remained constant (0.20–0.52 μmol P g^{-1}DW d^{-1}) until January 2019. Based on these results, the uptake rate exceeded the demand during winter, suggesting the accumulation of phosphorus into the tissues. In contrast, the uptake rates from March to November 2018 were less than 0.8 times lower than the demand, suggesting the use of phosphorus-tissue contents to maintain growth under phosphorus limitation.

In Study 2, the pre-cultivations during the growth period in March 2019 and maturation period in August 2019 aimed to obtain individuals with different

phosphorus-tissue contents under multiple-nutrient conditions. Thereafter, the maximum photosynthetic rate was evaluated with oligotrophic condition to estimate "storage capacity", which is defined as the period capable of sustaining growth by using phosphorus reserves in tissue. The photosynthetic growth rate during growth period increased when phosphorus-tissue content was high. Conversely, no relationship between the growth rate and phosphorus-tissue content in mature thallus was found. The storage capacities for the growth and maturation periods were approximately 19 and more than 16 weeks, respectively, indicating that this alga sustain growth under long-term phosphorus depletion by using the phosphorus-tissue contents. In conclusion, *S. macrocarpum* can adapt well to phosphorus depleted-environments during the growth to maturation periods.

The general discussion section will discuss how this alga is adaptive in temporally phosphorus-depleted environments and multiple discussion points are described as follows: 1) future prediction for the nutrient environment, 2) adaptation strategy under long-term phosphorus limitation, 3) phosphorus availability in short-term changes in the nutrient environment, 4) abiotic factors effect on the distributional change of *S. macrocarpum*. In summary, this alga, characterized as slow-growing, has a high P-storage capacity, and can mature under long-term P limitation condition by using P-tissue contents and P pulse-supplied to *in situ* environment.

Chapter I

General introduction

1.1 Trajectory of phosphorus depletion

Dissolved inorganic nitrogen (DIN) and phosphorus (DIP) play essential roles in the biological production, ecological functions and biogeochemical processes in marine environments (Asanuma et al. 2014; Li et al. 2014; Yang et al. 2018a). In these ecosystems, the distribution and dynamics of nutrients varies depending on various supply and removal processes. Generally, the nutrients are supplied to coastal waters through terrestrial input, regeneration of organic matter, atmospheric deposition, submarine groundwater discharge and horizontal advection from the open sea (Liu et al. 2005; 2009; 2012). The continuous uptake from micro- and macro-algae is the main pathway for the external nutrient removal. Additionally, human activities such as aquaculture, agriculture, wastewater treatment, and the consumption of fossil fuels also have a significantly wide effect on the patterns of nutrient circulation (Liu et al. 2012). In recent decades, due to human population growth and agricultural, urban, and industrial expansion since the mid-20th century, many coastal ecosystems are under significant pressure due to the anthropogenic loading of nitrogen (N) and phosphorus (P) from agricultural and urban runoff (e.g., de Jonge et al. 2002; García-Pintado et al. 2007; Dwight et al. 2002; Hale et al. 2015), which can then lead to eutrophication (e.g., Bell 1992; Jiang et al. 2014; Van Wijnen et al. 2015; Wan et al. 2017). Consequently, eutrophication results in harmful algal blooms and shifts of algal composition (Cloern 2001; Cardoso et al. 2004; Govers et al. 2014; Gubelit et al. 2016; Yang et al. 2018b), resulting in great economic damage for aquaculture and fishing industry (Tada et al.

2010). Therefore, there is a strong interest in understanding long-term trends in water quality and eutrophication (Bricker et al. 2008; Andersen et al. 2017; Wan et al. 2017; Li et al. 2018).

To create a sustainable environment, the negative impacts from human activities need to be balanced by the positive impacts of coastal remediation (Zhou et al. 2020). In Europe, the water framework directive (WFD, in 2000) has been established to reduce eutrophication impacts and various anthropogenic pressures, and has aimed to achieve the improved ecological state in groundwater and surface waters (Le Fur et al. 2019). Furthermore, the concept of "Satoumi", which aims at a well-balanced nutrient cycle between land and sea, is based on sustainable management of coastal waters developed in Japan (Matsuda and Kokubu, 2016). With laws and regulations to promote countermeasures against eutrophication, the anthropogenic nutrient loadings by various point sources from industrial effluents (Stockner et al. 2000; Yamamoto 2003; Kronvang et al. 2005; Yanagi 2016) and dams (Gong et al. 2006; Chai et al. 2009; Morais et al. 2009), and nonpoint sources (Hennessey et al. 1994) were managed. Consequently, due to stringent regulations reducing nutrient loadings, site-specific oligotrophication has occurred in European (Conley et al. 2000; Stockner et al. 2000; Le Fur et al. 2019), Chinese (Zhou et al. 2020) and Japanese coastal waters (Yamamoto 2003; Nishikawa et al. 2010a; Yanagi 2016; Tsuchiya et al. 2018).

In particular, P depletion has caused an imbalance of N/P ratio in the north-western European coasts (Grizzetti et al. 2012; Burson et al. 2016). In southern Japan Sea, phosphate concentrations in the surface layers tend to decline during summer and winter for a few decades, while nitrate concentration showed no significant linear trend (Kodama et al. 2016). The incidence of the declining trend for P seems to more

forward (Turner et al. 2003) because the development of stratification (Ono et al. 2001; Tadokoro et al. 2009) and horizontal advection (Kim et al. 2013; Kim and Kim 2013; Kodama et al. 2016) have been attributed to the gradual increases in water temperature induced by global warming.

1.2 Long-term changes in coastal ecosystems

The recovery of coastal ecosystems after the regulation of nutrient loadings discharged from wastewater treatment process has received plenty of attention from European (Leruste et al. 2016; Riemann et al. 2016; Pasqualini et al. 2017; Lefcheck et al. 2018; Le Fur et al. 2019) and Japanese researchers (Yamamoto 2003; Yanagi 2016) over past few decades. Le Fur et al. (2019) illustrated the long-term changes in the coastal ecosystem states and vegetation assemblages along oligotrophication trajectories. They predicted that regime shifts in the order of (1) phytoplankton-dominated states, (2) opportunistic macroalgae-dominated states, and (3) perennial macroalgae and seagrasses-dominated states are deeply related to the environmental conditions such as ambient nutrient concentration, chl-*a* concentration and turbidity. Under non-eutrophic conditions, benthic macroalgae and seagrasses are mainly distributed in shallow lagoons (Strain et al. 2014; Leruste et al. 2016) because the low suspended solids lead to improved underwater light penetration and enhanced light availability on their macroalgal production (Lloret and Marín 2009; Le Fur et al. 2018).

Recently, oligotrophication has actual impact on declines in macroalgal coverage or the increase in barren grounds (“isoyake”) in coastal embayments (Steneck et al. 2002). In southern California, nutrient-depleted water mass induced by El Niño events has negative impact on kelp population (Zimmerman and Robertson 1985;

Dayton et al. 1992; Edwards and Estes 2006). In Japan, a decrease in nutrient concentrations caused by the increases in the flux of the Tsushima Warm Current waters (Onishi and Ohtani 1997) may lead to a loss of kelp forest (Nabata et al. 2003). The degraded seaweed beds are expected to expand due to the ambient nutrient concentration below a threshold level. Hence, how seaweed coverage is influenced by the long-term oligotrophic trajectories which need to be investigated.

The Goto Islands, Nagasaki, Japan are located in the western part of Kyushu and the eastern part of the East China Sea, and are strongly affected by the Tsushima Warm Current, the Yellow Sea Cold Water and tidal current from Jeju Island. The Islands are rich in fishery resources, namely, the productive fishing grounds are due to the complicated submarine topography. However, the fishery production in the surrounding ocean area of Goto Islands has been gradually decreasing (Statistics Bureau of Japan) which is probably linked to the formation of barren grounds. Previous investigations from the Fisheries Department in Nagasaki Prefectural Government suggested that increase in water temperature enhances grazing pressure by herbivores causing barren grounds in the area.

Incidentally, the horizontal distribution in concentrations for DIN and DIP around the northern Goto Islands was seasonally investigated. The results indicated that the DIP concentration during summer and autumn was under the detection limit (< 0.09 μM) (Tsuchiya et al. 2018). The terrestrial P loadings discharged from local activities are almost completely removed by the wastewater treatment process, leading to the supply of oligotrophic-discharged water into the natural environment through the river (Soka University 2015). Therefore, the coastal embayment in the northern Goto Islands is characterized as an oligotrophic region close to the offshore area due to passing

oligotrophic warm current, indicating an unfavorable environment for the formation of seaweed beds.

Canopy-forming perennial algae such as Laminariales and Fucales play essential roles to provide an ecological habitat and a harvestable resource for various aquatic organisms throughout the year (Graham 2004; Christie et al. 2009; Yatsuya et al. 2005). A loss of seaweed beds undermines the important ecological functions. Therefore, an understanding of the physiological responses such as nutrient uptake, growth and photosynthetic characteristics) of temperate seaweeds to oligotrophic trajectory (i.e., P depletion) is essential.

1.3 Nutrient availability of seaweeds

Seaweeds take up nutrients to drive photosynthetic growth and productivity. The rate of nutrient uptake is depending on the availability of a nutrient supply from the surrounding seawater and the specific potential of nutrient uptake (Douglas et al. 2014). Previous studies reported that nutrient uptake characteristics are affected by abiotic factors such as temperature (e.g., Nishihara et al. 2005; Ohtake et al. 2020a), water flow (e.g., Hurd 2017; Inoue et al. 2020), light (e.g., Gordillo et al. 2002; Pereira et al. 2008) and carbon dioxide (Zou 2005; Fernández et al. 2017a, b).

Moreover, seaweeds can accumulate plenty of nutrients in their tissues (Ryther et al. 1982; Lundberg et al. 1989; Chopin et al. 1990; Hanisak 1990; Mizuta et al. 2003). The accumulation of P is also enhanced where phosphate uptake is higher than P-demand to sustain growth (Pedersen et al. 2010). Phosphate-absorbed in seaweed is transformed into different compounds in different parts of the alga, and transferred to processes of the incorporation and the storage. Organic P contents in tissue are

incorporated into many macromolecules, such as nucleic acids (i.e., ribosomal RNA and DNA), proteins, and phospholipids (Elser et al. 2000; Mizuta et al. 2003). Indeed, ATP and high-energy compounds play important roles in energy flow through photosynthesis and respiration processes of the plant (Cembella et al. 1984). Furthermore, intracellular polyphosphate and vacuolar inorganic phosphate can be served as the storage in macroalgal (Lundberg et al. 1989) and higher plant cells (Lee & Ratcliffe 1983; Roberts et al. 1984). These P reserves can be utilized to maintain growth when P demands are not met by P uptake (Birch et al. 1981; Gordon et al. 1981; Lundberg et al. 1989; Pedersen & Borum 1996; Pedersen et al. 2010).

The amount of P content in tissue can vary in response to the balance between input (the net uptake of external nutrient) and output (the biological demand of internal nutrient for growth, reproduction and tissue loss) (Douglas et al. 2014). Pedersen et al. (2010) examined the uptake kinetics and growth-related demands for P in six macroalgal species with different growth characteristics. Fast-growing algae (*Ceramium rubrum* and *Ulva lactuca*) periodically suffer from long-term P limitation because of their high P demands, whereas slow-growing algae (*Ascophyllum nodosum* and *Laminaria digitata*) can meet the P demands throughout a year. This finding concurs with the shift from the dominance of opportunistic macroalgae (i.e., fast-growing algae) to submerged macrophytes-dominated states observed in Mediterranean coasts (Le Fur et al. 2019). However, under oligotrophication, temperate slow-growing algae potentially face P limitation during the periods of P-depleted condition due to the insufficient P supply, which is unable to satisfy their P demand, unless they can rely on P reserves. The growth limitation causing P depletion has occurred less commonly than N limitation cases (Birch et al. 1981; Pedersen et al. 2010). Therefore, it is necessary to

focus on clarifying the adaptation strategy of the seaweeds to P-depleted seasons and environments.

According to the previous study, the annual variations of P uptake rates and *in situ* demands for macroalgal species with different growth strategies were estimated based on the seasonal variations of environmental factors such as phosphate concentration and PAR (Pedersen et al. 2010). It has been suggested that the characteristics of the P availability in seaweeds were classified into three types according to growth strategies (i.e., fast-, intermediate-, and slow-growing algae). This seems to be an appropriate approach to reveal the changes in macroalgal community composition in oligotrophic trajectory in coastal areas. However, there is still considerable uncertainty with regard to physiological changes along with the life cycle in the recent findings concerning macroalgal P-dynamics. Indeed, the inherent physiological roles of seaweeds are different between the growth and maturation periods. Therefore, focusing on the mutation in algal life stages must be considered in the understanding of the characteristics of the uptake and demand for P.

1.4 *Sargassum* species

The genus *Sargassum* (Sargassaceae, Fucales) can form dense *Sargassum* beds on rocky intertidal and subtidal areas throughout the temperate and subarctic regions (Schiel & Foster 1986). Canopy-forming *Sargassum* beds play various ecological roles in food source and shelter for a wide variety of associated aquatic organisms (e.g., Murase 2000a, 2000b, Yatsuya et al. 2005; Gouvêa et al. 2020), providing biodiversity in coastal ecosystems. According to the reports from Terawaki et al. (2003), *Sargassum* beds along the Japanese coasts composed of approximately 30% of the total coverage of

the vegetated benthic ecosystem. *S. macrocarpum* C. Agardh is known as one of the major perennial brown algae commonly found throughout temperate regions of Japan including the Sea of Japan, the Seto Inland Sea and the Pacific coast of Honshu Island (Yoshida 1983; Shimabukuro 2018; Terada et al. 2019), which are exposed to the effects of the Kuroshio and Tsushima warm current and Oyashio cold current. According to the report on the distribution of seaweed beds by local government in Shin-kamigoto, Nagasaki, dense *Sargassum* beds composed of *S. macrocarpum* has only formed in Arikawa Bay of the eastern Nakadori Island, situated in northern Goto Islands.

The details in morphology, phenology, community structure and the productivity of *S. macrocarpum* have been fully clarified (e.g., Murase and Kito 1998; Murase et al. 2000a, 2000b; Murase 2001; Yatsuya et al. 2005; Endo et al. 2013a). The estimated annual net productivities of the communities ranged from ca. 1,600 to 2,100 g dry weight m^{-2} $year^{-1}$, which were approximately the same levels to those of terrestrial plant (Murase et al. 2000a; Yatsuya et al. 2005). The responses of photosynthesis and nutrient uptake to temperature changes have recently been studied for this alga (Terada et al. 2020; Ohtake et al. 2020a). The maximum gross photosynthetic rate occurred at 27.8°C and the maximum quantum yields of photosystem II (Fv/Fm) in the optimal temperature was from 8.9 to 11.1 °C (Terada et al. 2020). Ohtake et al. (2020a) revealed that the maximum uptake rate (V_{max}) for phosphate was constant from 15 to 25 °C, and increased at 30 °C due to high P demand caused by high respiration rate. These results suggest that this alga has tolerance to a broad range of temperature, resulting that the geographical distribution is widely found within temperate areas of Japan. However, year-round variations of the P uptake and how this alga adapts to long-term low-P condition remain to be elucidated.

1.5 Aims of the doctoral thesis

This doctoral thesis aims to evaluate P dynamics during the growth and maturation periods of *S. macrocarpum*. In Study 1, the annual variations between P-uptake rate and demand were examined based on monthly incubations to estimate phosphate uptake kinetics and photosynthetic parameters, and monthly field observations of environmental factors. The period in which *S. macrocarpum* was exposed to seasonal P limitation was evaluated by the balance between *in situ* uptake and demand for P. Based on the results of Study 1, in Study 2, the P-storage capacity of *S. macrocarpum* was evaluated as the photosynthetic growth and adaptation to P-depleted condition. The P-storage capacities during the growth and maturation periods were examined by pre-cultivation with nutrient-enriched condition and short-term photosynthesis experiment under nutrient-depleted condition. Finally, this study discusses how this alga is adaptive throughout these life stages under oligotrophic coastal environments. The aim of this study is to broaden current knowledge of year-round P dynamics for canopy-forming temperate seaweeds. The P dynamics of *S. macrocarpum* along with the growth stages examined in this study have many contributions in the field of aquatic plant physiology.

Chapter II

Phosphorus uptake and demand during growth and maturation of *Sargassum macrocarpum*

2.1 Introduction

According to previous studies (Thomas et al. 1985; Yoshida et al. 2011; Sato et al. 2016), the N uptake characteristics of seaweeds vary with life stage. The ammonium and nitrate uptake rates of germlings or younger sporophytes in *Fucus distichus* and *Undaria pinnatifida* were relatively higher than those of mature sporophytes (Thomas et al. 1985; Sato et al. 2016). However, the variations of P uptake characteristics with different life stages are poorly understood. The estimated uptake rate for phosphate in *Saccharina ochotensis* during the growing period varied little from January to July 2001 (Sato & Agatsuma 2016). *In situ* uptake rates of phosphate, estimated by the subtidal seaweeds, varied seasonally with the seasonal patterns of P contents in their tissues (Douglas et al. 2014). Indeed, the nutrient contents in tissues showed seasonality and life stage-based variations coupled with changes in the external nutrient concentrations (Niel 1976). These findings hypothesize that the uptake characteristics of nutrients work closely with the nutrient accumulation which can facilitate the active growth of young sporophytes.

The P demands of seaweeds were estimated based on the relationship between the growth rates and critical P-tissue contents (Q_c) needed to maintain maximum growth rate (Pedersen et al. 2010). In fact, the Q_c was calculated from a non-linear model (i.e., Droop model) described by plotting growth rates against total P contents in tissues (Hanisak 1979). The P demand is assumed to be estimated by light-saturated

photosynthesis determined as a proxy for the maximum growth rate (Pedersen et al. 2010). However, the photosynthetic parameters for seaweeds have been found to vary with the thallus location. In macroalgae with leathery, leaf-like sections (hereafter, these sections of the thallus will be referred to as leaves) or cartilaginous branches, photosynthesis can occur throughout the thallus (Gao & Umezaki 1988, Gao 1991). In various parts of the *S. macrocarpum* thallus, the maximum photosynthetic rate (P_{max}) was found to be highest in the upper leaves, followed by the lower leaves, bladders, and main branches (Murase 2000a). The P_{max} and dark respiration rate of *S. fusiforme* were also much higher in the receptacles compared to the leaves (Zou & Gao 2005). Thus, it is predicted that there is a difference in P demand between the juvenile, which is composed of a main branch and some leaves, and the adult, which is composed of a main branch and many leaves, bladders, and receptacles.

The purpose of Study 1 is to estimate the annual variations between the *in situ* uptake rate and growth-related demands for P during the growth and maturation periods of *S. macrocarpum*. This study developed a hypothesis indicating that these annual variations vary depending on not only the seasonality of environmental factors, but the life stage of *S. macrocarpum*. In Study 1, the phosphate uptake kinetics and photosynthetic parameters were examined by monthly incubations and fitted to a model. Concurrently, the concentrations of dissolved inorganic nutrients and photosynthetically active radiation (PAR) in *in situ* environments, and nutrient contents in tissue were monitored every month.

2.2 Materials and methods

2.2.1 Field observation

In this study, the collections of algal samples and measurements of environmental factors (Figure 2-1) were conducted within seaweed beds in Arikawa Bay, Nakadori Islands, Nagasaki, Japan (32°59'17.0"N; 129°07'07.3"E). The coastline of Arikawa Bay is composed of wave-dissipating blocks and large natural rocks. In the subtidal zone (2–7 m depth), *S. macrocarpum*, *Dictyopteris prolifera* and *D. undulata* were dominant throughout the year, however *S. horneri* and *S. thunbergii* were only found during spring and early summer. This coastal area is characterized as a P-depleted environment, as reported by a previous investigation (Tsuchiya et al. 2018).

To monitor PAR, a cosine-corrected PAR sensor (Odyssey, Dataflow Systems Ltd.) was attached on the seabed inside the *Sargassum* beds. The PAR data was monitored every 15 minutes. To monitor *in situ* nutrient concentration, seawater samples were collected at the surface and within the *Sargassum* beds (~7 m deep) once a month. The particles contained in water samples were immediately removed through 0.45-μm pore size filters (Millex SLHA, Millipore). The filtered samples stored in 10-mL plastic tubes were transported to the Institute for East China Sea Research at Nagasaki University and were stored in a freezer (< -20°C) until nutrient analysis.

2.2.2 Collection of seaweeds

The experimental design and the procedure of Study 1 are shown in Figure 2-2. The collections of *S. macrocarpum* were conducted in Arikawa Bay (1–5 m deep) every month between December 2017 and January 2019 other than January 2018. The tested samples were collected with permission from local fisheries cooperatives after required

procedures. The algal collections in this study were based on the life stages through the juvenile and mature thallus for *S. macrocarpum*. The maturation of *Sargassum* species is generally induced from early summer, thus producing antheridium and oogonium on receptacles (Murase and Kito 1998; Cho et al. 2012). In this study, as the formation of receptacles in apical tissue of *S. macrocarpum* were observed during May and August in 2018, the "maturation period" of this alga was defined as the period. To track yearly morphological changes, the collections of the juveniles (2nd generation) continued between September 2018 and January 2019. Hence, growth periods in this study were divided into two periods as follows: "first-growth period": December 2017 to April 2018; "second-growth period": September 2018 to January 2019. Specimens collected during monthly sampling events were kept in cooled boxes and were immediately transported to an 80-L storage tank at the laboratory. The collected samples were pre-cultivated below a light shielding net under natural sunlight (ca. 500 μmol photons m^{-2} s^{-1}) and ambient temperature until the experiments started. Sand-filtered seawater was continuously supplied to the samples.

2.2.3 Nutrient uptake kinetics

To examine the phosphate uptake characteristics of *S. macrocarpum*, the algal samples were incubated under multiple concentrations of nutrients (Figure 2-2; Incubation 1). All individuals used for Study 1 were collected based on life stages to compensate different wet weights (WW; 1.4–83.2 g-WW). Prior to the experiments, samples were gently rinsed with filtered seawater (< 0.5 μm) to remove fouling organisms on algal surface. The large PVC tank used for experiments (Figure 2-3) was indoors in the institute. A LED lamp (High spec high disk V2, Nichido Ind.Co., Ltd.)

was set just above the tank to provide saturated irradiance. Plastic buckets (13-L volume; n = 3) were placed inside the tank and seated under the lamp to provide even irradiance to the buckets. Tested samples (n = 3) were incubated in each bucket, which was filled with filtered seawater. The sample buckets were sealed by a transparent acrylic board, and immersed into the seawater to prevent the loss of dissolved oxygen (DO) and fluctuations in temperature during incubation. A mini pump was used to vertically stir the filtered seawater in each bucket while the samples were fixed on the bottom of the bucket by weights.

The seawater in each bucket was enriched with sodium nitrate ($NaNO_3$), ammonium chloride (NH_4Cl), and sodium dihydrogen phosphate (NaH_2PO_4). The nutrient conditions were adjusted with 5 different concentrations as follows: ammonium and nitrate concentrations at 40, 80, 160, 320 and 500 μM and phosphate concentrations at 2, 4, 8, 16 and 25 μM. The N:P ratio of the nutrient conditions was constant at 20 to examine uptake characteristics for P and N. The algal samples (n = 3) were pre-cultured with a nutrient-depleted condition for more than 24 h. To quantify the nutrient uptake rates, incubation periods were selected according to the size of tested samples as follows: 4–6 h for mature thalli (July and August 2018); 1–2 h for juveniles (the other months mentioned above).

Triplicate seawater samples (10 mL) for nutrient analysis were collected from each bucket between before and after the incubation. Ammonium, nitrate, and phosphate concentrations of seawater samples were analyzed by an auto-analyzer (SWAAT, BL-TEC), in reference to previous method (Parsons 2013). The rate of nutrient uptake (μmol g^{-1}-DW h^{-1}) was estimated based on the depleted nutrients in the medium over a given incubation period and were represented using the following equation:

$$\text{uptake rate} = \frac{(N_0 - N_t) \times Vol}{DW \times t} \quad 1)$$

where N_0 and N_t are initial and final concentrations of nutrient (μM), respectively; Vol is seawater volume (L); DW is algal dry weight (g-DW); and t is incubation period (h). Michaelis–Menten function was fitted to the relationship between the calculated uptake rates at each nutrient condition and the average concentration during incubation, based on least-square regression:

$$V = \frac{V_{max} \times S}{K_m + S} \quad 2)$$

where V is uptake rate (μmol g^{-1}DW h^{-1}); V_{max} is maximum uptake rate (μmol g^{-1}DW h^{-1}); S is nutrient concentration of substrate (μM); and K_m is half-saturation constant (μM). In addition, the ratio of V_{max} to K_m (V_{max}/K_m) which quantifies the availability of nutrient at low nutrient concentration was estimated in this study (Healy 1980).

2.2.4 Photosynthetic response

To examine algal photosynthetic rate of *S. macrocarpum*, the samples were incubated under multiple light conditions (Figure 2-2; incubation 2). The photosynthetic rates were estimated as oxygen production under dark (0 μmol photons m^{-2} s^{-1}) and 5 or 6 light conditions (40–600 μmol photons m^{-2} s^{-1}). The experimental arrangement was the same as former one. After more than 15-min acclimation to each light condition, the incubations were conducted for 30–60 min. Respiration rate was measured in dark condition. Net photosynthetic rate was estimated under light conditions. The highest irradiance (~600 μmol photons m^{-2} s^{-1}) was provided without light obstruction and the lower irradiances (~40–350 μmol photons m^{-2} s^{-1}) were supplied using a lightproof

sheet. The light-saturated photosynthetic rates were evaluated by using a photosynthesis-irradiance (P-I) curve (Equation 4).

Prior to the photosynthetic experiment, the PAR sensor was calibrated outdoors from early morning to after sunset. The light intensity recorded by the PAR sensor was estimated from < 10 μmol photons m^{-2} s^{-1} to ~2,100 μmol photons m^{-2} s^{-1} by means of a LI-190 quantum sensor (LI-COR Biosciences). To measure the integrated photon flux density (μmol photons m^{-2} s^{-1}) during incubation, the PAR sensor recorded every 10 min. Additionally, temporal changes in DO and temperature during incubation were measured every minute using a DO logger (ProODO, YSI Inc.). The DO concentrations linearly changed with experimental period. The photosynthetic rates (P_n) and respiration rates (R_d) over the experimental periods were calculated by the following equation:

$$P_n \text{ and } R_d = \frac{([O_2]_t - [O_2]_0) \times Vol}{WW \times t} \quad 3)$$

where $[O_2]_0$ and $[O_2]_t$ represent the initial and final DO concentrations (mg L^{-1}), respectively; Vol is seawater volume (L); WW is algal wet weight (g-WW); and t is incubation period (h). The P-I curve was fitted to the calculated photosynthetic rates against light intensities (e.g., Jassby and Platt 1976):

$$P_{net} = P_{max}\left(1 - \exp\left(-\frac{\alpha}{P_{max}} E\right)\right) - R_d \quad 4)$$

where P_{net} is net O_2 production rate (mg O_2 g^{-1}WW h^{-1}); P_{max} is maximum O_2 production rate (mg O_2 g^{-1}WW h^{-1}); α is an initial slope of photosynthesis versus irradiance; E is incident irradiance; and R_d is respiration rate. The saturation irradiance (E_k) was calculated from P_{max}/α. The compensation irradiance (E_c) was estimated by $P_{max} \ln\left(\frac{P_{max}}{R_d - P_{max}}\right) / \alpha$ (Fujimoto et al. 2014).

To evaluate maximum growth rate, the values subtracting R_d from P_{max} were determined. Additionally, based on monthly average of *in situ* PAR monitored at the bottom of Arikawa Bay, *in situ* growth rate was estimated from the photosynthetic rate by assigning PAR to P-I curve. The growth rate was estimated based on photosynthetic quotient (PQ) ratio, expressed as a molar ratio of CO_2 uptake to O_2 release (e.g., Thomas & Wiencke 1991; Rosenberg et al. 1995; Mercado et al. 2003). In this study, a review of median PQ ratios (1.29 mol CO_2 mol^{-1} O_2), 10% and 90% percentiles (1.05 to 2.22 mol CO_2 mol^{-1} O_2) were referred to estimate the growth rates (Pedersen et al. 2010). These ratios were multiplied by the estimated photosynthetic rates (mg O_2 g^{-1}WW h^{-1}). The daily growth rate (g C g^{-1} tissue C d^{-1}) was converted to relative growth rate (d^{-1}), assuming diurnal period (ca. 12 h) recorded from December 2017 to January 2019.

2.2.5 Phosphorus demand

To analyze the total C and P contents of the algal samples, they were dried at 60 °C until the DW was stable. The dried *S. macrocarpum* samples were divided into leaves, branches, and holdfast, and the leaves were only broken into a powder by means of a small pestle and mortar. The total C contents were measured with a CHN analyzer (FLASH 2000, Thermo Fisher Scientific). Prior to the analysis of the total P contents, the mixture of tiny amount of powdered samples (approximately 0.1 g-DW) with a 2% aqueous solution of $K_2S_2O_8$ was autoclaved at 120 °C for 30 min. After the pre-treatment, the total P contents were measured by the nutrient auto-analyzer.

The P demands (μmol g^{-1}DW d^{-1}) were estimated by multiplying the calculated growth rate (d^{-1}) by the P-tissue content (μmol P g^{-1}DW) in this study. The maximum

demands were calculated from maximum growth rates, and *in situ* demands were based on *in situ* growth rate. To evaluate the annual variation of P demands during the growth and maturation periods, the monthly changes in these growth rates and P-tissue contents were analyzed.

2.2.6 Statistical analysis

Statistical analyses and model fittings were done using R version 3.3.4 (R Development Core Team 2019). To reveal the seasonal differences between P-uptake rate and demand in *S. macrocarpum*, the pairwise comparisons were analyzed by using two-sample t-test, leading to a systematized analysis for which seasons this alga is exposed to P limitation.

2.3 Results

2.3.1 Environmental factors

The *in situ* PAR monitored in Arikawa Bay seasonally changed and was relatively low during winter and high during summer (Figure 2-4a). The seasonal change in *in situ* phosphate concentration was also observed; relatively higher (~0.2–0.3) in winter and lower (~0.1 μM) in summer (Figure 2-4b). The nitrate concentrations also varied seasonally with a peak during spring (Figure 2-4c). The ammonium concentrations fluctuated ranging from ~0.1 μM to ~0.9 μM (Figure 2-4d).

2.3.2 Phosphorus uptake

The uptake rates for phosphate increased with rising DIP concentrations from culture medium then saturated (Figure 2-5). The kinetic parameters of phosphate uptake

are shown in Table 2-1. The V_{max} for phosphate seasonally changed, with a peak in January (1.73 μmol g^{-1} DW h^{-1}). There was no trend of the K_m ranging from 4.7 μM in March 2018 to 10.5 μM August 2018. The seasonal change in the ratio of V_{max} to K_m (V_{max}/K_m) for phosphate was found and relatively higher in winter than summer. The annual variations of V_{max} and V_{max}/K_m coincided with *in situ* concentrations for phosphate. Additionally, the experimental temperature seasonally varied, from 15.0°C in February 2018 to 28.6°C in August 2018 (Table 2-1). The temperature during incubation for up to 6 h was stable.

2.3.3 Photosynthetic characteristics

The net photosynthetic rates tended to increase with raising PAR, and saturated at higher PAR levels (Figure 2-6). The photosynthetic parameters obtained by P-I curve are shown in Table 2-2. The P_{max} during the growth period were relatively higher than those in the mature period, ranging from 0.33 mg O_2 g^{-1}WW h^{-1} in February 2018 to 1.19 mg O_2 g^{-1}WW h^{-1} in March 2018. No seasonality in α (initial slope of the photosynthetic rate versus irradiance) and R_d were observed, but these values were the highest in December 2017 (0.016 ± 0.009) and August 2018 (0.23 mg O_2 g^{-1}WW h^{-1}), respectively. The highest values of E_k and E_c were observed in August 2018.

2.3.4 Phosphorus contents in tissues and growth rate

The total P content increased from December 2017 to the highest in March 2018 and was constantly low (Figure 2-7) corresponding to low *in situ* concentrations for phosphate (Figure 2-4b). The estimated maximum growth rates tended to be higher during the two growth periods compared to the maturation period, ranging from 0.002

d^{-1} in February 2018 to 0.007 d^{-1} in March, October, and December 2018 (Table 2-3). The *in situ* growth rate, calculated from *in situ* PAR, ranged from 0.001 d^{-1} in December 2017 and February 2018 to 0.005 d^{-1} in March, September, and October 2018 (Table 2-3).

2.3.5 Uptake rate and demand of phosphorus

The P-uptake rate estimated by *in situ* concentrations of DIP seasonally changed, and was relatively low (~0.2 μmol P g^{-1}DW d^{-1}) between spring and late summer, and high (~0.4 to 1.7 μmol P g^{-1}DW d^{-1}) in winter (Figure 2-8). The maximum P-demands were relatively low (~0.3 μmol P g^{-1}DW d^{-1}) in winter and the highest (1.44 μmol P g^{-1}DW d^{-1}) in March 2018. Thereafter, the P demand between May and August 2018 during maturation period (~0.5 μmol g^{-1}DW d^{-1}) was relatively lower than that between September 2018 and January 2019 during second growth period (~0.7 μmol g^{-1}DW d^{-1}) (Figure 2-8). In addition, the *in situ* demand for P increased from the lowest (0.12 μmol P g^{-1}DW d^{-1}) in December 2017 to a single peak in March 2018 (1.02 μmol P g^{-1}DW d^{-1}), and then changed with a constant (0.20–0.52 μmol P g^{-1}DW d^{-1}) until January 2019 (Figure 2-8).

2.3.6 Relationship between uptake and demand of phosphorus

The differences between the P-uptake rate and demand were compared seasonally. During winter, the uptake rates were significantly higher than the *in situ* demand (Figure 2-9; $p = 0.016$). During spring, summer, and autumn, the median *in situ* demand exceeded the median uptake rate, but significant difference was only found in summer (Figure 2-9; $p = 0.033$). Consequently, the relationship between uptake rates

and demand for P changed with season. Additionally, the uptake rate was inadequate to meet the demand during the late growth period to the maturation period, resulting in P limitation for approximately 26 weeks (Figure 2-8).

2.4 Discussion

2.4.1 Annual change in phosphate uptake kinetics

Given that annual changes in *in situ* phosphate concentrations and V_{max}/K_m for phosphate showed a similar trend, *S. macrocarpum* seem to experience high ample phosphate when ambient concentration in Arikawa Bay was relatively high. The increasing trend in V_{max}/K_m (increase of V_{max} and constant K_m) suggests heightened characteristics to take up nutrients at low ambient concentrations (Dunlop et al. 1997; Harrison & Hurd 2001; Perini & Bracken 2014). According to Douglas et al. (2014), the *in situ* uptake rates for phosphate examined in subtidal algae (*Melanthalia abscissa* and *Pterocladia lucida*) were the highest when peaks in P contents in tissue were found under an intermediate level (~0.4 μM) of the *in situ* phosphate concentration. Generally, the increased growth rates are induced by the increases of water temperature and *in situ* PAR from spring onward. Thus, seaweeds have high P-requirement and the large amount of P input is enhanced by a demand-driven uptake of phosphate.

2.4.2 Growth characteristics during growth and maturation periods

The physiological changes of *S. macrocarpum* in this study have a similar pattern to those from a previous study (Murase & Kito 1998). Estimated annual variation of *in situ* growth rates (0.001 day^{-1} to 0.005 day^{-1}) of *S. macrocarpum* examined in this study was lower than the experimental values from a previous study

(Ohtake et al. 2020a). During semi-continuous cultivation for 10 days, the specific growth rates in the nutrient-enriched conditions (0.015 to 0.025 g-WW day^{-1}) were significantly higher than those in the non-enriched conditions (0.006 g-WW day^{-1}) (Ohtake et al. 2020a). Growth rates of *Sargassum* species examined by previous studies (Lapointe 1986; Endo et al. 2013b) tend to be higher than those of *S. macrocarpum* estimated in this study. Endo et al. (2013b) examined that there were no significant differences ($p < 0.05$) in relative growth rates of *S. patens* cultivated with nutrient enriched medium (0.06 g-WW day^{-1}) and nutrient-depleted condition (0.06 g-WW day^{-1}) at 20 °C and 30 °C. Additionally, the growth rates of *S. fluitans* and *S. natans* cultured in phosphate enriched medium were ranging from 0.05 to 0.08 g-WW day^{-1} (Lapointe 1986). From a methodological point of view, the photosynthesis-based growth rate in this study may be an underestimate compared to the WW-based growth rate. In fact, although the C assimilation during night was previously identified in the C metabolism of temperate macroalgae (Kremer 1981), the estimated growth rate in this study was derived from the C assimilation through photosynthesis during the daytime. In a brown alga *Laminaria hyperborea*, the C assimilation rate in dark condition was approximately 5% of those in light-saturated condition (Kfippers and Kremer 1978). Hence, the estimation process of the photosynthetic growth rate in *S. macrocarpum* ignores the processes of the dark assimilation. Additionally, the intracellular C discharge may need to be considered as a possible reason for the underestimation of growth rate. According to a previous study (Suzuki 1997), the parts of the total macroalgal production lose in the form of organic C. The estimation process used in this study allows evaluation of the algal photosynthetic growth rate in the short-term, and remains to be improved for the accuracy.

2.4.3 Availability and dynamics of phosphorus contents in tissues

The nutrient-tissue levels of seaweeds infer the internal nutrient status and are involved in growth and maturation (Mizuta et al. 2003). The high-energy compounds (e.g., ATP) play a vital role in energy transfer during the photosynthesis process (Cembella et al. 1984). Indeed, a peak in the total P contents of *S. macrocarpum* coincided with the highest growth rate (Figure 2-7; Table 2-3). To develop reproductive tissues (e.g., gametes and spores) during maturation, the mature individuals require P and utilize the P contents in tissues. The kelps *Undaria pinnatifida* and *Alaria crassifolia* sustain high levels of P reserves to form sporophyll and zoospore (Kumura et al. 2006), and *Saccharina* species require critical tissue contents for N and P to develop reproductive sori (Nimura et al. 2002). This indicate that the Laminariales (i.e., kelp) commonly mature when an ambient concentration of nutrients are high (i.e., winter).

However, the maturation of *Sargassum* species (i.e., *S. macrocarpum*) coincides when P-tissue contents and external P concentration are low (Figure 2-7; Yatsuya et al. 2008). This critical phase can be related to the storage capacity that is defined as the period that the nutrient-tissue contents are available to sustain growth with no uptake from ambient DIN and DIP (Pedersen et al. 2010; Pedersen & Johnsen 2017). Thus, the P-storage capacities of *S. macrocarpum* require evaluation based on the relationship between the estimated growth rates and total P-tissue contents.

2.4.4 Relationship between uptake and demand of phosphorus

Pedersen et al. (2010) examined whether P-uptake kinetics and growth-related P demands differed systematically among fast- and slow-growing algae. Slow-growing

algae can assimilate more ambient nutrients at low concentrations due to low P requirement, or continue the growth during summer by using P-tissue contents obtained during winter, when nutrient availability is high. Indeed, slow-growing species have both strategies to continue the growth potential under P-depleted environment (Pedersen & Borum 1996, 1997; Pedersen et al. 2010). The balance between uptake characteristics and inherent demands for nutrient, and thus the risk of suffering nutrient limitation, is approximately related to specific growth rate. Fast-growing species permanently or periodically suffer from nutrient limitation, while slow-growing species have a competitive advantage in low nutrient availability due to low nutrient demands (Pedersen & Borum 1996, 1997; Pedersen et al. 2010).

Compared to previous study (Pedersen et al. 2010), the balance of the P uptake and demand in *S. macrocarpum* would be similarly characterized as a slow-growing species. However, the uptake rate only exceeded the *in situ* demand in winter (Figure 2-8). This indicates that the P-uptake could not meet the demand under P-depleted conditions during spring and summer. However, *S. macrocarpum* can probably meet the demand by means of the following characteristics: (1) an elevated availability of P supplied through rainfall event within a short period, and (2) an effective use of P contents in tissue (high P-storage capacity).

Table 2-1 Nutrient-uptake kinetics (V_{max}, K_m, and V_{max}/K_m) of *Sargassum macrocarpum* and experimental temperature during the growth (December 2017 to April 2018 and September 2018 to January 2019) and maturation (May 2018 to August 2018) periods (Ohtake et al. 2020b modified). The dashed line in this table represents the switch between maturation and growth periods.

Year	Month	V_{max} ($\mu mol\ g^{-1}DW\ h^{-1}$)	K_m (μM)	V_{max}/K_m ($L\ g^{-1}DW\ h^{-1}$)	Experimental temperature* (°C)	r^2
2017	Dec.	0.95±0.16	5.02±2.18	0.13	16.8±0.4	0.75
2018	Feb.	1.76±0.31	7.12±2.80	0.14	15.0±0.3	0.84
	Mar.	0.33±0.05	4.68±1.78	0.04	15.5±0.7	0.76
	Apr.	0.61±0.11	7.84±3.02	0.05	19.4±0.5	0.84
	May	0.24±0.04	7.45±2.86	0.02	21.7±0.7	0.84
	Jun.	0.24±0.05	7.86±3.65	0.02	23.3±0.9	0.77
	Jul.	0.15±0.02	7.02±2.11	0.01	26.9±0.9	0.89
	Aug.	0.32±0.07	10.50±5.12	0.02	28.6±0.6	0.86
	Sep.	0.85±0.18	9.45±4.55	0.06	23.9±0.7	0.77
	Oct.	1.05±0.16	6.45±2.54	0.13	22.7±0.7	0.86
	Nov.	0.80±0.13	7.61±3.09	0.08	19.2±0.4	0.83
	Dec.	1.40±0.21	6.16±2.41	0.17	18.2±0.7	0.83
2019	Jan.	1.73±0.20	10.26±2.61	0.15	15.5±1.2	0.93

*: The experimental temperature was measured with a dissolved oxygen (DO) logger every minute during photosynthetic experiments each month. V_{max}: maximum uptake rate; K_m: half–saturation constant; r^2: coefficient of determination. Shown are the means and standard error of the means (n = 3).

Table 2-2 Photosynthetic parameters of *Sargassum macrocarpum* during growth (December 2017 to April 2018 and September 2018 to January 2019) and maturation (May 2018 to August 2018) periods (Ohtake et al. 2020b modified). The dashed line in this table represents the switch between maturation and growth periods.

Year	Month	P_{max} (mg O^2 g^{-1}WW h^{-1})	α (mg O^2 g^{-1}WW h^{-1} (μmol m^{-2} s^{-1}) $^{-1}$)	R_d (mg O^2 g^{-1}WW h^{-1})	E_k (μmol m^{-2} s^{-1})	E_c (μmol m^{-2} s^{-1})	r^2
2017	Dec.	0.58±0.09	0.016±0.009	0.15±0.08	37.2	9.4	0.74
2018	Feb.	0.33±0.02	0.003±0.001	0.06±0.02	115.6	21.6	0.93
	Mar.	1.19±0.21	0.008±0.003	0.13±0.11	144.2	15.8	0.78
	Apr.	0.68±0.07	0.005±0.001	0.09±0.04	131.6	16.7	0.92
	May	0.65±0.08	0.003±0.001	0.06±0.03	254.1	24.9	0.94
	Jun.	0.41±0.05	0.002±0.001	0.07±0.03	187.7	30.4	0.88
	Jul.	0.61±0.05	0.004±0.001	0.10±0.02	172.5	27.8	0.95
	Aug.	0.64±0.05	0.002±0.000	0.23±0.02	304.7	109.8	0.95
	Sep.	0.92±0.18	0.004±0.001	0.03±0.06	209.1	7.6	0.87
	Oct.	1.10±0.19	0.005±0.002	0.16±0.11	210.1	30.1	0.79
	Nov.	1.01±0.13	0.004±0.001	0.07±0.04	277.4	18.2	0.94
	Dec.	1.11±0.10	0.009±0.002	0.16±0.07	126.9	18.0	0.91
2019	Jun.	0.74±0.10	0.003±0.001	0.06±0.04	234.6	21.7	0.93

P_{max}: maximum O_2 production rate; α: initial slope of the photosynthesis versus light intensity; R_d: respiration rate under dark condition; E_k :saturation irradiance; E_c: compensation irradiance; r^2: coefficient of determination. Shown are the mean ± S.D. (n = 3).

Table 2-3 Maximum and *in-situ* growth rates of *Sargassum macrocarpum* during the growth (December 2017 to April 2018 and September 2018 to January 2019) and maturation (May 2018 to August 2018) periods (Ohtake et al. 2020b modified). These growth rates were estimated with the photosynthetic quotient (PQ) ratio. The dashed line in this table represents the switch between maturation and growth periods.

Year	Month	Maximum growth rate (d^{-1})		*In situ* growth rate (d^{-1})	
		Medium	10-90 percentiles	Medium	10-90 percentiles
2017	Dec.	0.003	0.002-0.004	0.001	0.001-0.002
2018	Feb.	0.002	0.001-0.003	0.001	0.001-0.002
	Mar.	0.007	0.006-0.012	0.005	0.004-0.009
	Apr.	0.004	0.003-0.007	0.004	0.003-0.007
	May.	0.004	0.003-0.006	0.003	0.003-0.006
	Jun.	0.003	0.002-0.004	0.003	0.002-0.004
	Jul.	0.003	0.003-0.006	0.003	0.003-0.005
	Aug.	0.003	0.002-0.004	0.002	0.002-0.003
	Sep.	0.006	0.005-0.011	0.005	0.004-0.008
	Oct.	0.007	0.006-0.012	0.005	0.004-0.008
	Nov.	0.006	0.005-0.010	0.003	0.002-0.005
	Dec.	0.007	0.006-0.012	0.003	0.003-0.006
2019	Jan.	0.005	0.004-0.009	0.002	0.001-0.003

Median PQ ratios and 10% and 90% percentiles were reviewed by Pedersen et al. (2010).

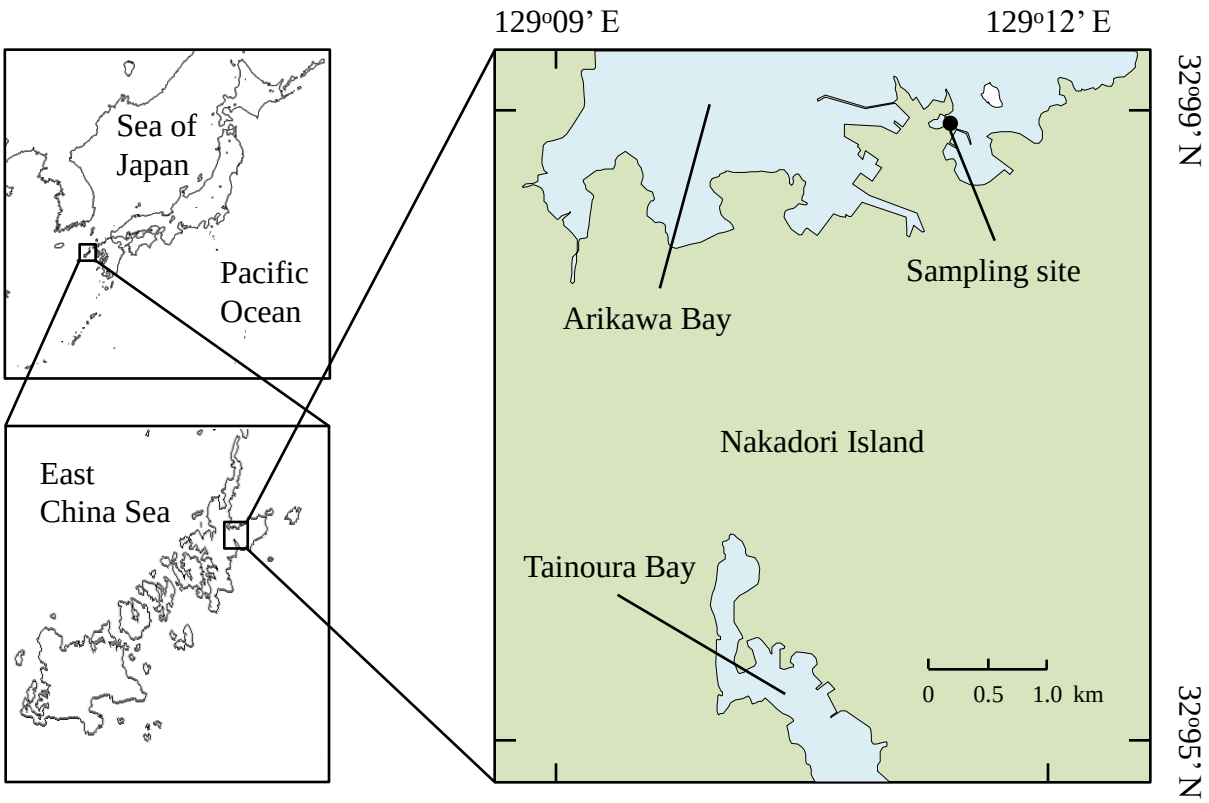

Figure 2-1 The map of Goto Islands, Nagasaki, Japan. The black circle represents the sampling site of *Sargassum macrocarpum* in a subtidal coastal area in Arikawa Bay situated in Nakadori Island (Ohtake et al. 2020c modified).

Life cycle of *Sargassum macrocarpum*

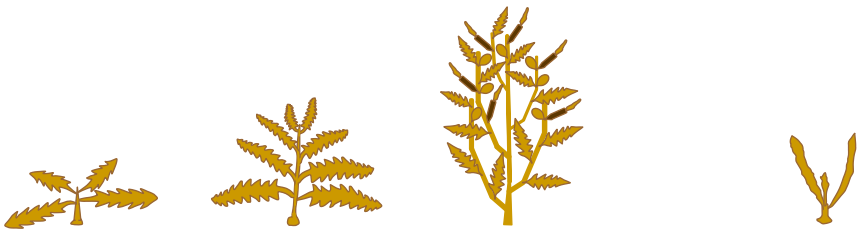

1st growth period | Maturation period | 2nd growth period

Period	December 2017 to April 2018	May to August 2018	September 2018 to January 2019

Algal collections

were conducted in Arikawa Bay every month from December 2017 to January 2019 (except January 2018)

Sampling site

Pre-incubation in 80-L storage tank (Outdoor)

Incubation 1 in an indoor seawater tank was aimed to evaluate nutrient uptake characteristics of *S. macrocarpum* under multiple-nutrient concentrations

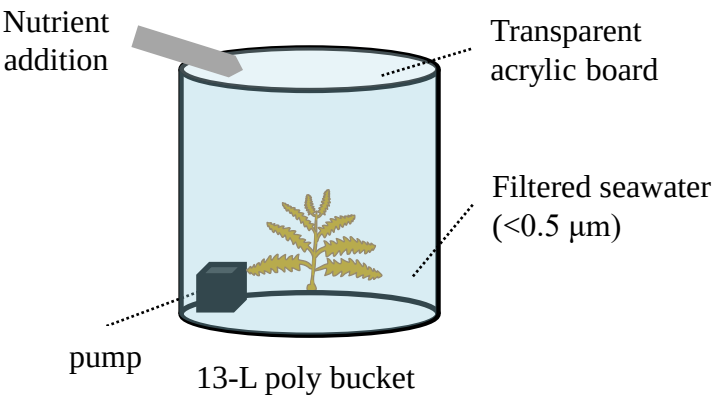

Incubation 2 in an indoor seawater tank was aimed to evaluate photosynthetic rate of *S. macrocarpum* under multiple-light conditions

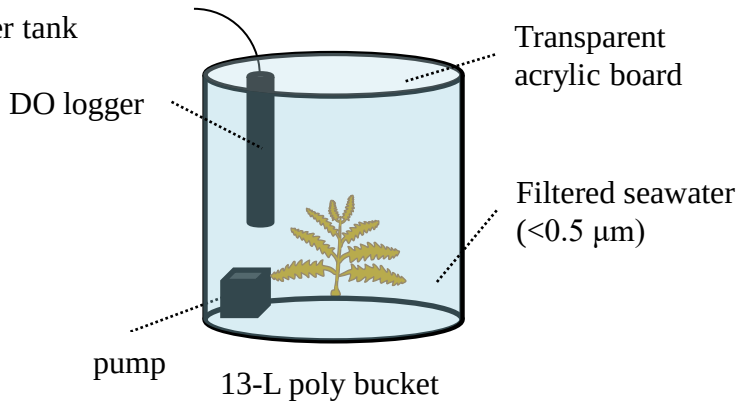

Figure 2-2 The experimental design and the procedure of Study 1.

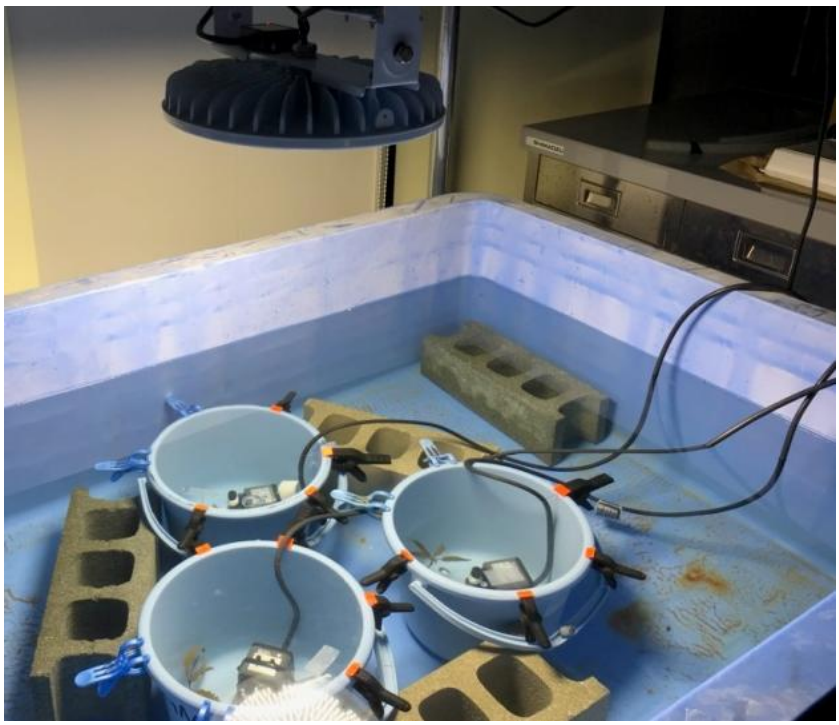

Figure 2-3 The incubation system used in Study 1 and Study 2. The seawater tank was indoors at the Institute for East China Sea Research at Nagasaki University and was illuminated by a LED lamp (High spec high disk V2). Three 13 L-plastic buckets were placed in a triangular shape in the center of the tank and set just below one LED lamp to maintain the constant and even light intensity to all buckets.

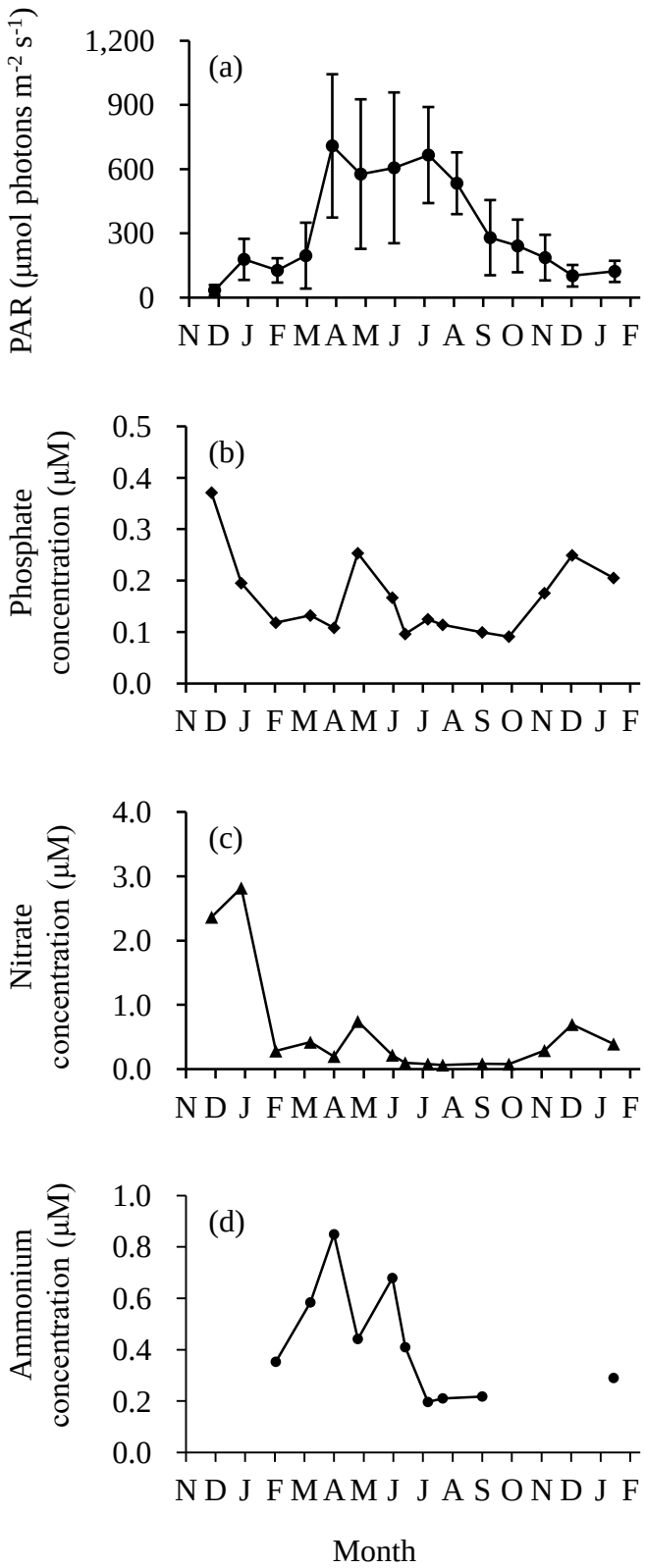

Figure 2-4 Seasonal variations in PAR (a), phosphate concentration (b), nitrate concentration (c), and ammonium concentration (d) in Arikawa Bay from December 2017 to January 2019. The PAR variation are expressed as mean ± standard deviation (S.D.) (Ohtake et al. 2020b modified).

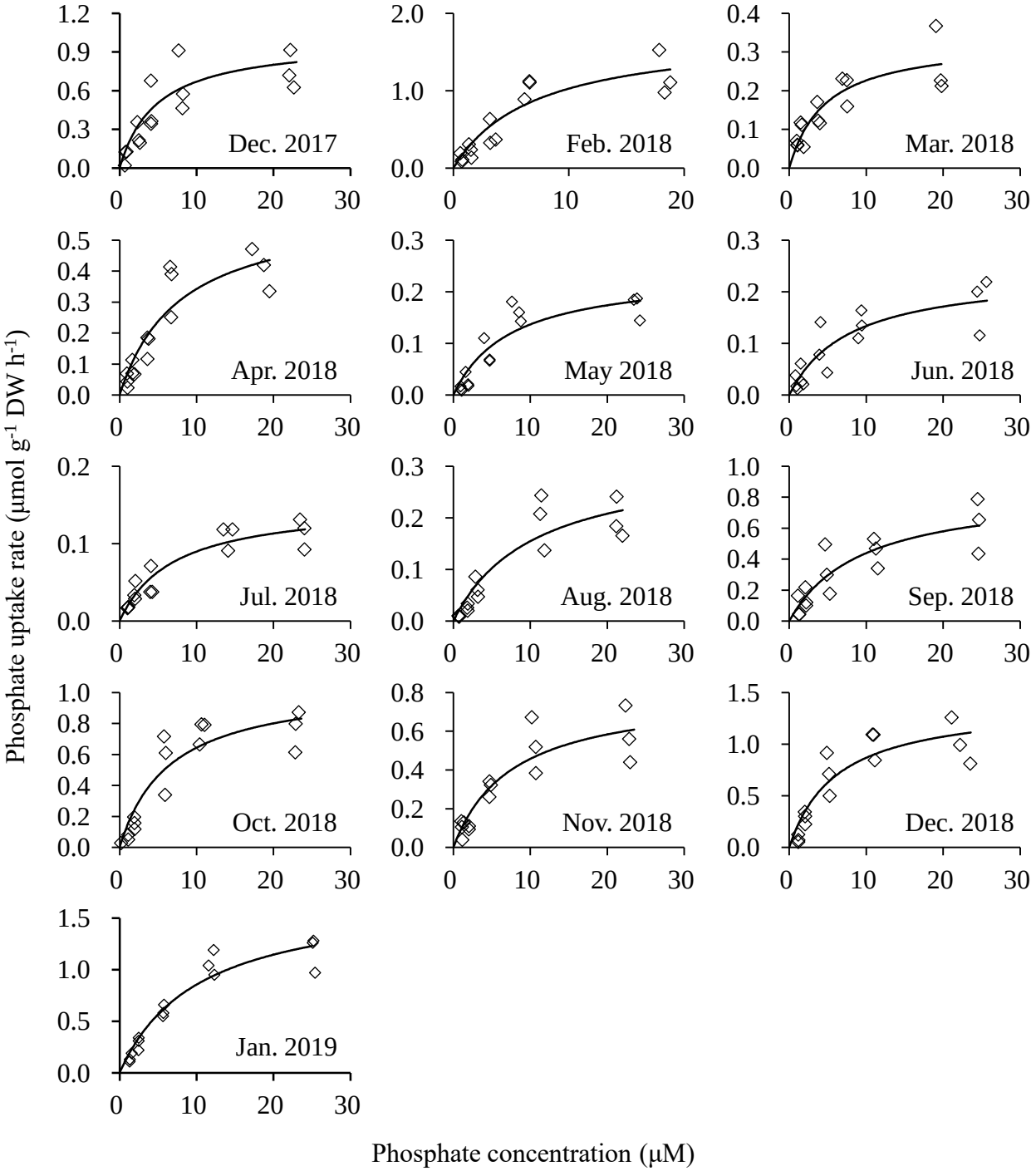

Figure 2-5 Monthly change of phosphate uptake kinetics: the relationship between phosphate uptake rate of *Sargassum macrocarpum* and phosphate concentration from December 2017 to January 2019. The Michaelis–Menten function was fitted to the data (n = 15) (Ohtake et al. 2020b modified).

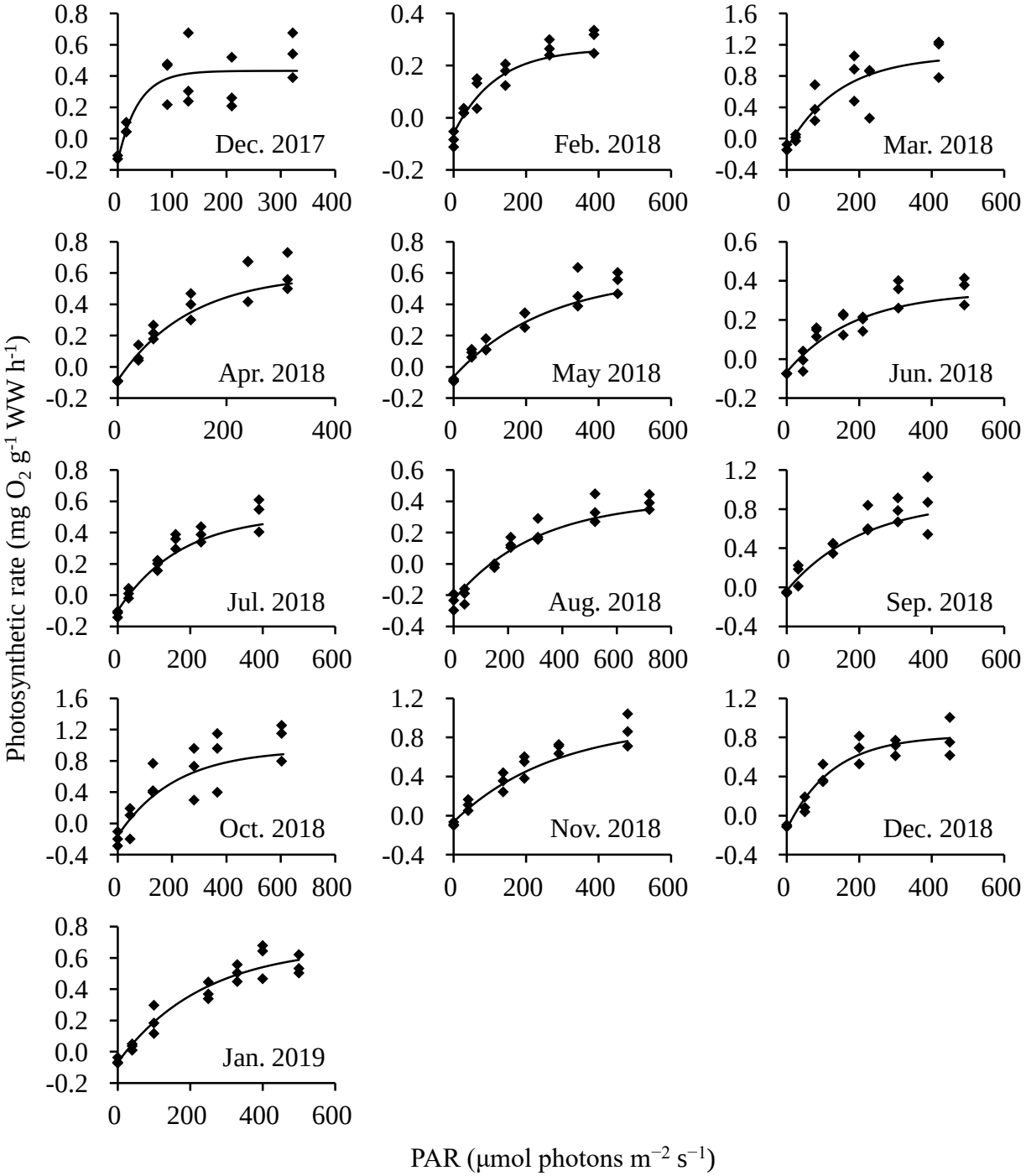

Figure 2-6 Monthly change of photosynthetic characteristics: the relationship between photosynthetic rate of *Sargassum macrocarpum* and PAR from December 2017 to January 2019. A photosynthesis-irradiance (P-I) curve was fitted to the data (n = 18–21) (Ohtake et al. 2020b modified).

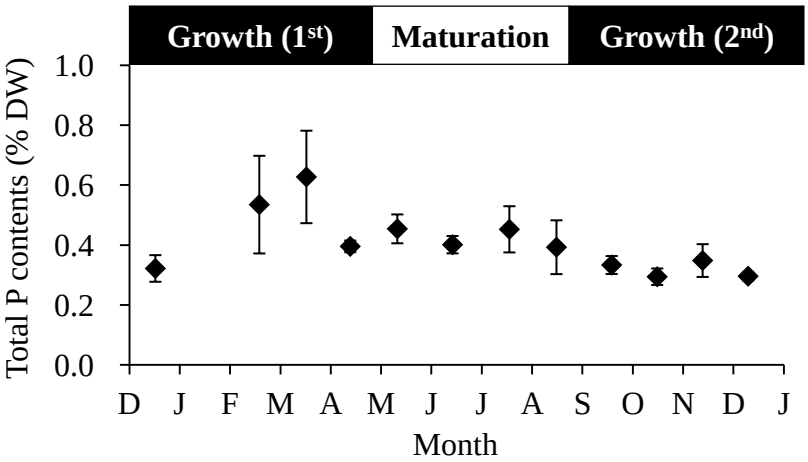

Figure 2-7 Total P content of *Sargassum macrocarpum* during the first-growth (December 2017 to April 2018), the maturation (May 2018 to August 2018) and the second-growth (September 2018 to January 2019) periods. Total P content is expressed as mean ± S.D. (n = 3) (Ohtake et al. 2020b modified).

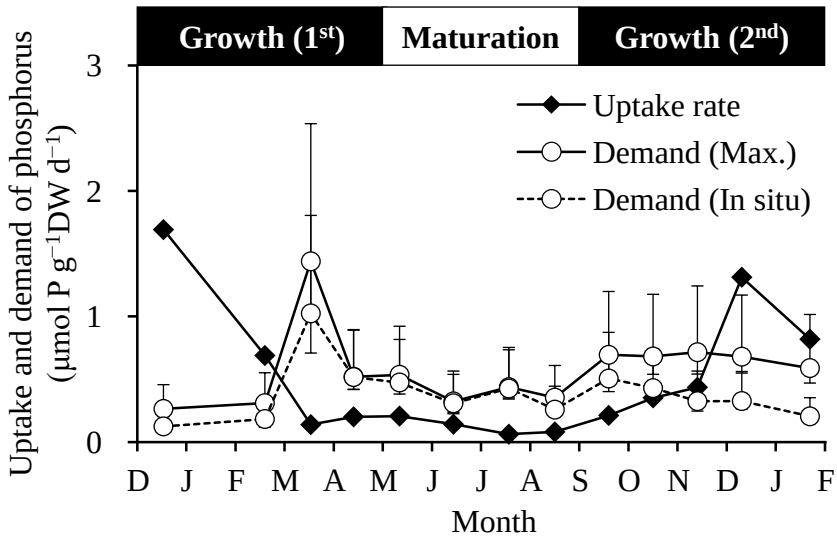

Figure 2-8 Uptake rate, maximum and *in-situ* demands for P of *Sargassum macrocarpum* during the first-growth (December 2017 to April 2018), the maturation (May 2018 to August 2018) and the second-growth (September 2018 to January 2019) periods. Maximum demand was estimated as the product of the maximum growth rate and total P contents. *In-situ* demand was estimated by the *in-situ* photosynthetic rate as a result of assigning photosynthetically active radiation (PAR) to the photosynthesis-irradiance (PI) curve. The range of error bars are expressed based on 10% and 90% percentiles of photosynthetic quotient (PQ) ratios (Pedersen *et al*. 2010) (Ohtake et al. 2020b).

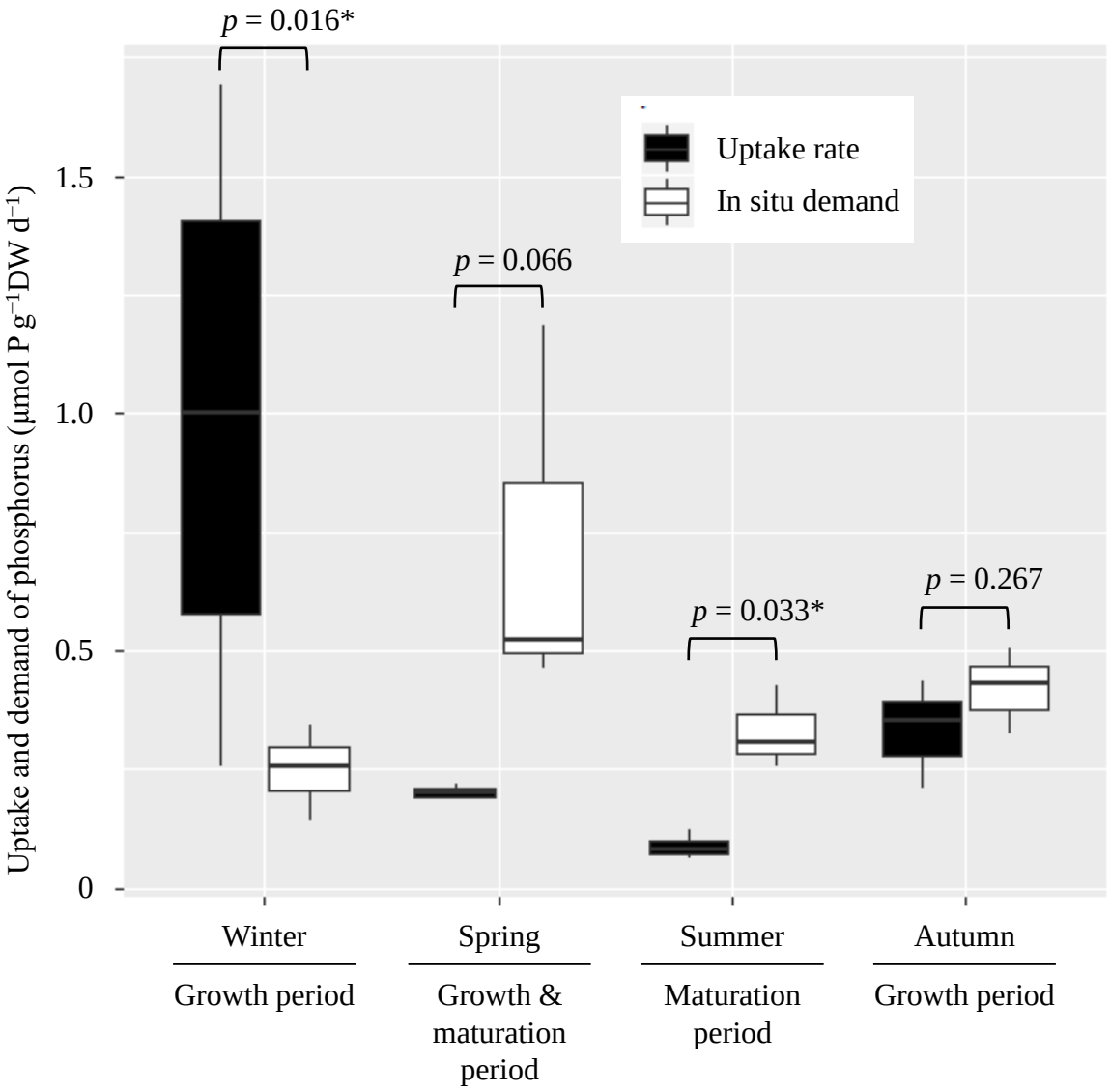

Figure 2-9 Mean comparison of uptake rate and *in-situ* demands for P of *Sargassum macrocarpum* during four seasons: (a) winter (growth period; December 2017 to February 2018 and December 2018 to January 2019), (b) spring (growth period and maturation period; March to May 2018), summer (maturation period; June to August 2018), and autumn (growth period; September to November 2018). The horizontal line within the box is the median, the upper and lower boundaries of the box represent the 25 and 75 percentiles and the whiskers mark the minimum and maximum values. Each box is expressed as means ± S.D. ($n \geq 3$), and different letters on bars indicate significant differences between uptake rate and *in-situ* demands according to two-sample t-test (*: $p < 0.05$) (Ohtake et al. 2020b).

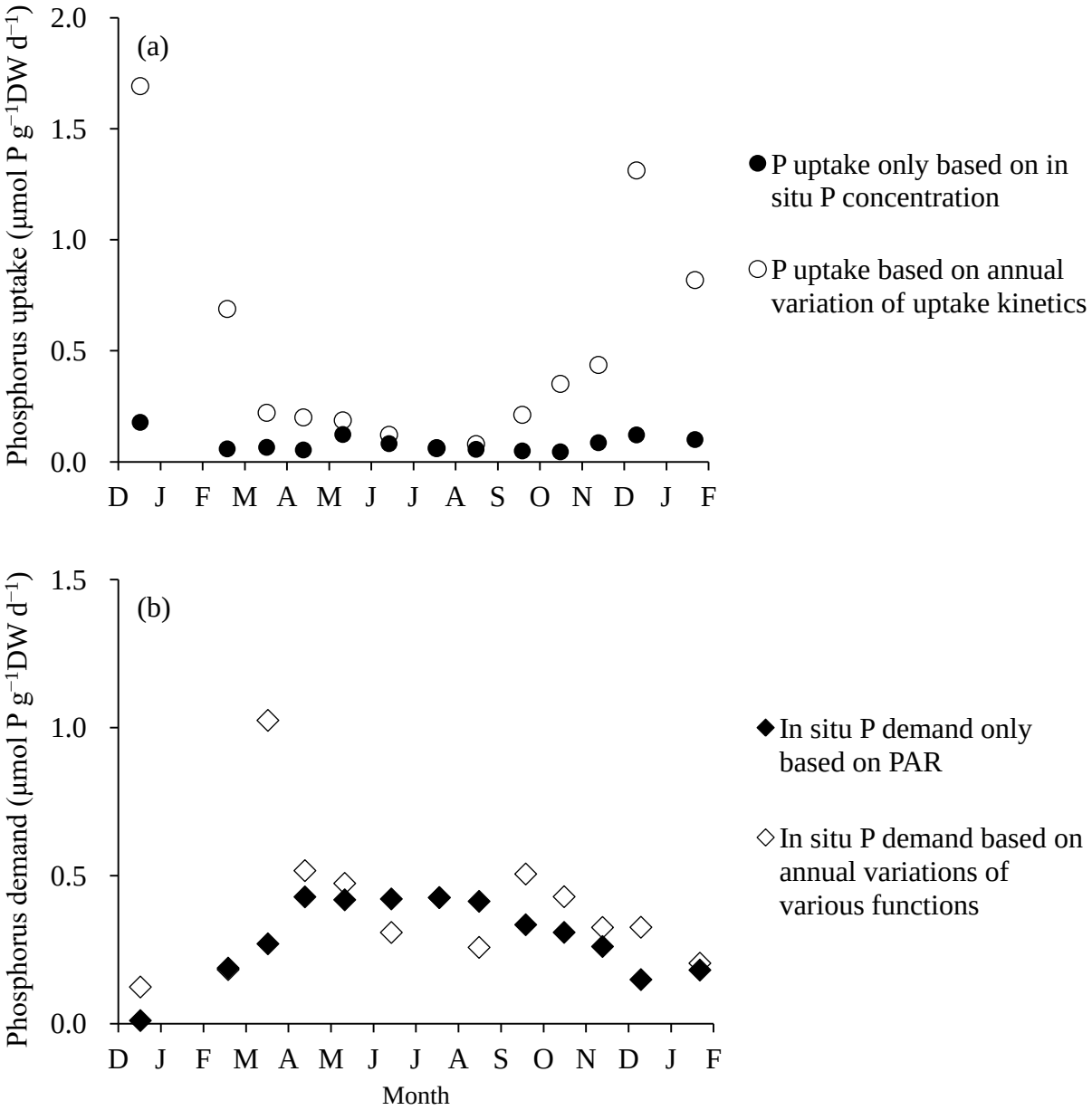

Figure 2-10 Annual variations of uptake rates (a) and *in-situ* demands (b) for P in *Sargassum macrocarpum*. Estimated P uptake (black circle) only based on uptake kinetics on July 2018 (Table 2-1) and annual variation of external P concentration (Figure 2-4b). P uptake (white circle) estimated by annual variation of uptake kinetics (Figure 2-8). Estimated in situ P demand (black diamond) only based on annual variation of PAR (Figure 2-4a). In situ P demand (white diamond) based on annual variations of various functions such as growth rate (Table 2-3), total P contents (Figure 2-7) and PAR estimated in this study.

Chapter III

Storage capacity for phosphorus during growth and maturation in *Sargassum macrocarpum*

3.1 Introduction

Dissolved inorganic nutrients are playing a vital role in supporting of seaweed physiology (Harrison & Hurd 2001). Uptake rates of nutrients are affected by the continuous supply of nutrients through water exchange between algal surface and the surrounding seawater, and specific nutrient availability (Douglas et al. 2014). Since nutrient concentrations of temperate regions are often depleted due to the seasonality, temperate seaweeds face temporal limitation of nutrients throughout their life history. However, they can adapt to such unfavorable conditions since the nutrient storage in their tissues (Ryther et al. 1982; Hanisak 1990), and the availability of the stored nutrients under oligotrophic condition (Birch et al. 1981; Gordon et al. 1981) is developed. Storage capacity of nutrients is clearly essential to quantify the availability of internal nutrients in tissue to sustain a continuous growth with no uptake of external nutrients (Pedersen et al. 2010). The storage capacities among species differ from growth characteristics of seaweeds such as fast- and slow-growing species. Perennial algae, characterized as a slow-growing, have the superior storage capacity to sustain growth, and probably induce maturation in nutrient-depleted environment. However, there is a still need for the long-term availability of internal P in accordance with their life stages.

Phosphorus (P) contents in tissue are accumulated as various P compounds such as nucleic acids, proteins and phospholipids (Chopin et al. 1990; Mizuta et al.

2003). Although these intracellular P compounds have an influence on the processes of growth and maturation, little is known about P dynamics in seaweed tissue. Yatsuya et al. (2008) revealed that the P reserves accumulated in the apical parts of *S. macrocarpum* have seasonal changes, and are more than those in the base during winter. Presumably, phosphate-absorbed in seaweeds under P-replete environment can be formed as growth-associated P compounds (e.g., nucleic acids) to induce growth and maturation. Since juvenile and adult stages play different physiological roles, P-storage capacity of *S. macrocarpum* may differ between these stages. Consideration is given to be clarified how growth is sustained in seasonally oligotrophic environments throughout the life stage.

The purpose of Study 2 is to evaluate the P-storage capacity of *S. macrocarpum* during the growth and maturation periods. In this study, the P-storage capacity was examined by the combination of two experiments as follows: (1) “pre-cultivation” aimed to obtain algal samples with different nutrient-tissue contents under several nutrient-enriched conditions; (2) “photosynthetic experiment” to evaluate the maximum photosynthetic rates of *S. macrocarpum* as a proxy of maximum growth rates after pre-cultivation. The P-storage capacity was estimated based on the relationship between the growth rates and P contents in tissue, leading to estimation of how long this alga can endure under P depletion condition.

3.2 Materials and methods

3.2.1 Field observation

To monitor the daily variations of the salinity and phosphate concentrations in Arikawa Bay, daily water samplings every morning were conducted by skin diving with

a plastic bottle (50 mL volume) at the surface (0 m depth) and near the surrounding of the *Sargassum* beds in the bottom (ca. 5 m depth) in Arikawa Bay during the experimental period from August 25 to 31, 2019. The amount of daily precipitation (mm day^{-1}) in the Arikawa area (32°58.9'N; 129°07.1'E; 10 m height above sea level) during the experimental period was referred to from the integrated data from Japan Meteorological Agency (2019).

3.2.2 Collection of seaweeds

Collections of *S. macrocarpum* specimens were conducted in Arikawa Bay (approximately 2 m deep) during the growth period (March 2019) and maturation period (August 2019) (Figure 2-1). All specimens were immediately transported to the institute at Nagasaki University, and kept in a storage tank under natural ambient light and temperature condition. The continuous supply of the aerated- and sand-filtered seawater to the specimens was to preserve their activity.

3.2.3 Pre-cultivation with nutrient supply

To provide tested specimens with a variety of nutrient-tissue contents, all individuals were pre-cultured for 9 days in multiple nutrient-enriched conditions. Prior to the experiments, diatoms and debris attached to the juvenile and mature thallus were gently removed using filtered seawater. The algal wet weights (WW) ranged from 0.7 to 5.5 g WW for juveniles (n = 18) and from 2.5 to 6.0 g WW for mature thalli (n = 18). Prior to the cultivations, three sub-samples were used to analyze the initial total P contents (% DW) during the cultivation.

The experimental design and the procedure of Study 2 are shown in Figure 3-1.

To induce the accumulation of P-tissue contents in the thallus, pre-cultivations of the juveniles and mature thalli of *S. macrocarpum* were conducted under multiple-nutrient conditions (Figure 3-1). Sodium nitrate ($NaNO_3$), ammonium chloride (NH_4Cl), and sodium dihydrogen phosphate (NaH_2PO_4) were supplied to 500 mL of filtered seawater (< 0.5 μm) in a 600 mL glass beaker. The nutrient-enriched media were prepared at the following concentrations: 8, 60, 120, 240 and 400 μM ammonium and nitrate and 0.4, 3, 6, 12 and 20 μM phosphate. The highest nutrient concentration treatment was labeled "1", and the subsequent conditions were labeled 2, 3, 4, and 5, which corresponded with a high to low gradient of nutrient conditions. Specimens were assigned to all treatments (n = 3) with an equivalent WW distribution. All beakers filled with the culture media were set in an incubator (MLR-350HT, SANYO; Figure 3-2). The culture media were gently aerated by using an air pump. The low irradiance (ca. 80 μmol photons m^{-2} s^{-1} in a 12: 12 h light–dark cycle) was supplied to all beakers to enhance the nutrient accumulation in tissues during the cultivation rather than growth. The temperatures were actually set to 18 °C (±1 °C) in March 2019 and 25 °C (±1 °C) in August 2019. The exchange of culture media was conducted every 3 days to recover the initial nutrient concentration in each treatment.

To monitor change in nutrient concentration during cultivation, triplicate samples (10 mL) were collected from media every 3 days. The maximum quantum yield (Fv/Fm) was measured before and after cultivation by using a Chlorophyll Fluorometer (Pocket PEA, Hansatech) to measure the variations in photosynthetic activity of specimens cultivated with different nutrient conditions. All specimens were immersed in filtered seawater contained in a plastic tray (40 × 30 × 7 cm) to acclimate a dark condition for more than 15 min. The tray was placed in the incubator to keep a stable

seawater temperature. Fv/Fm at 0 μmol photons m^{-2} s^{-1} was measured after the dark acclimation. Finally, the WW change of each specimen was monitored every 3 days by using an electronic balance (0.1 mg accuracy). Prior to the measurement, moisture on surface of specimens was removed by blotting with paper towels. After 9 days-cultivation, specimens were reused for incubation aimed to evaluate the maximum photosynthetic rate.

3.2.4 Incubation under nutrient-depleted condition

In order to estimate the maximum photosynthetic rate of *S. macrocarpum* after pre-cultivation, the specimens were incubated under nutrient-depleted and light-saturated conditions (Figure 3-1). The large PVC tank was indoors in the institute and illuminated by the LED lamp that can provide sufficient irradiance (ca. 500 μmol m^{-2} s^{-1}) to allow *S. macrocarpum* to keep light-saturated photosynthetic rate (Terada et al. 2020; Study 1). Three 13 L-buckets were installed in the same arrangement as the nutrient uptake-experiment (Chapter 2). All specimens were individually incubated in each bucket, which was filled with fresh sand-filtered seawater. The recirculation flow each bucket was provided by a mini pump.

The maximum photosynthetic rates were estimated in light-saturated irradiance. Before deployment, the PAR sensor was calibrated by using the quantum sensor according to the method mentioned above. The variations of DO and temperature over time in each bucket were measured every 60 seconds by using the DO logger. The photosynthetic rate (P_n) was determined using Eq. (3).

In study 2, photosynthetic growth rates were estimated from photosynthetic quotient (PQ) ratios (Pedersen et al. 2010). The growth rates were estimated assuming

daily light exposure (ca. 12 h) and expressed in units of g C g^{-1} tissue C day^{-1}. Finally, the exponential growth rate (ln unit day^{-1}) was calculated.

Photosynthesis based-growth rates were plotted against P-tissue contents, and the Droop model was fitted to the data using least squares, non-linear regression.

$$\mu = \mu_{\max} \times \left(1 - \frac{Q_s}{Q}\right), \quad 5)$$

where μ is relative growth rate (day^{-1}), μ_{max} is maximum growth rate, Q_s is subsistence cell quota (in % DW)—the lowest P-tissue content that allows growth—and Q is P-tissue concentration. The critical P-tissue content (Q_c) is defined as the P-tissue contents above which growth is not limited by a lack of the P contents in tissues. The P requirements guaranteed to maximum growth rates were estimated based on the observed maximum growth rate and critical P-tissue contents (i.e., Q_c). Corresponding to the intercept of the two lines between the maximum growth rate and the initial slope of the curve (Pedersen & Borum 1996), the Q_c was defined that the growth rate equaled 67% of the estimated μ_{max}.

The magnitude of P that could be accumulated in tissue was calculated based on the difference between the highest P-tissue contents (Q_{max}) and the Q_s. The storage capacity was evaluated using the following equation:

$$T = \frac{ln(Q_{\max}) - ln(Q_s)}{\mu}, \quad 6)$$

where T is the duration required for P consumption from Q_{max} to Q_s and μ is the estimated growth rate (e.g., 67% of μ_{max}; day^{-1}).

Until nutrient analysis, filtered seawater samples (< 0.45 μm) stored in 10 mL plastic tube were frozen (< -20 °C) at a deep freezer. Concentrations of dissolved

inorganic-nitrogen (DIN) and -phosphorus (DIP) were measured by the nutrient auto-analyzer, according to Parsons (2013). The little concentration of nitrate contained in seawater is treated as parts of DIN concentration.

The specimens collected before and after the 2 phase-experiment were dried at 60 °C to remove moisture. The leaves of juveniles were separated between upper and lower, whereas mature thalli were allocated to the leaves, receptacles and bladders. The dried samples were powdered by a small mortar, and stored at a desiccator until analysis for total C and P contents. Prior to the analysis, a small amount of the powdered samples (ca. 1 mg-DW) were weighted using the electrical balance. Total C contents were analyzed using the CHN analyzer. As the pre-treatment of analysis for total P contents, the mixture of powdered samples (ca. 1 mg-DW) with a 2% aqueous solution of $K_2S_2O_8$ was autoclaved at 120 °C for 30 min. After pre-treatment, total P contents were measured by the nutrient auto-analyzer.

3.2.5 Statistical analysis

Statistical analyses were conducted using R version 3.3.4. The data were analyzed by one-way ANOVA, and the differences among treatment means were analyzed using Dunnett multiple comparison tests.

3.3 Results

3.3.1 Precipitation, salinity, and phosphate concentration

The daily changes in precipitation, salinity and phosphate concentration at Arikawa Bay were shown in Figure 3-3. Precipitation from August 27 to 28 were more than 60 mm day^{-1} and other sampling dates were less than 20 mm day^{-1} (Figure 3-3a).

The daily change in salinity at the surface sharply decreased from 34.5 on August 26 to 29.0 on August 27 (Figure 3-3b) due to periodic precipitation and then maintained the same level (ca. 31.0) (Figure 3-3a). No change in the daily salinity at the bottom was observed during August 25 to 28, thereafter a decreasing trend was found (Figure 3-3b). The daily variation of phosphate concentration at the surface sharply increased from ca. 0.1 μM on August 26 to 0.6 μM (the highest value) on August 27, and then a decreasing trend was reported after the precipitation events passed (Figure 3-3c). On the other hand, the phosphate concentration at the bottom was stable, ranging from 0.07 to 0.17 μM (Figure 3-3c).

3.3.2 Phosphorus contents in tissues

During growth period of *S. macrocarpum*, the total P contents ranged from 0.36 ± 0.06% to 0.52 ± 0.07% dry weight (DW) (Figure 3-4a), and those in treatment 1 and 2 after the cultivation were significantly higher than those in initial stages (Dunnett's test: $t = 4.81$, $p = 0.004$, df = 5; $t = 5.42$, $p = 0.002$, df = 5, respectively; Figure 3-4a). Similarly, the total P content of mature thallus ranged from 0.36 ± 0.02 to 0.52 ± 0.10 % DW (Figure 3-4b), and those in treatment 1 was significantly higher than those in initial stages (Dunnett's test: $t = 2.93$, $p = 0.011$, df = 8; Figure 3-4b).

In treatment 1, total P contents in the upper leaves of juveniles were significantly higher than those in the lower leaves (T-test: $t = 24.37$, $p = 0.002$, df = 2; Figure 3-5a). Focusing on mature thallus cultured in treatment 1, the total P content in the receptacles tended to be significantly higher than those in the bladders (T-test: $t = 5.71$, $p = 0.030$, df = 2; Figure 3-5b).

3.3.3 Maximum growth rate

Maximum growth rates of juveniles taken during March 2019 increased from 0.004 ± 0.001 day^{-1} in treatment 5 to 0.006 ± 0.001 day^{-1} in treatment 3, 4, and 5 (Table 3-1). On the other hand, no trend of maximum growth rates for mature thallus collected during August 2019 was observed, ranging from 0.004 ± 0.001 day^{-1} in treatment 2 to 0.005 ± 0.001 day^{-1} in treatment 5 (Table 3-1). Maximum quantum yields (Fv/Fm) of juvenile and mature thallus during the cultivation were stable more than 0.6 in all treatments (Table 3-2).

3.3.4 Storage capacity for phosphorus

Maximum photosynthetic growth rates during the growth period correlated with the total P contents (Figure 3-6a), and the data can be fitted to the Droop model (Equation 5). Conversely, during maturation period, no trend between maximum growth rates and total P contents was found (Figure 3-6b). Critical P concentrations (Q_c) during the growth period were determined by the lowest P content (119.5 μmol P g^{-1} DW; Table 3-3) because of the Q_s (subsistence cell quota: 0.20 %-DW) deviated from the data set. The Q_c during the maturation period was defined as less than the lowest P content (108.1 μmol P g^{-1} DW) in this study (Table 3-3) because no results were obtained relatively low growth rates at low total P contents in the experiment. Thus, μ of the juveniles and mature thalli were defined as 67% of the estimated highest growth rate. The P requirements of the juveniles and mature thalli were 0.6 and less than 0.5 μmol P g^{-1} DW day^{-1}, respectively (Table 3-3). The P-storage capacities during growth and maturation periods (Equation 6) were approximately 19 weeks and more than 16 weeks, respectively (Table 3-3).

3.4 Discussion

3.4.1 Phosphorus pulse supply caused by rainfall

After the precipitation event on August 27 to 28, the salinity at the surface and bottom was stable at low level (ca. 31.0) (Figure 3-3b). This is because low-salinity water mass at the surface was transported to the bottom through vertical mixing. However, since the average wind speed on August 27 to 28 was less than 3 m s^{-1}, there was scarcely wind-induced vertical mixing during this rainy period. Given that the vertical mixing was caused by strong waves, P-contained in surface water may be transported to the bottom where *S. macrocarpum* grow with dense patches. Thus, the phosphate concentration at the bottom was stable throughout the sampling period (Figure 3-3c), which means the balance between supply (i.e., horizontal and vertical transportation) and loss (phosphate uptake by primary producers such as micro- and macro-algae) for P.

To have better sense of the daily change in amount of precipitation (mm day^{-1}) in the Arikawa area (32°58.9'N; 129°07.1'E) during 2019, the integrated data from Japan Meteorological Agency (2019) was summarized in Figure 4-4. The daily precipitation amounts, as well as the occurrence frequency of the precipitation events in summer (i.e., May to August) in 2019, tended to be more than that during other seasons (Figure 3-7). Therefore, there is evidence to support the hypothesis that the bioavailable P supplied by rainfall is one of the important sporadic-nutrient sources for mature thallus of *S. macrocarpum* exposed to P-depleted environments.

3.4.2 Phosphorus storage for growth and maturation

The P compounds in tissue are stored as various macromolecules such as nucleic acids, phospholipids, and proteins (Chopin et al. 1990; Mizuta et al. 2003). These P-containing molecules are likely to play central roles in processes of growth and maturation for seaweeds, although the P dynamics throughout their life cycles remain to be clarified. In a previous study on N dynamics of *Saccharina japonica* (Mizuta et al. 1994), the total length decreased with rising ammonium contents in the apical tissues. The N-reserves in the apical tissues are probably transported downward into a growing point in the base of thallus, resulting in the survival in N-depleted environments (Mizuta et al. 1994).

The P-tissue contents were higher in the upper leaves than the lower leaves (Yatsuya et al. 2008), suggesting a high P-requirement to induce growth during winter. In this study, as phosphate-absorbed into juvenile *S. macrocarpum* was accumulated at the upper leaves (Figure 3-5a), the similar pattern in the distribution of P-reserves was found. These results infer that the enhanced availability of P-reserves may lead to the elongation growth, and this evidence is likely to be linked to the findings of N dynamics.

During maturation period of seaweeds, an increased P-demand cause a decreased P-tissue contents because of the release of gametes and spores. Kumura et al. (2006) revealed that *Alaria crassifolia* and *Undaria pinnatifida* have high P-demands of P-reserves to develop sporophyll and zoospores. According to Nimura et al. (2002), *Laminaria* species also demand N- and P-tissue concentration above critical levels to form reproductive sori. The findings in this study regarding higher P contents in receptacles other than tissues (Figure 3-5b) suggest a possible function of P

accumulation in reproductive tissue. Presumably, P compounds accumulated in *S. macrocarpum* during winter may be transported to the P-requiring points until maturation.

3.4.3 Growth characteristics

The maximum growth rates of *S. macrocarpum* examined through photosynthesis experiments in Study 2 were within those variations (0.002 to 0.007 day^{-1}) estimated by Study 1. Compared with a previous study (Pedersen et al. 2010), the maximum growth rates of fast-growing *Ulva lactuca* (0.196 day^{-1}) and *Ceramium rubrum* (0.136 day^{-1}) were particularly higher than those of two *Fucus* species (0.040 day^{-1}), slow-growing *Ascophyllum nodosum* (0.014 day^{-1}) and *Laminaria digitata* (0.006 day^{-1}) (Table 3-3). Hence, *S. macrocarpum* seems to be characterized as a slow-growing alga.

In study 2, the estimated growth rate (μ) of *S. macrocarpum*, defined as 67% of the highest growth rate in photosynthetic experiment, may require more than 119.5 μmol P g^{-1} DW (0.37%-DW) of critical P-tissue concentration (Q_c) (Table 3-3). Above the Q_c value (0.37%-DW), the growth rate is saturated and the amount of P is enough to be accumulated in tissues. On the other hand, when the P-tissue content is lower than the Q_c value, the P-limited growth is expected to be found. In Study 1, total P content in September 2018 during second-growth period ranged from 0.29 to 0.33%-DW, resulting in below the Q_c value (Figure 2-7). This result appears to be reflected in the aftereffects of P-limitation during summer. Conversely, maximum growth rate which was obtained on March 2018 during the first-growth period (Table 2-3) coincided with the highest total P content (ca. 0.6% DW) (Figure 2-7). This indicates the highest P-demands for

rapid growth (Figure 2-8). These physiological responses lead to the increases in P-storage capacity.

The Fv/Fm values from juvenile and mature thallus of *S. macrocarpum* examined in this study did not change between the beginning and the end of experiments in all treatments (Table 3-2). Lubsch and Timmermans (2019) investigated the long-term changes in Fv/Fm, targeted for the perennial brown algae *Saccharina latissima* and *Laminaria digitata*. Fv/Fm values in these tested algae exposed to nutrient-enriched conditions (DIN: 50 μM; DIP: 3 μM) were stable with a high levels (approximately 0.7) for more than 8 weeks. However, in case of nutrient-depleted condition (DIN: 0 μM; DIP: 0 μM), these Fv/Fm values showed the significant decrease throughout the experiment due to the gradual consumption of nutrient reserves in their tissues. Based on these results, *S. macrocarpum* cultivated in multiple nutrient-enriched conditions seems to be unaffected by nutritional stress-limitation, regardless of the life stages.

3.4.4 Storage capacity for phosphorus

In this study, P-tissue contents in *S. macrocarpum* were utilized to support the growth for 19 weeks during growth period and more than 16 weeks during maturation period. *S. macrocarpum* was comparable in the P-storage capacities to slow-growing species (Table 3-3; Pedersen et al. 2010). They have relatively low P requirements (Table 3-3), and can absolve enough *in situ* P to meet the P demands during most of the year, leading to potential adaptability to long-term oligotrophic conditions. On the other hand, for fast-growing algae, the P contents in tissue last for only 2 weeks because of high P requirements for fast growth (Table 3-3). Hence, slow-growing algae have a

competitive advantage compared to fast-growing algae in oligotrophic environments (Pedersen & Borum 1996, 1997; Pedersen et al. 2010). The availability of P-tissue contents for maturation would be slow due to slow growth (Table 2-3) and low P-requirements (Table 3-3). Therefore, the metabolism required for the formation of antheridium or oogonium in *S. macrocarpum* may be maintained in nutrient-depleted environments.

Contrary to the hypothesis in this study, the storage capacities were not dissimilar between both periods due to similar growth rates (Table 3-1). Maximum total P content of juveniles cultivated in Study 2 (Figure 3-4a) were comparable to those during the growth periods in March 2018 (Figure 2-7) reported in Study 1. The juveniles can utilize the P-tissue contents largely obtained in winter to continue to growth under P-depleted environments, leading to high P-storage capacity. The high potential to accumulate a large amount of P contents in mature thallus was clarified through two-phase experiments in Study 2. However, the total P content of naturally mature thallus exposed to P depletion over a long-term period was low (Study 1). The estimated value (more than 16 weeks) should therefore be treated with considerable caution. These findings would seem to imply that the actual availability for P-tissue contents may be different between juvenile and mature thallus even if the potential capacities for P storage are not largely different between them. Based on the results, the use of external P supplied from rainfall is further essential to enhance the reproduction and regrowth for mature thallus.

Table 3-1 Maximum growth rates of *Sargassum macrocarpum* during the growth period (March 2019) and maturation period (August 2019) (Ohtake et al. 2020c). The growth rate was estimated with the photosynthetic quotient (PQ) ratio.

Treatment	Growth period (Mar 2018)		Maturation period (Aug. 2018)	
	Medium	10-90 percentiles	Medium	10-90 percentiles
1	0.006	0.005-0.010	0.004	0.004-0.007
2	0.006	0.005-0.010	0.004	0.003-0.007
3	0.006	0.005-0.011	0.005	0.004-0.009
4	0.005	0.004-0.008	0.005	0.004-0.008
5	0.004	0.003-0.007	0.005	0.004-0.009

Table 3-2 The response of the maximum quantum yield (Fv/Fm)-at all treatments (1, 2, 3, 4, 5) in *Sargassum macrocarpum* during the growth period (March 2019) and maturation period (August 2019) (Ohtake et al. 2020c). The day 0 was the initial Fv/Fm and day 9 was the final Fv/Fm during in pre-cultivation.

Treatment	Growth period		Maturation period	
	Day 0	Day 9	Day 0	Day 9
1	0.77 ± 0.03	0.78 ± 0.01	0.76 ± 0.01	0.78 ± 0.01
2	0.74 ± 0.06	0.77 ± 0.02	0.72 ± 0.03	0.75 ± 0.01
3	0.75 ± 0.03	0.77 ± 0.01	0.76 ± 0.01	0.69 ± 0.03
4	0.75 ± 0.06	0.75 ± 0.03	0.74 ± 0.03	0.72 ± 0.03
5	0.76 ± 0.06	0.74 ± 0.02	0.76 ± 0.01	0.65 ± 0.04

Table 3-3 Calculated maximum growth rates, critical and maximum P-tissue concentrations, estimated P-requirements and storage capacity that stored P can support maximum growth in 6 species of macroalgae reported from Pedersen et al. (2010) and *S. macrocarpum* from this study (Ohtake et al. 2020c).

Species	Max. growth rate (d^{-1})	Critical P-tissue concentration (μmol P g^{-1} DW)	Max. P-tissue concentration (μmol P g^{-1} DW)	P-requirements for max. growth (μmol P g^{-1} DW d^{-1})	Storage capacity at max. growth rate (week)
Ulva lactuca [a]	0.196 ± 0.018	65.5	125 ± 20	12.8	2
Ceramium rubrum [a]	0.136 ± 0.012	142.9	186 ± 22	19.4	1
Fucus vesiculosus [a]	0.040 ± 0.006	<38.7	173 ± 7	<1.5	>10
Fucus serratus [a]	0.040 ± 0.006	71.9	161 ± 20	2.9	8
Ascophyllum nodosum [a]	0.014 ± 0.003	48.1	90 ± 9	0.7	12
Laminaria digitata [a]	0.006 ± 0.001	69.4	133	0.4	19
Sargassum macrocarpum Growth season [b]	0.005 ± 0.001	119.5	184	0.6	19
Sargassum macrocarpum Maturation season [b]	0.005 ± 0.001	<108.1	173	<0.5	>14

a: Pedersen et al. 2010; b: this study

Life stages of *Sargassum macrocarpum*

Growth period — Maturation period

Period March 2019 August 2019

1) Algal collections

were conducted in Arikawa Bay on March 2019 and August 2019

Sampling site

2) Pre-incubation in 80-L storage tank (Outdoor)

3) Pre-cultivation in an incubator

was aimed to accumulate P-tissue contents of *S. macrocarpum* under multiple-nutrient concentrations

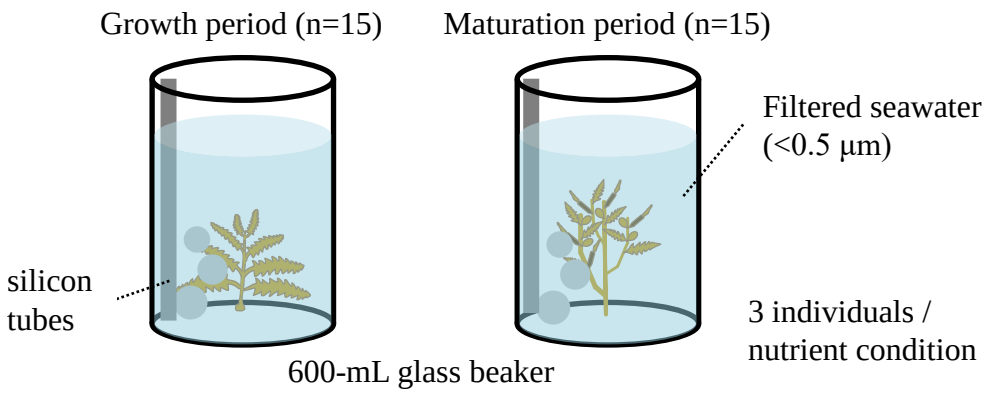

4) Incubation in an indoor seawater tank

was aimed to evaluate P-storage capacity of *S. macrocarpum* under nutrient-depleted condition.

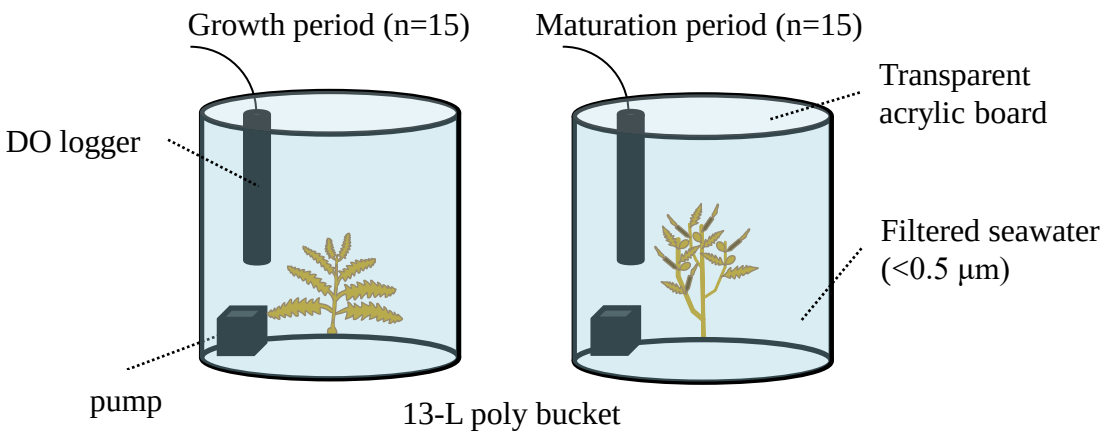

Figure 3-1 The experimental design and the procedure of Study 2.

Figure 3-2 The incubator (MLR-350HT) used in study 2. The 600 mL-glass beakers with a total volume of 500 mL of seawater enriched with $NaNO_3$, NH_4Cl and NaH_2PO_4 were set in the incubator. In all beakers, the culture media were gently supplied with air pumped through sterile silicon tubes.

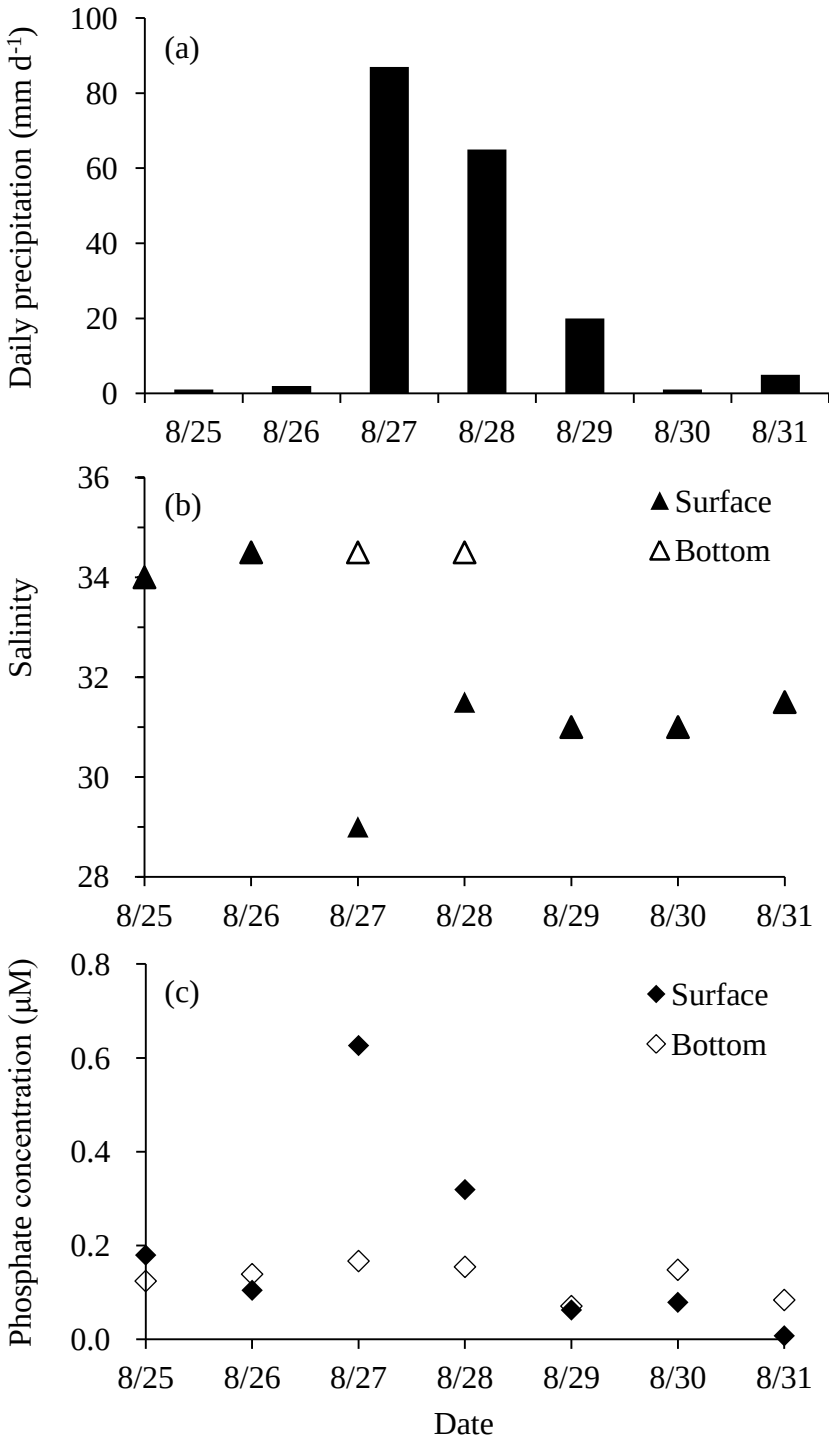

Figure 3-3 Daily changes in precipitation (a), salinity (b) and phosphate concentration (c) in Arikawa Bay during experimental period from August 25 to 31, 2019. The amount of daily precipitation (mm day^{-1}) in the Arikawa area (32˚58.9'N; 129˚07.1'E; 10 m height above sea level) during the experimental period was referred to the integrated data from Japan Meteorological Agency (http://www. jma.go.jp/jp/typh/). The samples of the salinity and phosphate concentration in Arikawa Bay were collected at the surface (black mark; 0 m depth) and the near surrounding of the *Sargassum* beds in the bottom (white mark; ca. 5 m depth).

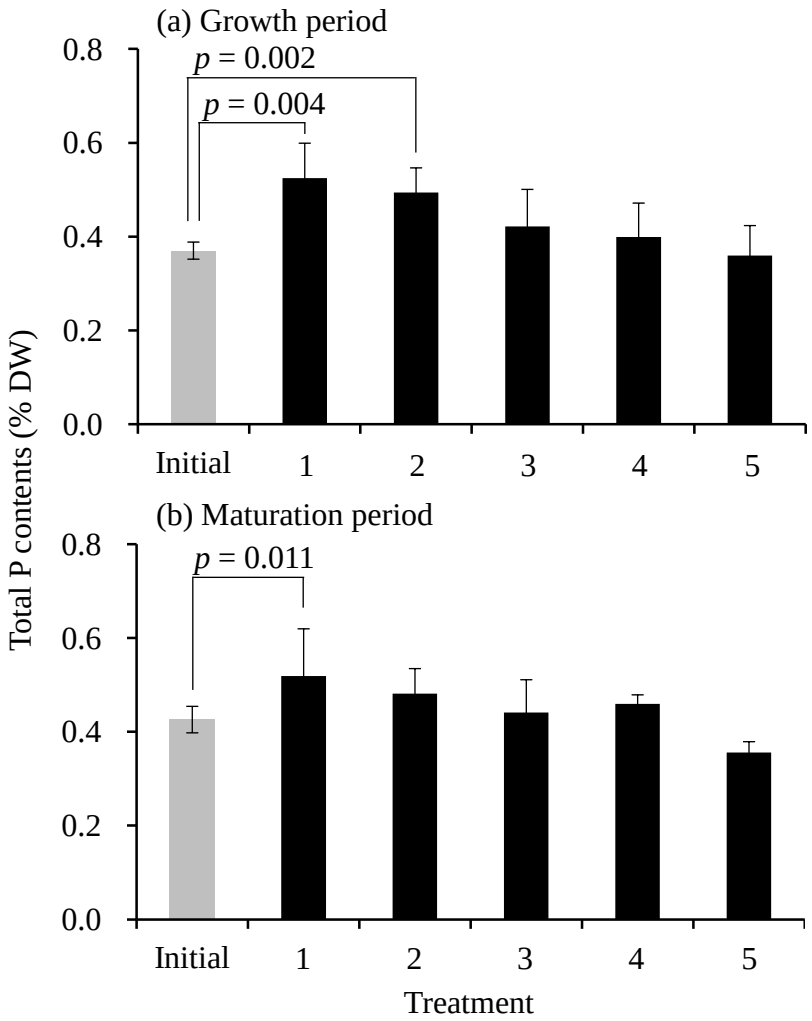

Figure 3-4 Total P content of *Sargassum macrocarpum* during the growth period (a; March 2019) and maturation period (b; August 2019) in initial and 9 days after culture in each treatment (1, 2, 3, 4, 5). Total P content is expressed as mean ± one standard deviation and the *p*-values are determined with a Dunnett's test (Ohtake et al. 2020c modified).

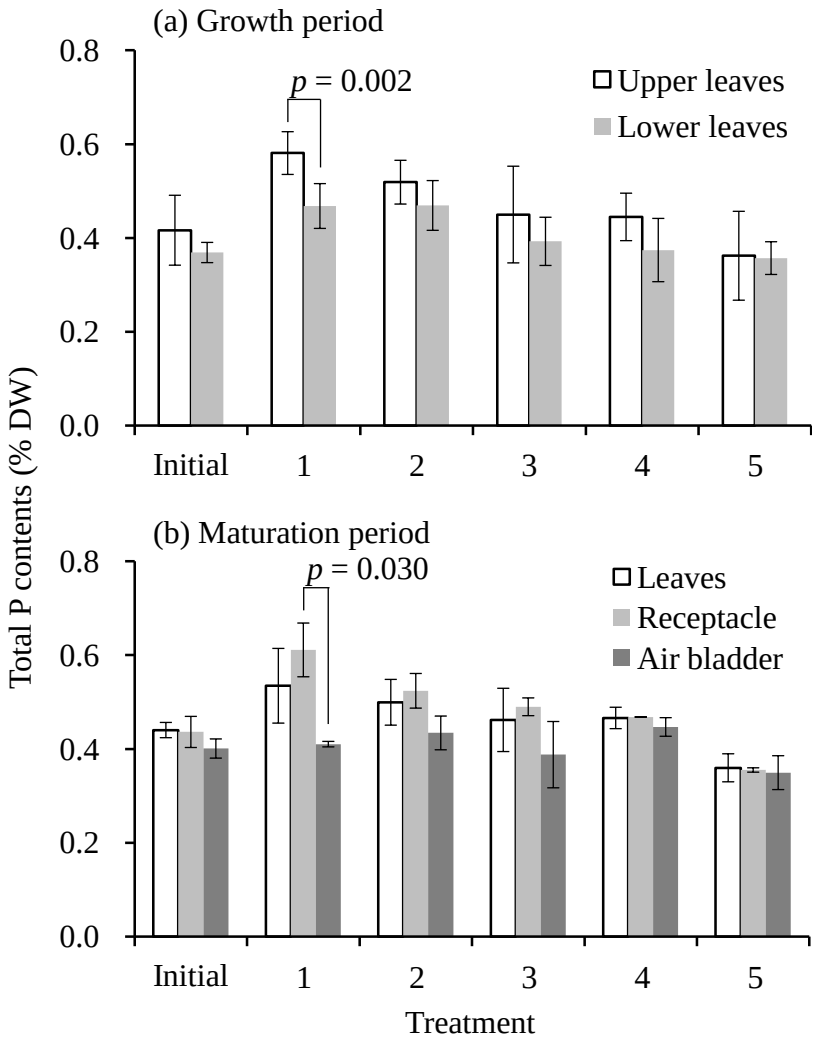

Figure 3-5 Total P contents of upper and lower leaves (a), and those of leaves, receptacle and air bladder (b) of *Sargassum macrocarpum* in initial stage and each treatment (1, 2, 3, 4, 5). Total P content is expressed as mean ± one standard deviation and the *p*-values are determined with a t-test (Ohtake et al. 2020c modified).

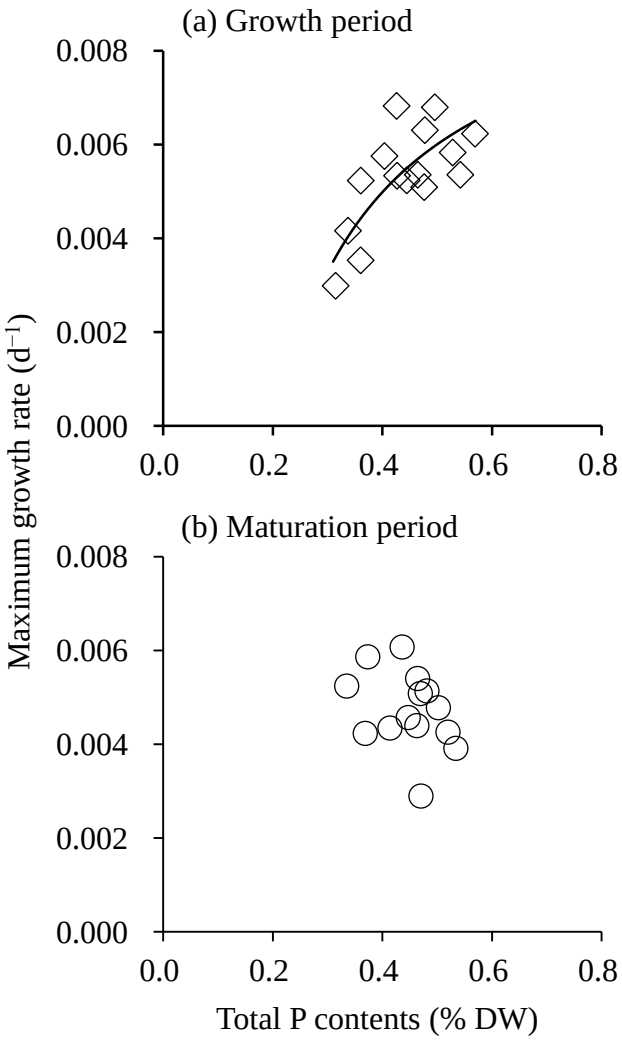

Figure 3-6 The relationships between total P contents and specific growth rate of *Sargassum macrocarpum* during the growth period (a; March 2019) and maturation period (b; August 2019). The model indicates the Droop equation (Eq. 2) (Ohtake et al. 2020c modified).

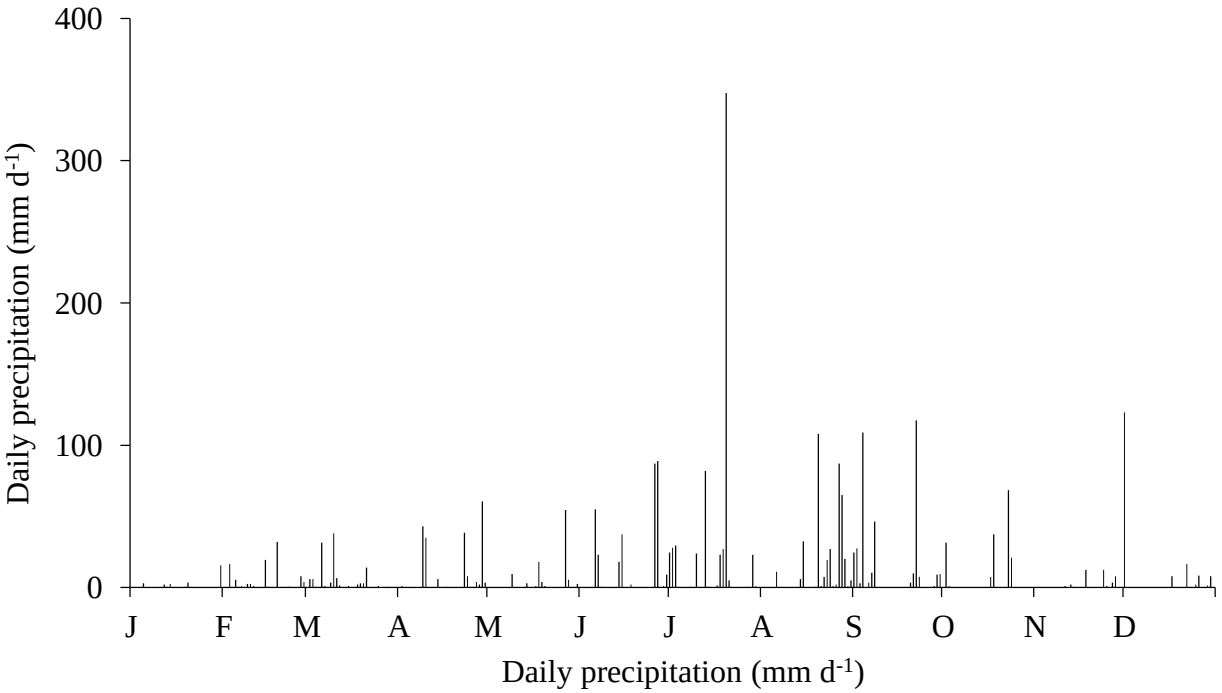

Figure 3-7 Daily change in amount of precipitation (mm day^{-1}) in the Arikawa area (32° 58.9'N; 129° 07.1'E) within 2019. The data was referred to Japan Meteorological Agency (2020).

Chapter IV

General discussion

4.1 Future prediction for nutrient environment

The anthropogenic oligotrophication of coastal regions has caused long-term changes in global- and local-scale nutrient cycles. Regionally, to eradicate the risk of eutrophication, countermeasures reducing anthropogenic P loadings from wastewater treatment have been promoted in developed counties (Conley et al. 2000; Yamamoto 2003; Howarth and Marino 2006; Nishikawa et al. 2010a). Consequently, the oligotrophication trend has been site-specifically found in coastal areas adjacent to megacities (watershed population: more than 10 million) such as Tokyo Bay (Kubo et al. 2019), Osaka Bay (Yamamoto et al. 2017) and Shenzhen Bay (Zhou et al. 2020). The phosphate concentrations in the surface waters of Tokyo Bay were frequently below detection limits (< 0.05 μM) during spring and summer after the 2000s (Kobo et al. 2019), reflecting the effect on reduced P loadings. Importantly, the incidence of P depletion will have increased effects in the coastal embayment of developed countries. In these circumstances, regime shifts from opportunistic macroalgae-dominated states to seagrass-dominated states were observed in Mediterranean lagoons, probably due to oligotrophic trajectories with the EU water framework directive (Le Fur et al. 2019). The dynamic cross-interaction between the vegetative shift to avoid loss of macrophytes (i.e., barren grounds) and oligotrophication remain to be clarified in Mediterranean lagoons. Hence, the anticipated regime shift under oligotrophication trajectories may require more long-term monitoring.

On a global scale, El Niño events in the equatorial Pacific cause

oligotrophication of surface waters, subsequently leading to macroalgal deforestation (Tegner and Dayton 1991; Paine et al. 1998) and reduced geographic distribution of kelp beds living closest to the tropics (Steneck et al. 2002). The episodic ocean warming events caused by El Niño results in developed thermohaline stratification (Sarmiento et al. 2004). In the Oyashio and Oyashio-Kuroshio transition areas located along the coastal line in north-eastern part of Japan, the trend for phosphate concentration in the surface layers and the middle layers were decreasing and increasing, respectively, which was linked to the development of stratification (Ono et al. 2001; Tadokoro et al. 2009). On the other hand, Kodama et al. (2016) revealed that an increase in phosphate concentrations of the Kuroshio and the Tsushima Warm Current was not found in any deep layers. Hence, the decrease in the P supply from the deeper layer did not constitute a major cause of P depletion in the surface layer during summer (Kodama et al. 2016). Alternatively, the horizontal advection of the oligotrophic warm current is an important factor that could reduce phosphate concentrations in the surface water (Kim et al. 2013; Kim and Kim 2013; Kodama et al. 2016). Kodama et al. (2016) reported that the declining trend for phosphate concentrations in the southern Japan Sea was quantified as 1.8–3.3 nM yr^{-1} while those for nitrate concentrations was not detected. These oligotrophic warm currents will be warmer with sea surface temperature (SST) increases (Wu et al. 2012). The warmer SST induced by global warming is strongly linked to the vertical and horizontal alterations of phosphate concentration in coastal environments.

The case of oligotrophication in Goto Islands is also related to the nutrient cycles on global- and local-scales. The oligotrophication is remarkably linked to depopulation for several decades (the population has fallen to about two-thirds from ca.

27,600 in 2000 to ca. 18,500 in 2020; National Institute of Population and Social Security Research). It appears possible that the decrease in anthropogenic nutrient loadings from land due to the decrease of the population is the cause of the local oligotrophication. According to a previous survey to clarify the terrestrial P flow in the northern Goto Islands, treated wastewater with low-P concentration is supplied to watershed drainage (Soka University 2015). Even though no data regarding the long-term variations of phosphate concentration were collected in the coastal waters, the following data may explain the oligotrophication trend. Phosphate depletion (< 0.09 μM) during summer and autumn was reported in the coastal embayment of the northern Goto Islands (Tsuchiya et al. 2018). Indeed, low P-concentrations during summer (~0.05 to 0.2 μM) were also reported in the offshore areas in the East China Sea (Chen 2009; Kim et al. 2009; Shiozaki et al. 2018). This trend may be affected by the horizontal advection of oligotrophic warm currents (e.g., the Tsushima Warm Current) to off the coast of the Goto Islands (Kodama et al. 2016). Another possible factor is the nutrient consumption by diazotrophs observed in the East China Sea (Shiozaki et al. 2018), also assumed to lead to nutrient depletion. In summary, in the coastal waters around the Goto Islands, if the SST increases in addition to the reduction of anthropogenic nutrient loadings, there is a possibility that the oligotrophication will progress further.

4.2 Adaptation strategy under long-term phosphorus limitation

The P dynamics of *S. macrocarpum* seem to vary according to life-stage (Figure 4-1). The annual variations between estimated *in situ* uptake and growth-related demands for P are implicitly related to the season (Figure 2-9). This species during

winter can accumulate external P because the P-uptake rate exceeded the P-demand (Figure 4-1). Conversely, during spring to late summer, this alga during the late growth and maturation periods utilizes P-tissue contents due to relatively high P-demand (Figure 4-1). In summary, this alga can adapt to long-term oligotrophic environment by means of the combined characteristics in both P accumulation in their tissue during winter and long-term availability of P-tissue contents from spring to summer.

The characteristics of the nutrient uptake and demand for seaweeds appear to be categorized with their species-specific growth potentials (Pedersen et al. 2010). They sampled algae annually and incubated the specimens to evaluate the seasonal variations of *in situ* P uptake rates and demands depending on seasonal environmental changes in phosphate concentration and irradiance levels, respectively. Since the P availability during early life stage potentially affects the growth and maturation of adults, the annual variations across life stages, including growth and maturation remain to be clarified. In this study, these variations of *S. macrocarpum* were estimated based on annual changes not only in environmental factors but also in physiological parameters such as phosphate uptake kinetics (i.e., V_{max} and K_m), photosynthetic-based growth rate, and total P contents. This estimation process capable of evaluating P-uptake and demand may be generalized to *Sargassum* species, which have similar physiological characteristics (i.e., functional form).

The annual variations between the uptake rate and demand were seasonally uncoupled and commonly observed between this study (Figure 2-8) and a previous study (Pedersen et al. 2010). However, from the perspective of physiological change, the method to estimate the annual variations of seaweeds was different between studies. To evaluate the accuracy in this study, a more practical approach is the comparison of

the estimated variations in the P-uptake rate and demand of *S. macrocarpum*, employing an estimation method for each study. The phosphate uptake kinetics, growth rate and total P contents obtained on July 2018 (referred to target period in Pedersen et al. 2010) were used for the comparison. As the results (Figure 2-10), the P uptake rate based only on *in situ* phosphate concentration ranged from 0.05 to 0.18 μmol P g^{-1} DW d^{-1}, and the annual average (0.08 μmol P g^{-1} DW d^{-1}) was approximately 6 times lower than those derived from this study (0.49 μmol P g^{-1} DW d^{-1}). During winter, the variation from this study was significantly higher than those from a previous study due to the V_{max}/K_m values in winter being higher than those in summer (Table 2-1). *In situ* P demand based only on PAR varied from 0.01 to 0.43 μmol P g^{-1} DW d^{-1} and the annual average (0.29 μmol P g^{-1} DW d^{-1}) derived from a previous method was relatively lower than those estimated by this study (0.39 μmol P g^{-1} DW d^{-1}) (Figure 2-10). Focusing on the P demands in March 2018 (Figure 2-10), the P demands derived from a previous study was significantly lower than those from this study due to the lack of the highest value for the growth rate and total P contents during main growth period of *S. macrocarpum*. Based on these results, the estimation process used in this study is suitable for evaluating the annual variations of P uptake rates and *in situ* demands for seaweeds, leading to an understanding of the P dynamics of seaweeds along with their life cycle.

Hypothetically, *S. macrocarpum* matures under P-depleted environment during summer by using P-tissue contents. The P contents in receptacles formed in mature thallus may be available to create reproductive tissues for more than 16 weeks (Table 3-3). However, in Study 1, P-tissue contents accumulated in winter could not support potential growth rate during spring and summer when the *in situ* P concentrations was low (i.e., March to August). Taking into account the uptake from external P, *in situ* DIP

concentrations varied from 0.1 to 0.3 μM from March to August in 2018, and were sufficient to supply 10 to 50% (averaged value: 30%) of the P demands. Consequently, the P-tissue contents were available more 1.1 to 2 times (averaged value: 1.4 times) longer when compared to the case of no uptake from *in situ* P. Thus, the storage capacity during growth period increased to approximately 27 weeks. This estimated term is approximately the same as those of P-limitation for this alga (ca. 26 weeks). Consequently, this alga could maintain growth under long-term P-limitation condition until maturation. However, the extended period of exposure to P-limitation condition results from a progressive oligotrophication, leading to that this alga will be difficult to survive in Arikawa Bay.

In summary, year-round availability of P enough to satisfy demands throughout *S. macrocarpum* life stages can be explained by the specific advantages for long-term use of P-reserves in tissue and continuous uptake of external P. Consequently, a series of studies revealed that this alga can adapt well to temporally P-depleted environment.

4.3 Phosphorus availability in short-term changes in nutrient environment

The high availability of P temporally supplied into the *in situ* environment is one of the adaptive strategies for temperate seaweeds under the oligotrophic coastal environment. The nutrient concentrations in coastal waters are often enhanced by physical disturbances such as upwelling events (e.g., Lin et al. 2003; Zheng & Tang 2007; Tsuchiya et al. 2013), terrestrial runoff (Zheng & Tang 2007; Chen et al. 2009), sediment resuspension (Fogel et al. 1999). These disturbances are induced by the passage of typhoons causing strong wind and heavy rain. Schaffelke and Klumpp (1998) examined the effect of pulse-supplied nutrient on the growth and net

photosynthesis rates of *S. baccularia* in the laboratory. Consequently, the nutrient reserves derived from substrates enable the alga to sustain enhanced growth and net photosynthesis rates for approximately 1 week. Indeed, three typhoons crossed over the Goto Islands during June to September 2018 (Japan Meteorological Agency 2018), and nutrient pulse supply was observed after the passage of a typhoon occurring in August 2018 (phosphate concentration: 0.1 to 0.3 μM increase; nitrate concentration: 0.1 to 1.2 μM increase; Nishihara et al. 2019 unpublished data). Hence, *S. macrocarpum* in Arikawa Bay may have obtained benefits from these transient pulses.

Considering that marine primary producers (e.g., micro- and macro-algae) absorb external nutrients, the following will discuss the competitive relationships in nutrient uptake characteristics among different species of macroalgae in addition to micro- and macro-algae. Since macroalgae with high-specific surface areas have a great advantage in nutrient uptake, the morphological differences reflect the variations of nutrient availability. Littler and Littler (1980) developed a theory called "functional form" where the algal morphology and internal structure are deeply related to the physiological characteristics (i.e., nutrient uptake and photosynthesis) (Littler & Arnold 1982; Littler et al. 1983). Sheet-shaped (e.g., *Ulva* sp. and *Phyropia* sp.) and filamentous-groups have a competitive advantage in nutrient uptake and photoreception because of the high-specific surface areas of their morphology. On the other hand, since Laminariales and Fucales species are categorized as a thick-leathery-group, the net photosynthesis per unit of thallus weight is relatively low. The V_{max}/K_m values for ammonium, nitrate, and phosphate in thick-leathery-groups show large anomalies, but are commonly lower than that in sheet-shaped group and filamentous-group (e.g., Haines & Wheeler 1978; Topinka 1978; Espinoza & Chapman 1983; Wallentinus 1984).

This indicates that *Ulva* sp. (i.e., sheet-shaped group) has generally advantageous characteristics for nutrient uptake under natural ambient levels of nutrient concentrations. However, *S. macrocarpum* found in Arikawa Bay do not seem to be competitive to sheet-shaped algae unbloomed in the bay for all seasons. This is because *Ulva* sp. could not meet the high nutrient requirements to sustain the rapid growth in such oligotrophic waters. Therefore, although the nutrient uptake kinetics of *Sargassum* species, composed of a thick-leathery leaves, are disadvantaged compared with those of sheet-shaped and filamentous-algae, the former can be abundant under such nutrient-depleted waters.

Indeed, bioavailable nutrients supplied by the physical disturbances in short term in Arikawa Bay might be directly used for both micro- and macro-algae. To evaluate the compatibility of nutrient uptake in both algae, it is necessary to standardize and compare their nutrient uptake characteristics. Importantly, half saturation constant (K_s) quantifies the affinity of substrate availability (Dugdale 1967). The K_s for phosphate in marine phytoplankton (e.g., *Skeletonema* sp. and *Chaetoceros* sp.) ranged from 0.7 to 133 μM with large anomalies (Nakamura 1985; Tarutani 1999; Nishikawa et al. 2009, 2010b; Yamamoto et al. 2004). The K_s variation of marine phytoplankton is approximately 10 times larger than those of seaweeds (<1 to 10 μM; e.g., Wallentinus 1984; Hurd & Dring 1990; Pedersen et al. 2010; Appendix 2). The K_m (i.e., K_s) for phosphate in *S. macrocarpum* examined in this study changed from ca. 5 to 10 μM with no seasonal trend (Table 2-1) which is an equivalent anomaly compared with the variation from various brown algae mentioned above (Appendix 2). In eutrophicated environments, high phytoplankton densities induced by high-concentrations of external nutrients lead to insufficient light availability for the growth of benthic macrophytes due

to high turbidity in the water column (e.g., Scheffer et al. 1993). However, variations of K_s values suggest that the growth of seaweeds is more suitable than those of phytoplankton under low-concentrations of nutrients. Hypothetically, phytoplankton (e.g., *Skeletonema* sp. and *Chaetoceros* sp.) with high affinity for low nutrient concentration (i.e., low K_s) grow and take up nutrients in cases which the temporal increases in an *in situ* phosphate concentration (ca. 0.2 to 0.6 μM) induced by the physical disturbances in Arikawa Bay. It is reasonable to hypothesize that the short-term nutrient supply in nutrient-depleted conditions during summer supports the maturation of seaweeds.

4.4 Abiotic factors effect on distributional change of *Sargassum macrocarpum*

This study revealed that a brown alga *S. macrocarpum* can adapt to seasonal P limitation in Arikawa Bay. Based on the results regarding the horizontal distribution of DIP concentration around the northern Goto Islands (Tsuchiya et al. 2018), seasonal depletion of P was found in the coastal waters other than Arikawa Bay. However, according to the guideline from Fisheries Department in Nagasaki Prefectural Government (2018), *Sargassum* beds predominantly composed of *S. macrocarpum* were observed only in Arikawa Bay out of the survey areas. In the barren grounds around the northern Goto Islands, the abiotic factors not involving DIP concentration that prevent the formation of *Sargassum* beds remain unclear. This dissertation describes the other factors causing the degraded seaweed beds as follows: (1) low-current velocity and (2) high-water temperature (i.e., global warming).

Seaweed beds depend on the water motion to supply the essential materials (e.g., dissolved-nutrients, oxygen, carbon) for photosynthesis and growth. The material

supply to the surface of macrophytes is regulated by the concentration boundary layer formed on the adjacent surface at the micro level (Hurd 2000), and is affected by the concentration and water flux (Nishihara & Ackerman 2006). These boundary layers become thinner (i.e., the formation of a diffusive boundary layer) as the water velocity near the surface of algal body increases, leading to increases in the amount of materials supplied to the algal body (Nishihara &Ackerman 2006). Therefore, on a micro-scale of the algal body surface, increasing the water velocity promotes not only photosynthesis but the uptake rate of nutrients for seaweeds (Wheeler 1980; Hurd et al. 1996; Larned & Atkinson 1997; Nishihara & Ackerman 2006, 2007). Furthermore, the coastal hydrodynamic environment is closely related to a variety of physiological processes in macrophytes, and plays a vital role in the formation of seaweed beds.

From April 2017 to February 2018, Nishihara et al. (unpublished data) investigated the daily mean current velocities within the *Sargassum* beds in the Arikawa Bay and barren grounds in Tainoura Bay (32°56’57’N, 129°06’45’E) (Nagasaki University 2018). As the results, In the Arikawa Bay, the monthly mean current velocities were low in summer and high in winter due to the wind-wave impacts, annually ranging from 2.0 ± 1.9 to 7.0 ± 5.0 cm s^{-1}. On the other hand, in Tainoura Bay, the annual change of the current velocities showed no trend (1.7 ± 0.6 to 2.4 ± 9.9 cm s^{-1}). Comparing the observed values between both coastal waters, the current conditions in Tainoura Bay are relatively calm, suggesting that the material supply required for the growth of seaweeds is limited. In other words, as the turbulence effect on the physiological processes is high in Arikawa Bay, the hydrodynamic condition of this embayment may be more suitable for the formation of seaweed beds.

The biogeographical distributions of algae were strongly limited by the

temperature gradient based on latitudinal variation and water current (Adey & Steneck 2001; Nishihara & Terada 2010; Fukumoto et al. 2018, 2019; Terada et al. 2018). However, global warming leads to the habitat shift of inherent seaweeds which will be poleward in the future. Therefore, the photosynthetic responses of saeweeds to temperature gradients are one of the important factors to understand the resilience to thermal changes in environment. Terada et al. (2019) reported that maximum gross photosynthetic rate of *S. macrocarpum* occurred at 27.8 °C which approximately equal the highest seawater temperature in August (28 to 29 °C) in the southern distributional limit of this alga (i.e., the southern part of Kyushu Island; Watanabe et al. 2014; Kokubu et al. 2015; Terada et al. 2018). The Fv/Fm values of this alga exposed to different temperature conditions for 72 h were stable above 0.6 from 8 to 28 °C, but sharply decreased to zero above 28 °C (Terada et al. 2019), suggesting that this alga is likely to face the deactivation of a photosystem II above 28 °C (Terada et al. 2018). Considering these results regarding the photosynthetic responses to summer temperatures, 28 °C is the critical temperature for their survival. Indeed, since the SST in the southern part of Kyushu Island (Kagoshima, Japan) has risen by approximately 1.8 °C over the last four decades, their southern limit of the distribution of this alga will be northward in the future.

According to the relationship between maximum uptake rate (V_{max}) for phosphate and temperate increase (Ohtake et al. 2020a), the V_{max} examined in *S. macrocarpum* was stable at the intermediate level under optimum temperature (e.g., 15 to 25 °C), but increased at unfavorable high temperature (e.g., 30 °C) probably caused by an increase in P demands. This result suggests that the survival of temperate seaweeds is threatened by the increased P demands if warm-season persistently

continues to be caused by global warming. Given that the habitat distribution of *S. macrocarpum* at the Arikawa Bay will be shifted northward along the Japanese coastal waters due to SST increases, the phosphate availability of this alga in new habitats needs to be clarified.

The observed data regarding monthly changes of average concentrations for phosphate were collected in Japanese coastal waters ranging from the southern Kyusyu islands to the northernmost island, Hokkaido, Japan. The ranges of phosphate concentrations in target coastal areas were summarized in Table 4-1. The variations of phosphate concentrations in all target areas changed with seasonality and that in the Arikawa Bay tended to be lower than in the others (Table 4-1). The *in situ* uptake rates of *S. macrocarpum* for phosphate in all target coastal waters were estimated based on monthly evaluated Michaelis-Menten models in this study. During winter, the estimated P-uptake rates for *S. macrocarpum* in Satsuma Peninsula in Kagoshima, Bisanseto Strait in Seto Inland Sea, Tosa Bay in Kochi, Ise Bay in Aichi, Japan Sea off Hokkaido were substantially higher than that in the Arikawa Bay (Figure 4-2). The P-uptake rates throughout all-year in other target areas such as Genkai-nada in Fukuoka and Suo-nada regions off Yamaguchi showed same levels, ranging from 0.01 to 0.39 μmol g^{-1} DW h^{-1}, compared with Arikawa Bay. This result suggests that *S. macrocarpum* is expected to not face the P limitation even if the distributional range extends northward due to global warming in the future.

Table 4.1 Summary of monthly changes in phosphate concentrations (μM) in domestic coastal areas. Each data were collected in different year.

Place	Month													
	Dec.	Jan.	Feb.	Mar.	Apr.	May	Jun.	Jul.	Aug.	Sep.	Oct.	Nov.	Dec.	Jan.
Southern coast of Satsuma Peninsula, Kagoshima [a]	-	0.21	0.84	0.33	-	0.02	0.01	-	0.28	0.21	0.84	0.33	0.87	-
Genkai-nada, Fukuoka [b]	-	0.30	0.10	-	0.10	0.10	-	0.10	-	0.10	0.10	-	0.30	-
Suo-nada regions off	-	0.13	0.07	0.04	0.03	0.04	0.06	0.13	0.08	0.18	0.20	0.21	0.20	-
Yamaguchi [c]	-	0.25	0.17	0.13	0.08	0.08	0.10	0.11	0.13	0.25	0.33	0.32	0.29	-
	-	0.16	0.07	0.08	0.04	0.08	0.06	0.12	0.15	0.34	0.39	0.23	0.18	-
Bisanseto Strait in Seto Inland Sea [d]	-	-	-	-	0.16	0.08	0.23	0.30	0.19	0.29	0.48	0.44	0.46	0.27
Tosa Bay, Kochi (surface) [e]	-	-	0.50	0.15	0.10	0.40	0.10	0.10	0.03	0.03	0.23	0.14	0.33	0.09
Tosa Bay, Kochi (bottom) [e]	-	0.24	0.65	0.20	0.24	0.34	0.01	0.04	0.10	0.03	0.29	0.14	0.14	0.29
Ise Bay, Aichi (surface) [f]	-	0.70	0.42	0.31	0.29	0.46	0.29	0.35	0.30	0.45	0.76	0.83	0.73	-
Ise Bay, Aichi (bottom) [f]	-	0.73	0.47	0.43	0.52	0.74	0.94	1.32	1.51	1.71	1.18	0.83	0.71	-
Sagami Bay, Kanagawa [g]	-	-	-	-	-	0.22	0.33	0.14	-	-	-	-	-	-
Japan Sea off Hokkaido [h]	-	-	0.40	-	0.20	-	0.10	-	0.10	-	0.10	-	0.30	-
	-	-	0.50	-	0.20	-	0.10	-	0.10	-	0.10	-	0.10	-
Arikawa Bay, Nagasaki [i]	0.37	0.20	0.12	0.13	0.11	0.25	0.17	0.12	0.11	0.10	0.09	0.18	0.25	0.21

a: Shimabukuro 2007; b: Ikeuchi et al. 1998; c: Wanishi 2007; d: Japan Fisheries Agency 2015; e: Serisawa and Ohno 1995; f: Mizuno et al. 2009; g: Fujiki et al. 2004; h: Kuribayashi 2016; i: This study

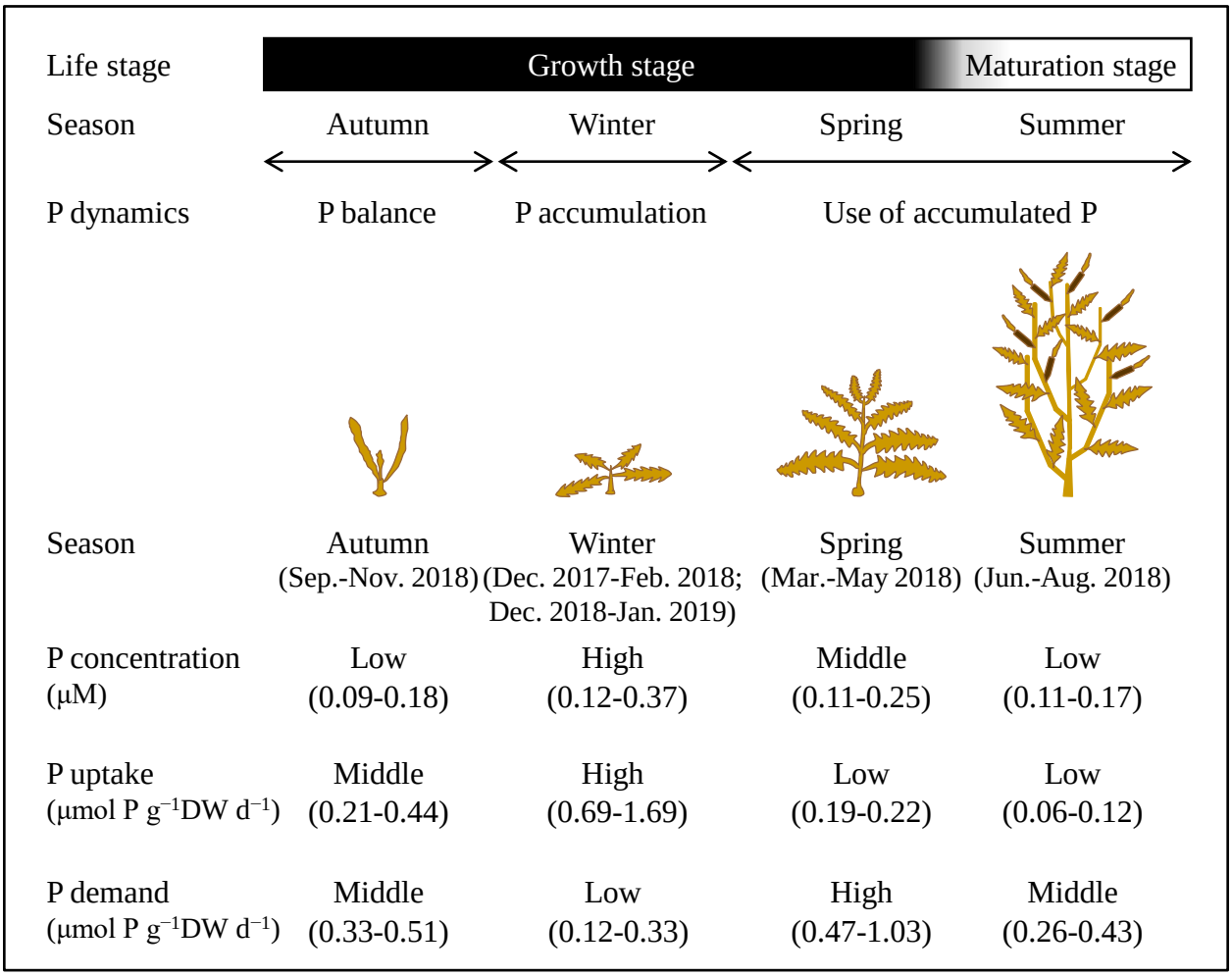

Figure 4-1 The schematic diagram of P dynamics of *Sargassum macrocarpum* during periods of growth and maturation. P concentration, P uptake and P demand are categorized into three levels such as low, middle and high based on these data in the present study and these levels were divided into each season. The P dynamics are defined as the following three types: P balance, P accumulation and availability of tissue P. The P equilibrium means that P uptake equals P demand. The P accumulation represents that P uptake exceeds P demand while the use of accumulated P is the inverse response.

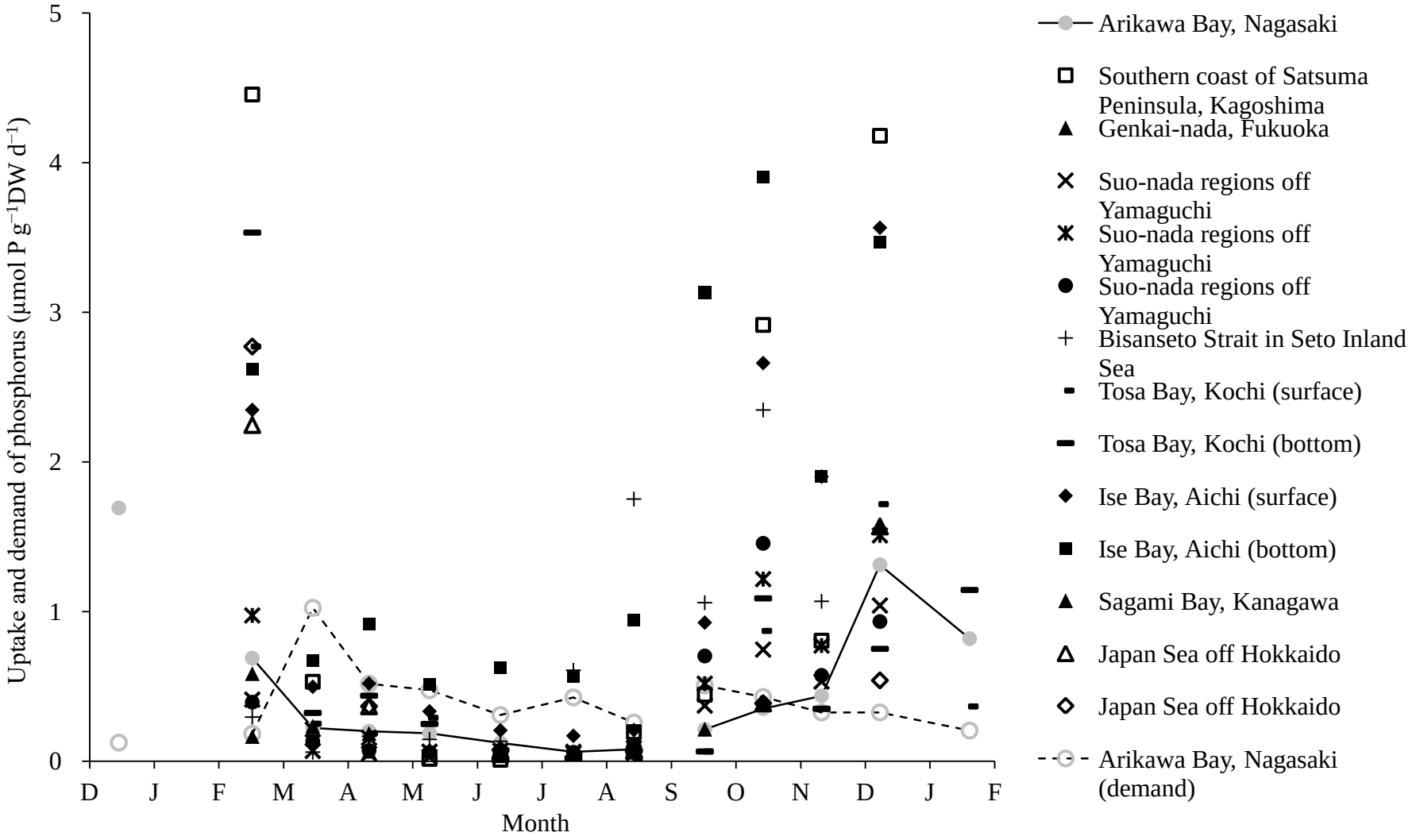

Figure 4-2 Monthly changes in estimated phosphate uptake rates of *Sargassum macrocarpum* in domestic coastal areas (various black symbols without line) and Arikawa Bay (gray circle with solid line) and those in *in-situ* demands (gray circle with dashed line) during the first-growth (December 2017 to April 2018), the maturation (May 2018 to August 2018) and the second-growth (September 2018 to January 2019) periods. The *in-situ* uptake rates in all target coastal areas were estimated based on monthly evaluated Michaelis-Menten model in this study and these phosphate concentrations. The *in-situ* demand was estimated by the *in-situ* photosynthetic rate as a result of assigning photosynthetically active radiation (PAR) to the photosynthesis-irradiance (PI) curve.

Conclusion

In Study 1, the annual variations between *in situ* uptake and growth-related demand for P examined in *S. macrocarpum* were investigated. These variations were uncoupled trends (Figure 2-8) and the P dynamics varied with season and life stage (Figure 2-9). The primary growth period of *S. macrocarpum* during autumn was a response to a balance between P-uptake rate and demand (Figure 4-1). Thereafter, P uptake exceeded P demand in late growth period during winter, indicating that sufficient external P can be accumulated in the tissue. Conversely, in maturation period during spring to late summer, this alga suffered from P-limitation, and probably utilized the P-tissue contents for growth (Figure 4-1).

In Study 2, the storage capacity of *S. macrocarpum* was evaluated as an indicator to sustain growth rate under nutrient depleted environment. The storage capacities during the growth and maturation periods were approximately 19 weeks and more than 16 weeks, respectively, suggesting that this species can endure P depletion for several months by using the P-tissue contents. During the growth period, the estimated capacity may be extended for a longer period (ca. 27 weeks) if external P uptake is considered. Additionally, the availability of P-tissue contents during maturation period may be partly supported by an effective uptake of external P supplied from rainfall. Consequently, *S. macrocarpum* is able to adapt to seasonally oligotrophic waters until the species matures. In this study, considerable progress has been gained with regard to the understanding of year-round P dynamics of the perennial brown seaweeds until maturation.

Further study needs to be performed to understand how fecundity is influenced by P-tissue content during maturation of *S. macrocarpum*. This study suggests that there

is potential for P-reserves to be accumulated in the receptacle and reproduction (e.g., release of oospores and embryos) in mature thallus, leading to a population increase and the expansion of the seaweed beds.

The annual change in concentration of intracellular polyphosphate, known as a major tissue P compound, remains to be clarified in this study. According to a previous report (Lundberg et al. 1989), the polyphosphates accumulated in the tissue of the red alga *Ceramium* sp. were detected by nuclear magnetic resonance (NMR) analysis. Hypothetically, perennial brown seaweeds may also accumulate polyphosphates into the tissue, and can utilize it to sustain growth under P-depleted condition. In the present study, since the number of individuals collected for the experiment was limited by the authority of local fisheries cooperatives, only the total P-tissue contents of *S. macrocarpum* was examined in Study 1 and 2. Further analysis regarding the seasonal variation of polyphosphate contents can help to promote a better understanding of the long-term change of internal P dynamics in seaweeds.

References

Adey WH and Steneck RS (2001) Thermogeography over time creates biogeographic regions: a temperature/space/time-integrated model and an abundance-weighted test for benthic marine algae. *J Phycol* **37**: 677–698

Andersen JH, Carstensen J, Conley DJ, Dromph K, et al. (2017) Long-term temporal and spatial trends in eutrophication status of the Baltic Sea. *Biol Rev* **92**(1): 135–149

Asanuma I, Zhang XG, Zhao C, Huang B and Hasegawa D (2014) Nutrients distribution in the coastal water of East Asia relative to the Kuroshio. *Landsc Ecol Eng* **10**(1): 191–199

Birch PB, Gordon DM and McComb AJ (1981) Nitrogen and Phosphorus Nutrition of *Cladophora* in the Peel-Harvey Estuarine System, Western Australia. *Bot Mar* **24**(7): 381–387

Braga ADC and Yoneshigue-Valentine Y (1996) Nitrogen and phosphorus uptake by the Brazilian kelp *Laminaria abyssalis* (Phaeophyta) in culture. *Hydrobiologia* **326**(1): 445–450

Bricker S, Longstaff B, Dennison W, Jones A, et al. (2008) Effects of Nutrient Enrichment in the Nation's Estuaries: A Decade of Change. *Harmful Algae* **8**: 21–32

Bell P (1992) Eutrophication and coral reefs—some examples in the Great Barrier Reef lagoon. *Water Res* **26**(5): 553–568

Burson A, Stomp M, Akil L, Brussaard CPD and Huisman J (2016) Unbalanced reduction of nutrient loads has created an offshore gradient from phosphorus to nitrogen limitation in the North Sea. *Limnol Oceanogr* **61**(3): 869–888

Cardoso PG, Pardal MA, Lillebø AI, Ferreira SM, Raffaelli D and Marques JC (2004)

Dynamic changes in seagrass assemblages under eutrophication and implications for recovery. *J Exp Mar Biol Ecol* **302**(2): 233–248

Cembella A, Antia NJ and Harrison PJ (1984) The utilization of inorganic and organic phosphorus compounds as nutrients by eukaryotic microalgae: a multidisciplinary perspective. *CRC Crit Rev Microbiol* **10**: 317–391

Chai C, Yu Z, Shen Z, Song X, Cao X and Yao Y (2009) Nutrient characteristics in the Yangtze River Estuary and the adjacent East China Sea before and after impoundment of the Three Gorges Dam. *Sci Total Environ* **407**: 4687–4695

Chen YL, Chen H, Jan S and Tuo SH (2009) Phytoplankton productivity enhancement and assemblage change in the upstream Kuroshio after typhoons. *Mar Ecol Prog Ser* **385**: 111–126

Cho SM, Lee SM, Ko YD, Mattio L and Boo SM (2012) Molecular systematic reassessment of *Sargassum* (Fucales, Phaeophyceae) in Korea using four gene regions. *Bot Mar* **55**(5): 473–484

Chopin T, Hourmant A, Floc'h J-Y and Penot M (1990) Seasonal variations of growth in the red alga *Chondrus crispus* on the Atlantic French coasts. II. Relations with phosphorus concentration in seawater and internal phosphorylated fractions. *Can J Botany* **68**(3): 512–517

Christie H, Norderhaug KM and Fredriksen S (2009) Macrophytes as habitat for fauna. *Mar Ecol Prog Ser* **396**: 221–233

Cloern JE (2001) Our evolving conceptual model of the coastal eutrophication problem. *Mar Ecol Prog Ser* **210**: 223−253

Conley DJ, Kaas H, Møhlenberg F, Rasmussen B and Windolf J (2000) Characteristics of Danish Estuaries. *Estuaries* **23**(6): 820–837

Dayton PK, MJ Tengner, PE Parnell and PB Edwards (1992) Tempral and spatial patterns of disturbance and recovery in a kelp forest community. *Ecol Monogr* **62**(3): 421–445

de Jonge VN, Elliott M and Orive E (2002) Causes, historical development, effects and future challenges of a common environmental problem: eutrophication. In Nutrients and eutrophication in estuaries and coastal waters. Springer, Dordrecht, pp. 1−19

Díez I, Muguerza N, Santolaria A, Ganzedo U and Gorostiaga JM (2012) Seaweed assemblage changes in the eastern Cantabrian Sea and their potential relationship to climate change. *Estuar coast shelf S* **99**: 108–120

Douglas EJ, Haggitt TR and Rees TAV (2014) Supply- and demand-driven phosphate uptake and tissue phosphorus in temperate seaweeds. Aquat Biol **23**(1): 49–60

Dugdale RC (1967) Nutrient limitation in the sea: dynamics, identification and significance. *Limnol Oceanogr* **12**: 685–695

Dunlop J, Phung HT, Meeking R and White DWR (1997) The kinetics associated with phosphate absorption by *Arabidopsis* and its regulation by phosphorus status. *Funct Plant Biol* **24**(5): 623–629

Dwight RH, Semenza JC, Baker DB and Olson BH (2002) Association of urban runoff with coastal water quality in Orange County, California. *Water Environ Res* **74**(1): 82–90

Edwards MS and Estes JA (2006) Catastrophe, recovery and range limitation in NE Pacific kelp forests: a large-scale perspective. *Mar Ecol Prog Ser* **320**: 79–87

Elser JJ, Sterner RW, Gorokhova EA, Fagan WF, et al. (2000) Biological stoichiometry from genes to ecosystems. *Ecol lett* **3**(6): 540–550

Endo H, Nishigaki T, Yamamoto K and Takeno K (2013a) Ageand size-based

morphological comparison between the brown alga *Sargassum macrocarpum* (Heterokonta; Fucales) from different depths at an exposed coast in northern Kyoto, Japan. *J Appl Phycol* **25**: 1815–1822

Endo H, Suehiro K, Kinoshita J, Gao X and Agatsuma Y (2013b) Combined effects of temperature and nutrient availability on growth and phlorotannin concentration of the brown alga *Sargassum patens* (Fucales; Phaeophyceae). *Am J Bot* **4**(12): 14–20

Espinoza J and Chapman ARO (1983) Ecotypic differentiation of *Laminaria longicruris* in relation to seawater nitrate concentration. *Mar Biol* **74**(2): 213–218

Fernández PA, Roleda MY, Leal PP and Hurd CL (2017a) Seawater pH, and not inorganic nitrogen source, affects pH at the blade surface of *Macrocystis pyrifera*: implications for responses of the giant kelp to future oceanic conditions. *Physiol Plantarum* **159**(1): 107–119

Fernández PA, Roleda MY, Leal PP, Hepburn CD and Hurd CL (2017b) Tissue nitrogen status does not alter the physiological responses of *Macrocystis pyrifera* to ocean acidification. *Mar Biol* **164**(9): 177

Fisheries Department in Nagasaki Prefectural Government (2018) Guidelines concerning the technical countermeasures for barren grounds in Nagasaki prefecture (In Japanese: 長崎県における磯焼け対策ガイドライン, 平成 30 年度改訂版)

Fogel ML, Aguilar C, Cuhel R, Hollander DJ, et al. (1999) Biological and isotopic changes in coastal waters induced by Hurricane Gordon. *Limnol Oceanogr* **44**(6): 1359–1369

Fujiki T, Toda T, Kikuchi T, Aono H and Taguchi S (2004) Phosphorus limitation of primary productivity during the spring-summer blooms in Sagami Bay, Japan. *Mar Ecol Prog Ser* **283**: 29–38

Fujimoto M, Nishihara GN and Terada R (2014) The effect of irradiance and temperature on the photosynthesis of two agarophytes *Gelidium elegans* and *Pterocladiella tenuis* (Gelidiales) from Kagoshima, Japan. *Fisheries Sci* **80**(4): 695–703

Fukumoto R, Borlongan IA, Nishihara GN, Endo H and Terada R (2018) The photosynthetic responses to PAR and temperature including chilling-light stress on the heteromorphic life istory stages of a brown alga, *Cladosiphon okamuranus* (Chordariaceae) from Ryukyu Islands, Japan. *Phycol Res* **66**: 209–217

Fukumoto R, Borlongan IA, Nishihara GN, Endo H and Terada R (2019) Effect of photosynthetically active radiation and temperature on the photosynthesis of two heteromorphic life history stages of a temperate edible brown alga, *Cladosiphon umezakii* (Chordariaceae, Ectocarpales), from Japan. *J Appl Phycol* **31**: 1259–1270

Gao K (1991) Comparative photosynthetic capacities of different parts of *Sargassum horneri* (Phaeophyta). *Jpn J Phycol* **39**: 245–252

Gao K and Umezaki I (1988) Comparative photosynthetic capacities of the leaves of upper and lower parts of *Sargassum* plants. *Bot Mar* **31**(3): 231–236

García-Pintado J, Martínez-Mena M, Barberá GG, Albaladejo J and Castillo VM (2007) Anthropogenic nutrient sources and loads from a Mediterranean catchment into a coastal lagoon: Mar Menor, Spain. *Sci Total Environ* **373**(1): 220–239

Gong GC, Chang J, Chiang KP, Hsiung TM, et al. (2006) Reduction of primary production and changing of nutrient ratio in the East China Sea: Effect of the Three Gorges Dam? *Geophys Res Lett* **33**: L07610

Gordillo FJL, Dring MJ and Savidge G (2002) Nitrate and phosphate uptake characteristics of three species of brown algae cultured at low salinity. *Mar Ecol Prog Ser* **234**: 111–118

Gordon DM, Birch PB and McComb AJ (1981) Effects of inorganic phosphorus and nitrogen on the growth of an estuarine *Cladophora* in Culture. *Bot Mar* **24**(2): 93–106

Gouvêa LP, Assis J, Gurgel CF, Serrão EA, et al. (2020) Golden carbon of *Sargassum* forests revealed as an opportunity for climate change mitigation. *Sci Total Environ* **729**: 138745

Govers LL, Lamers LP, Bouma TJ, de Brouwer JH and van Katwijk MM (2014) Eutrophication threatens Caribbean seagrasses–An example from Curaçao and Bonaire. *Mar Pollut Bull* **89**(1-2): 481–486

Graham MH (2004) Effects of local deforestation on the diversity and structure of southern California giant kelp forest food webs. *Ecosystems* **7**(4): 341–357

Grizzetti B, Bouraoui, F and Aloe A (2012) Changes of nitrogen and phosphorus loads to European seas. *Global Change Biol* **18**(2): 769–782

Gubelit Y, Polyak Y, Dembska G, Pazikowska-Sapota G, et al. (2016) Nutrient and metal pollution of the eastern Gulf of Finland coastline: sediments, macroalgae, microbiota. *Sci Total Environ* **550**: 806–819

Haines KC and Wheeler PA (1978) Ammoniun and nitrate uptake by the marine macrophytes *Hypnea musvuformis* (rhodophyta) and *Macrocystis pyrifera* (phaeophyta). *J Phycol* **14**(3): 319–324

Hale RL, Grimm NB, Vörösmarty CJ and Fekete B (2015) Nitrogen and phosphorus fluxes from watersheds of the northeast US from 1930 to 2000: role of anthropogenic nutrient inputs, infrastructure, and runoff. *Global Biogeochem Cy* **29**(3): 341–356

Hanisak MD (1979) Nitrogen limitation of *Codium fragile* ssp. tomentosoides as determined by tissue analysis. *Mar Biol* **50**(4): 333–337

Hanisak MD (1990) The use of *Gracilaria tikvahiae* (Gracilariales, Rhodophyta) as a

model system to understand the nitrogen nutrition of cultured seaweeds. *Hydrobiologia* **204**(1): 79–87

Harrison PJ and Hurd CL (2001) Nutrient physiology of seaweeds: application of concepts to aquaculture. *Cah Biol Mar* **42**(1–2): 71–82

Healy FP (1980) Slope of the Monod equation as an indicator of advantage in nutrient competition. *Microb Ecol* **5**(4): 281–286

Hennessey TM (1994) Governance and adaptive management for estuarine ecosystems: the case of Chesapeake Bay. *Coast Manag* **22**(2): 119–145

Howarth RW and Marino R (2006) Nitrogen is the limiting nutrient for eutrophication in coastal marine ecosystems: evolving views over three decades. *Limnol Oceanogr* **51**(1 part 2): 364–376

Hurd CL (2000) Water motion, marine macroalgal physiology, and production. *J Phycol* **36**: 453–472

Hurd CL (2017) Shaken and stirred: the fundamental role of water motion in resource acquisition and seaweed productivity. *Pers Phycol* **4**(2): 73–81

Hurd CL and Dring MJ (1990) Phosphate uptake by intertidal algae in relation to zonation and season. *Mar Biol* **107**(2): 281–289

Hurd CL, Harrison PJ and Druehl LD (1996) Effect of seawater velocity on inorganic nitrogen uptake by morphologically distinct forms of *Macrocystis integrifolia* from wave-sheltered and exposed sites. *Mar Biol* **126**: 205–214

Ikeuchi J, Kamizono M and Sugino K (1998) Distributions of nutrient and plankton in the Genkai-nada and the Eastern Tsushima Channel. *Agriculture, Forestry and Fisheries Research Information Technology Center (AFFRIT)* **8**: 97–106

Inoue Y, Osaki K, Terada R and Nishihara GN (2020) Effects of seaweed deformation

on photosynthesis rate and nutrient uptake rate. *Jpn J Phycol (Sôrui)* **68**: 1–8

Japan Fisheries Agency (2015) [cited on 20 May 2020]. Available from: https://www.jfa.maff.go.jp/j/koho/pr/pamph/attach/pdf/index-6.pdf

Japan Meteorological Agency (2018) Meteorological Data Acquisition System (AMeDAS). [cited on 28 May 2019]. Available from: http://www.jma.go.jp/.

Japan Meteorological Agency (2019) Publications/Periodicals. [cited on 23 March 2020]. Available from: https://www.jma.go.jp/jma/menu/menureport.html.

Jassby AD and Platt T (1976) Mathematical formulation of the relationship between photosynthesis and light for phytoplankton. *Limnol Oceanogr* **21**(4): 540–547

Jiang Z, Liu J, Chen J, Chen Q, et al. (2014) Responses of summer phytoplankton community to drastic environmental changes in the Changjiang (Yangtze River) estuary during the past 50 years. *Water Res* **54**: 1–11

Kfippers U. and Kremer BP (1978) Longitudinal profiles of carbon dioxide fixation capacities in marine macroalgae. *Plant Physiol* **62**(1): 49−53

Kim DS, Choi H, Kim KH, Sim J, et al. (2009) Spatial and temporal variations in nutrient and chlorophyll-a concentrations in the northern East China Sea surrounding Cheju Island. *Cont Shelf Res* **29**(11–12): 1426–1436

Kim SK, Chang KI, Kim B and Cho YK (2013) Contribution of ocean current to the increase in N abundance in the Northwestern Pacific marginal seas. *Geophys Res Lett* **40**(1): 143–148

Kim TH and Kim G (2013) Changes in seawater N:P ratios in the northwestern Pacific Ocean in response to increasing atmospheric N deposition: Results from the East (Japan) Sea. *Limnol Oceanogr* **58**(6): 1907–1914

Kodama T, Igeta Y, Kuga M and Abe S (2016) Long-term decrease in phosphate

concentrations in the surface layer of the southern Japan Sea. *J Geophys Res Oceans* **121**(10): 7845–7856

Kokubu S, Nishihara GN, Watanabe Y, Tsuchiya Y, et al. (2015) The effect of irradiance and temperature on the photosynthesis of a native brown alga, *Sargassum fusiforme* (Fucales) from Kagoshima, Japan. *Phycologia* **54**(3): 235–247

Kremer BP (1981) Aspects of carbon metabolism in marine macroalgae. *Oceanogr Mar Biol Annu Rev* **19**: 41–94

Kronvang B, Jeppesena E, Daniel J, Conley DJ, et al. (2005) Nutrient pressures and ecological responses to nutrient loading reductions in Danish streams, lakes and coastal waters. *J Hydrol* **304**(1–4): 274–288

Kubo A, Hashihama F, Kanda J, Horimoto-Miyazaki N and Ishimaru T (2019) Long-term variability of nutrient and dissolved organic matter concentrations in Tokyo Bay between 1989 and 2015. *Limnol Oceanog* **64**(S1): S209–S222

Kumura T, Yasui H and Mizuta H (2006) Nutrient requirement for zoospore formation in two alariaceous plants *Undaria pinnatifida* (Harvey) Suringar and *Alaria crassifolia* Kjell- man (Phaeophyceae: Laminariales). *Fish Sci* **72**(4): 860−869

Kuribayashi T (2016) Historical evaluation of nutrient supply characteristics of the Japan Sea off Hokkaido with the hydrographic monitoring and δ15N records in paleo-*Saccharina* specimens. Doctoral thesis, Hokkaido University. 12490

Lapointe BE (1986) Phosphorus-limited photosynthesis and growth of *Sargassum natans* and *Sargassum fluitans* (Phaeophyceae) in the western North Atlantic. *Deep Sea Res* Part A **33**(3): 391–399

Larned ST and Atkinson MJ (1997) Effects of water velocity on NH_4 and PO_4 uptake and nutrient-limited growth in the macroalga *Dictyosphaeria cavernosa*. *Mar Ecol Prog*

Ser **157**: 295–302

Le Fur I, De Wit R, Plus M, Oheix J, et al. (2018) Submerged benthic macrophytes in Mediterranean lagoons: distribution patterns in relation to water chemistry and depth. *Hydrobiologia* **808**(1): 175−200

Le Fur I, De Wit R, Plus M, Oheix J, et al. (2019) Re-oligotrophication trajectories of macrophyte assemblages in Mediterranean coastal lagoons based on 17-year time-series. *Mar Ecol Prog Ser* **608**: 13–32

Lee RB and Ratcliffe RG (1983) Phosphorus nutrition and the intracellular distribution of inorganic phosphate in pea root tips: A Quantitative Study using 31 P-NMR. *J Exp Bot* **34**(9): 1222–1244

Leruste A, Malet N, Munaron D, Derolez V, et al. (2016) First steps of ecological restoration in Mediterranean lagoons: shifts in phytoplankton communities. *Estuar Coast Shelf S* **180**: 190−203

Lefcheck JS, Orth RJ, Dennison WC, Wilcox DJ, et al. (2018) Long-term nutrient reductions lead to the unprecedented recovery of a temperate coastal region. *Proc Natl Acad Sci USA* **115**(14): 3658−3662

Li RH, Liu SM, Li YW, Zhang GL, et al. (2014) Nutrient dynamics in tropical rivers, lagoons, and coastal ecosystems of eastern Hainan Island, South China Sea. *Biogeosciences* **11**(2): 481–506

Liu SM, Zhang J, Chen HT and Zhang GS (2005) Factors influencing nutrient dynamics in the eutrophic Jiaozhou Bay, North, China. *Prog Oceanogr* **66**(1): 66–85

Liu SM, Hong GH, Zhang J, Ye XW and Jiang XL (2009) Nutrient budgets for large Chinese estuaries. *Biogeosciences* **6**(10): 2245–2263

Liu SM, Li LW, Zhang GL, Liu Z, et al. (2012) Impacts of human activities on nutrient

transports in the Huanghe (Yellow River) estuary. *J Hydrol* **430**: 103–110

Li T, Sun G, Yang C, Liang K, et al. (2018) Using self-organizing map for coastal water quality classification: towards a better understanding of patterns and processes. *Sci Total Environ* **628**: 1446–1459

Lin I, Liu WT, Wu CC, Wong GTF, et al. (2003) New evidence for enhanced ocean primary production triggered by tropical cyclone. *Geophys Res Lett* **30**(13): 51-1–4

Littler MM and Littler DS (1980) The evolution of thallus form and survival strategies in benthic marine macroalgae: field and laboratory tests of a functional form model. *Am Nat* **116**(1): 25–44

Littler MM and Arnold KE (1982) Primary productivity of marine macroalgal functional – form groups from southwestern north America. *J Phycol* **18**(3): 307−311

Littler MM, Littler DS and Taylor PR (1983) Evolutionary strategies in a tropical barrier reef system: functional-form groups of marine macroalgae. *J Phycol* **19**(2): 229−237

Lloret J and Marín A (2009) The role of benthic macrophytes and their associated macroinvertebrate community in coastal lagoon resistance to eutrophication. *Mar Pollut Bull* **58**(12): 1827−1834

Lubsch A and Timmermans KR (2019) Uptake kinetics and storage capacity of dissolved inorganic phosphorus and corresponding dissolved inorganic nitrate uptake in *Saccharina latissima* and *Laminaria digitata* (Phaeophyceae). *J phycol* **55**(3): 637–650

Lundberg P, Weich RG, Jensén P and Vogel HJ (1989) Phosphorus-31 and Nitrogen-14 NMR studies of the uptake of phosphorus and nitrogen compounds in the marine macroalgae *Ulva lactuca*. *Plant Physiol* **89**(4): 1380–1387

Manley SL (1985) Phosphate uptake by blades of *Macrocystis pyrifera* (Phaeophyta). *Bot Mar* **28**(6): 237–244

Matsuda O and Kokubu H (2016) Recent coastal environmental management based on new concept of Satoumi which promotes land-ocean interaction: A case study in Japan. *Estuar Coast Shelf S* **183**: 179–186

Mercado JM, Avilés A, Benítez E, et al. (2003) Photosynthetic production of *Ulva rotundata* Bliding estimated by oxygen and inorganic carbon exchange measurements in the field. *Bot Mar* **46**(4): 342–349

Mizuno T, Maruyama T and Higano J (2009) Transition and Prospect of Asari clam (*Ruditapes philippinarum*) Fisheries in Ise Bay, Mie Prefecture. *Bull Mie Oref Fish Res Inst* **17**: 1–21

Mizuta H, Maita Y and Kuwada K (1994) Nitrogen recycling mechanism within the thallus of *Laminaria japonica* (Phaeophyceae) under the nitrogen limitation. *Fisheries Sci* **60**(6): 763–767

Mizuta H, Ogawa S and Yasui H (2003) Phosphorus requirement of the sporophyte of *Laminaria japonica* (Phaeophyceae). *Aquat Bot* **76**(2): 117–126

Morais P, Chícharo MA and Chícharo L (2009) Changes in a temperate estuary during the filling of the biggest European dam. *Sci Total Environ* **407**(7): 2245–2259

Murase N and Kito H (1998) Growth and maturation of *Sargassum macrocarpum* C. Agardh in Fukawa Bay, the Sea of Japan. *Fisheries Sci* **64**(3): 393–396

Murase N, Kito H, Mizukami Y and Maegawa M (2000a) Productivity of *Sargassum macrocarpum* (Fucales, Phaeophyta) population in Fukawa Bay, Sea of Japan. *Fisheries Sci* **66**(2): 270–277

Murase N, Kito H, Mizukami Y and Maegawa M (2000b) Relationship between critical photon irradiance for growth and daily compensation point of juvenile *Sargassum macrocarpum*. *Fisheries Sci* **66**(6): 1032–1038

Murase N (2001) Ecological study of *Sargassum macrocarpum* C. Agardh (Fucales, Phaeophyta). *J Nat Fish Univ* **49**: 131–212

Nabata S, Takiya A and Tada M (2003) On the decreased production of natural kelp, *Laminaria ochotensis* in Rishiri Island, Northern Hokkaido. *Sci Rep Hokkaido Fish Res Inst* **64**: 127–136

Nagasaki University (2018) Reports on commissioned research work for verification experiment aimed at restoring barren grounds (in Japanese: 平成 30 年度　新上五島町磯焼け対策実証実験　委託業務報告書)

Nakamura Y (1985) Kinetics of nitrogen- or phosphorus-limited growth and effects of growth conditions on nutrient uptake in *Chattonella antique*. *J Oceanogr Soc Jpn* **41**: 381–387

National Institute of Population and Social Security Research [cited on 18 May 2020]. Available from: http://www.ipss.go.jp/

Niel FX (1976) C:N ratio in some marine macrophytes and its possible ecological significance. *Bot Mar* **19**(6): 347−350

Nimura K, Mizuta H and Yamamoto H (2002) Critical contents of nitrogen and phosphorus for sorus formation in four *Laminaria* species. *Bot Mar* **45**(2): 184−188

Nishihara GN and Ackerman JD (2006) The effect of hydrodynamics on the mass transfer of dissolved inorganic carbon to the freshwater macrophyte *Vallisneria americana*. *Limnol Oceanogr* **51**: 2734–2745

Nishihara GN and Ackerman JD (2007) The interaction of CO_2 concentration and spatial location on O_2 flux and mass transport in the freshwater macrophytes *Vallisneria spiralis* and *V. americana*. *J Exp Biol* **210**: 522–532

Nishihara GN, Terada R and Noro T (2005) Effect of temperature and irradiance on the

uptake of ammonium and nitrate by *Laurencia brongniartii* (Rhodophyta, Ceramiales). *J Appl Phycol* **17**(5): 371–377

Nishihara GN and Terada R (2010) Species richness of marine macrophytes is correlated to a wave exposure gradient. *Phycol Res* **58**(4): 280–292

Nishikawa T, Tarutani K and Yamamoto T (2009) Nitrate and phosphate uptake kinetics of the harmful diatom *Eucampia zodiacus* Ehrenberg, a causative organism in the bleaching of aquacultured *Porphyra thalli*. *Harmful Algae* **8**: 513–517

Nishikawa T, Hori Y, Nagai S, Miyahara K, et al. (2010a) Nutrient and phytoplankton dymamics in Harima-Nada, eastern Seto Inland Sea, Japan during a 35 year period from 1973 to 2007. *Estuar Coast* **33**(2): 417−427

Nishikawa T, Tarutani K and Yamamoto T (2010b) Nitrate and phosphate uptake kinetics of the harmful diatom *Coscinodiscus wailesii*, a causative organism in the bleaching of aquacultured *Porphyra thalli*. *Harmful Algae* **9**: 563–567

Ohtake M, Natori N, Sugai Y, Tsuchiya K, et al. (2020a) Growth and nutrient uptake characteristics of *Sargassum macrocarpum* cultivated with phosphorus-replete wastewater. *Aquat Bot* **163**: 103208

Ohtake M, Nishihara GN, Inoue Y, Tsuchiya K and Toda T (2020b) Phosphorus demand and uptake during growth and maturation of the brown alga *Sargassum macrocarpum*. *Phycol Res* https://doi.org/10.1111/pre.12430.

Ohtake M, Kurita R, Tsunogai M, Nishihara GN and Toda T (2020c) Storage capacity for phosphorus during growth and maturation in a brown alga *Sargassum macrocarpum*. *Sci Total Environ* **750**(1): 141221

Onishi M and Ohtani K (1997) Volume transport of the Tsushima warm current, west of Tsugaru Strait bifurcation area. *J Oceanogr* **53**(1): 27–34

Ono T, Midorikawa T, Watanabe YW, Tadokoro K and Saino T (2001) Temporal increases of phosphate and apparent oxygen utilization in the subsurface waters of western subarctic Pacific from 1968 to 1998. *Geophys Res Lett* **28**(17): 3285–3288

Ozaki A, Mizuta H and Yamamoto H (2001) Physiological differences between the nutrient uptakes of *Kjellmaniella crassifolia* and *Laminaria japonica* (Phaeophyceae). *Fish Sci* **67**(3): 415–419

Paine RT, Tegner MJ and Johnson EA (1998) Compounded perturbations yield ecological surprises. *Ecosystems* **1**(6): 535–545

Parsons TR (2013) A manual of chemical & biological methods for seawater analysis. in *Determination of Phosphate*. (Eds) Parsons TR, Maita Y and Lalli CM. Pergamon Press. Oxford. pp. 22–25

Pasqualini V, Derolez V, Garrido M and Orsoni V (2017) Spatiotemporal dynamics of submerged macrophyte status and watershed exploitation in a Mediterranean coastal lagoon: understanding critical factors in ecosystem degradation and restoration. *Ecol Eng* **102**: 1−14

Pedersen MF and Borum J (1996) Nutrient control of algal growth in estuarine waters. Nutrient limitation and the importance of nitrogen requirements and nitrogen storage among phytoplankton and species of macroalgae. *Mar Ecol Prog Ser* **142**: 261−272

Pedersen MF and Borum J (1997) Nutrient control of estuarine macroalgae: growth strategy and the balance between nitrogen requirements and uptake. *Mar Ecol Prog Ser* **8**(45): 155−163

Pedersen MF, Borum J and Fotel FL (2010) Phosphorus dynamics and limitation of fast-and slow-growing temperate seaweeds in Oslofjord, Norway. *Mar Ecol Prog Ser* **399**: 103−115

Pedersen MF and Johnsen KL (2017) Nutrient (N and P) dynamics of the invasive macroalga *Gracilaria vermiculophylla*: nutrient uptake kinetics and nutrient release through decomposition. *Mar Biol* **164**(8): 172

Pereira R, Kraemer G, Yarish C and Sousa-Pinto I (2008) Nitrogen uptake by gametophytes of *Porphyra dioica* (Bangiales, Rhodophyta) under controlled-culture conditions. *Eur J Phycol* **43**(1): 107–118

Perini V and Bracken ME (2014) Nitrogen availability limits phosphorus uptake in an intertidal macroalga. *Oecologia* **175**(2): 667−676

Riemann B, Carstensen J, Dahl K and Fossing H (2016) Recovery of Danish coastal ecosystems after reductions in nutrient loading: a holistic ecosystem approach. *Estuaries Coasts* **39**(1): 82−97

Roberts JK, Linker CS, Benoit AG, Jardetzky O and Nieman RH (1984) Salt stimulation of phosphate uptake in maize root tips studied by 31P nuclear magnetic resonance. *Plant Physiol* **75**(4): 947–950

Rosenberg G and Ramus J (1984) Uptake of inorganic nitrogen and seaweed surface area: volume ratios. *Aquat Bot* **19**(1-2): 65–72

Rosenberg G, Littler DS, Littler MM and Oliveira EC (1995) Primary production and photosynthetic quotients of seaweeds from Sao Paulo State, Brazil. *Bot Mar* **38**: 369–377

Ryther JH, Corwin N, DeBusk TA and Williams LD (1982) Nitrogen uptake and storage by the red alga *Gracilaria tikvahiae* (McLachlan, 1979). *Aquaculture* **26**(1978): 107–115

Sarmiento JL, Slater R, Barber R, Bopp L, et al. (2004) Response of ocean ecosystems to climate warming. *Geophys Res Lett* **18**(3): 1–23

Sato Y and Agatsuma Y (2016) Resource accumulation of the kelp *Saccharina ochotensis* based on photosynthetic rate and specific nutrient uptake kinetics. *J Appl Phycol* **28**(1): 499–509

Sato Y, Hirano T, Niwa K, Suzuki T, et al. (2016) Phenotypic differentiation in the morphology and nutrient uptake kinetics among *Undaria pinnatifida* cultivated at six sites in Japan. *J Appl Phycol* **28**(6): 3447–3458

Schaffelke B and Klumpp DW (1998) Short-term nutrient pulses enhance growth and photosynthesis of the coral reef macroalga *Sargassum baccularia*. *Mar Ecol Prog Ser* **170**: 95–105

Scheffer M, Hosper SH, Meijer ML, Moss B and Jeppesen E (1993) Alternative equilibria in shallow lakes. *Trends ecol evol* **8**(8): 275–279

Schiel DR and Foster MS (1986) The structure of subtidal algal stands in temperate waters. *Oceanogr Mar Biol* **24**: 265–307

Serisawa Y and Ohno M (1995) Succession of seaweed communities on artificial reefs in the inlet of Tosa Bay, Japan. *Aquacult Sci* **43**(4): 437–443

Shimabukuro H (2018) Temperate species of genus *Sargassum* in Japan (8): *Sargassum macrocarpum* distributed in Japan. *Aquabiology* 236 **40**(3): 268–273

Shimabukuro H, Terada R, Sotobayashi J, Nishihara GN and Noro T (2007) Phenology of *Sargassum duplicatum* (Fucales, Phaeophyceae) from the southern coast of Satsuma Peninsula, Kagoshima, Japan. *Bull J Soc Sci Fish* **73**(3): 454–460

Shiozaki T, Kondo Y, Yuasa D and Takeda S (2018) Distribution of major diazotrophs in the surface water of the Kuroshio from northeastern Taiwan to south of mainland Japan. *J Plankton Res* **40**(4): 407–419

Soka University (2015) Reports on research work for verification experiment aimed at

restoring barren grounds (in Japanese: 平成 26 年度　磯焼け対策のための実証実験に係る研究業務報告書)

Statistics Bureau of Japan, Portal Site of Official Statistics of Japan (2008-2018) [cited on 18 May 2020]. Available from: https://www.maff.go.jp/j/tokei/kouhyou/kaimen_gyosei/index.html

Steneck RS, Graham MH, Bourque BJ, Corbett D, et al. (2002) Kelp forest ecosystems: biodiversity, stability, resilience and future. *Environ Conserv* **29**(4): 436–459

Stockner JG, Rydin E and Hyenstrand P (2000) Cultural oligotrophication: causes and consequences for fisheries resources. *Fisheries* **25**(5): 7–14

Strain EM, Thomson RJ, Micheli F, Mancuso FP and Airoldi L (2014) Identifying the interacting roles of stressors in driving the global loss of canopy-forming to mat-forming algae in marine ecosystems. *Global Change Biol* **20**(11): 3300–3312

Suzuki M (1997) Marine biota and grobal carbon cycling, University of Tokyo Press, Tokyo

Tada K, Fujiwara M and Honjo T (2010) Water quality and nori (*Porphyra*) culture in the Seto Inland Sea. *Bunseki Kagaku* **59**: 945–955

Tadokoro K, Ono T, Yasuda I, Osafune S, et al. (2009) Possible mechanisms of decadal-scale variation in PO_4 concentration in the western North Pacific. *Geophys Res Lett* **36**(8): L08606

Tarutani K (1999) Ecophysiological studies on the population dynamics of toxic dinoflagellate *Alexandrium tamarense*. *Bull Fish Environ Inland Sea* **1**: 63–96

Taylor RB, Peek JT and Rees TAV (1998) Scaling of ammonium uptake by seaweeds to surface area: volume ratio: geographical variation and the role of uptake by passive diffusion. *Mar Ecol Prog Ser* **169**: 143–148

Tegner MJ and Dayton PK (1991) Sea urchins, El Niños, and the long term stability of southern California kelp forest communites. *Mar Ecol Prog Ser* **77**(1): 49–63

Terada R, Matsumoto K, Borlongan IA, Watanabe Y, et al. (2018) The combined effects of PAR and temperature including the chilling-light stress on the photosynthesis of a temperate brown alga, *Sargassum patens* (Fucales), based on field and laboratory measurements. *J Appl Phycol* **30**(3): 1893–1904

Terada R, Abe M, Abe T, Aoki M, et al. (2019) Japan's nationwide long-term monitoring survey of seaweed communities known as the “Monitoring Sites 1000”: Ten-year overview and future perspectives. *Phycol Res*

Terada R, Nakashima Y, Borlongan IA, Shimabukuro H, et al. (2020) Photosynthetic activity including the thermal-and chilling-light sensitivities of a temperate Japanese brown alga *Sargassum macrocarpum*. *Phycol Res* **68**(1): 70–79

Terawaki T, Yoshikawa K, Yoshida G, Uchimura M and Iseki K (2003) Ecology and restoration techniques for *Sargassum* beds in the Seto Inland Sea, Japan. *Mar Pollut Bull* **47**(1–6): 198–201

Thomas DN and Wiencke C (1991) Photosynthesis, dark respiration and light independent carbon fixation of endemic Antarctic macroalgae. *Polar Biol* **11**(5): 329–337

Thomas TE, Harrison PJ and Taylor EB (1985) Nitrogen uptake and growth of the germlings and mature thalli of *Fucus distichus*. *Mar Biol* **84**(3): 267–274

Topinka J (1978) Nitrogen uptake by *Fucus spiralis* (Phaeophyceae). *J Phycol* **14**: 241–247

Tsuchiya K, Yoshiki T, Nakajima R, Miyaguchi H, et al. (2013) Typhoon-driven variations in primary production and phytoplankton assemblages in Sagami Bay, Japan:

a case study of typhoon Mawar (T0511). *Plankton Benthos Res* **8**(2): 74–87

Tsuchiya K, Ehama M, Yasunaga Y, Nakagawa Y, et al. (2018) Seasonal and spatial variation of nutrients in the coastal waters of the northern Goto islands, Japan (in Japanese). *Bull Coast Oceanogr* **55**(2): 125–138

Turner RE, Rabalais NN, Justic D and Dortch Q (2003) Future aquatic nutrient limitations. *Mar Pollut Bull* **46**(8): 1032−1034

Van Wijnen J, Ivens WP, Kroeze C and Löhr AJ (2015) Coastal eutrophication in Europe caused by production of energy crops. *Sci Total Environ* **511**: 101–111

Wallentinus I (1984) Comparisons of nutrient uptake rates for Baltic macroalgae with different thallus morphologies. *Mar Biol* **80**(2): 215–225

Wan Y, Wan L, Li Y and Doering P (2017) Decadal and seasonal trends of nutrient concentration and export from highly managed coastal catchments. *Water Res* **115**: 180–194

Wanishi A (2007) Long-term variations of the Nutrient Environment in the Suo-Nada Region of Yamaguchi Prefecture. *Bull Yamaguchi Pref Fish Res Ctr* **5**: 1–8

Watanabe Y, Nishihara GN, Tokunaga S and Terada R (2014) The effect of irradiance and temperature responses and the phenology of a native alga, *Undaria pinnatifida* (Laminariales), at the southern limit of its natural distribution in Japan. *J Appl Phycol* **26**(6): 2405–2415

Wheeler WN (1980) Effect of boundary layer transport on the fixation of carbon by the giant kelp *Macrocystis pyrifera*. *Mar Biol* **56**: 103–110

Wu L, Cai W, Zhang L, Nakamura H, et al. (2012) Enhanced warming over the global subtropical western boundary currents. *Nat Clim Change* **2**(3): 161–166

Yamamoto T (2003) The Seto Inland Sea-Eutrophic or oligotrophic ? *Mar Pol Bull*

47(1-6): 37–42

Yamamoto T, Oh SJ and Kataoka Y (2004) Growth and uptake kinetics for nitrate, ammonium and phosphate by the toxic dinoflagellate *Gymnodium catenatum* isolate from Hiroshima Bay, Japan. *Fish Sci* **70**: 108–115

Yamamoto K, Nakajima M and Imai I (2017) Expansion of blooming in the toxic dinoflagellate *Alexandrium tamarense* and environmental fluctuation analyzed from long-term monitoring data in Osaka Bay, eastern Seto In land sera, Japan. *Plankton Soc J* **64**(1): 11–21 (In Japanese)

Yanagi T (2016) Eutrophication and Oligotrophication in Japanese Estuaries, Springer, Netherlands

Yang B, Gao X and Xing Q (2018a) Geochemistry of organic carbon in surface sediments of a summer hypoxic region in the coastal waters of northern Shandong Peninsula. *Cont Shelf Res* **171**: 113–125

Yang X, Zhang P, Li W, Hu C, et al. (2018b) Evaluation of four seagrass species as early warning indicators for nitrogen overloading: implications for eutrophic evaluation and ecosystem management. *Sci Total Environ* **635**: 1132–1143

Yatsuya K, Nishigaki T, Douke A and Wada Y (2005) Annual net production of the five Sargassaceae species in Yoro, western Wakasa Bay, Sea of Japan. *Fisheries Sci* **71**(5): 1098–1106

Yatsuya K, Nishigaki T, Douke A and Wada Y (2008) Seasonal changes in carbon, nitrogen, and phosphorus contents of some Sargassacean species in the coastal areas of Kyoto Prefecture, Sea of Japan (in Japanese). *Jpn J Phycol* **56**(2): 107–115

Yoshida G, Niimura Y, Tarutani K and Hamuguchi M (2011) Research review on the relationship between macroalgal-production and nutrients, and relative assessment of

the nutrient conditions on macroalgae in the Seto Inland Sea (in Japanese). *Bull Fish Res Agen* **34**: 1–31

Yoshida T (1983) Japanese species of *Sargassum* subgenus *Bactrophycus* (Phaeophyta, Fucales). *J Fac Sci Hokkaido Univ Ser 5 Bot* **13**(2): 99–246

Zheng GM and Tang D (2007) Offshore and nearshore chlorophyll increases induced by typhoon winds and subsequent terrestrial rainwater runoff. *Mar Ecol Prog Ser* **333**: 61–74

Zhou Y, Wang L, Zhou Y and Mao XZ (2020) Eutrophication control strategies for highly anthropogenic influenced coastal waters. *Sci Total Environ* **705**: 135760

Zimmerman RC and Robertson DL (1985) ODU Digital Commons Effects of El Nino on Local Hydrography and Growth of the Giant Kelp, *Macrocystis Pyrifera*, at Santa Catalina Island, California Repository Citation. *Limnol Oceanogr* **30**(6): 1298–1302

Zou D (2005) Effects of elevated atmospheric CO_2 on growth, photosynthesis and nitrogen metabolism in the economic brown seaweed, *Hizikia fusiforme* (Sargassaceae, Phaeophyta). *Aquaculture* **250** (3-4): 726–735

Zou D and Gao K (2005) Photosynthetic characteristics of the economic brown seaweed *Hizikia fusiforme* (Sargassaceae, Phaeophyta), with special reference to its “leaf” and receptacle. *J Appl Phycol* **17**(3): 255–259

APPENDICES

Appendix 1 Symbol definitions and units

Symbol	Unit	Definition
V_{max}	μmol g^{-1}DW h^{-1}	Maximum uptake rate of nutrient
K_m	μmol L^{-1}	Half-saturation constant
V_{max}/K_m	L g^{-1}DW h^{-1}	Availability of nutrients at low concentrations
P_{max}	mg O_2 g^{-1}WW h^{-1}	Maximum O_2 production rate
P_{net}	mg O_2 g^{-1}WW h^{-1}	Net O_2 production rate
R_d	mg O_2 g^{-1}WW h^{-1}	Respiration rate
E_k	μmol photons m^{-2} s^{-1}	Saturation irradiance
E_c	μmol photons m^{-2} s^{-1}	Compensation irradiance
μ	day^{-1}	Relative growth rate
$μ_{max}$	day^{-1}	Maximum growth rate
Q_{max}	% DW	Maximum tissue concentration of phosphorus
Q_c	% DW	Critical tissue concentration of phosphorus
Q_s	% DW	Lowest tissue concentration of phosphorus

Appendix 2 List of uptake kinetics parameters for phosphate in various brown alga (1/2)

Species	V_{max} (μmol g^{-1}DW h^{-1})	K_m (μM)	V_{max}/K_m (L g^{-1}DW h^{-1})	Temper-ature (°C)	Reference
Ascophyllum nodosum	0.09	1.85	0.05	12.0	Hurd & Dring (1990)
	0.05	0.59	0.09	12.0	
	0.45	3.75	0.12	18.0	Pedersen et al. (2010)
Acrosiphonia centralis	3.33	N.D.	N.D.	2.0	Wallentinus (1984)
Chorda filum	1.38	0.62	2.22	13.0	
Cystophora torulosa	0.24	4.09	0.06	17.5	Dougals et al. (2014)
Dictyosiphon foeniculaceus	11.14	2.12	5.24	13.0	Wallentinus (1984)
Ectocarpus siliculosus	0.75	1.22	0.61	12.0	
Eudesme virescens	3.55	0.67	5.26	11.0	
Fucus serratus	0.82	2.14	0.38	18.0	Pedersen et al. (2010)
	0.31	6.50	0.05	12.0	Hurd & Dring (1990)
	0.23	2.87	0.08	12.0	
	0.18	2.85	0.06	12.0	
Fucus spiralis	0.55	7.19	0.08	12.0	
	0.55	2.14	0.26	12.0	
	0.27	3.81	0.07	12.0	
Fucus vesiculosus	0.34	3.10	0.11	12.0	
	0.41	12.06	0.03	12.0	
Fucus vesiculosus "tip"	0.75	1.84	0.41	14.0	Wallentinus (1984)
	0.90	2.74	0.33	18.0	
	0.59	3.65	0.16	11.0	
Fucus vesiculosus "middle"	N.D.	1.70	N.D.	18.0	
Fucus vesiculosus "tip"	2.85	45.94	0.06	2.0	
Fucus vesiculosus	1.26	4.17	0.30	18.0	Pedersen et al. (2010)
Furcellaria lumbricalis	0.10	1.51	0.07	13.0	Wallentinus (1984)
	0.27	7.39	0.04	12.0	
	N.D.	0.02	N.D.	2.0	
Kjellmaniella crassifolia	not comparable	0.31	N.D.	5.0	Ozaki et al.. (2001)
Kaminaria japonica	not comparable	0.14	N.D.	5.0	

Appendix 2 List of uptake kinetics parameters for phosphate in various brown alga (2/2)

Species	V_{max} (μmol g_{-1}DW h_{-1})	K_m (μM)	V_{max}/K_m (L g_{-1}DW h_{-1})	Temperature (°C)	Reference
Laminaria abyssalis	0.83	2.21	0.38	18.0	Braga & Valentin, (1996)
Laminaria difitata	0.70	3.73	0.19	18.0	Pedersen et al. (2010)
Macrocystis pyrifera	not comparable	3.51	N.D.	24.0	Manley (1985)
Pelveti canaliculata	0.32	5.12	0.06	12.0	Hurd & Dring (1990)
Pelveti canaliculata	0.39	6.80	0.06	12.0	
Phyllophora truncata	0.12	N.D.	N.D.	14.0	Wallentinus, 1984
Rhodomela confervoides	0.64	N.D.	N.D.	4.0	
Sargassum baccularia	N.D.	0.26	N.D.	26.0	Schaffelke & Klumpp (1998)
Sargassum macrocarpum	0.19	1.28	0.15	10.0	Ohtake et al. (2020a)
	0.40	4.38	0.09	15.0	
	0.44	3.06	0.14	20.0	
	0.45	3.07	0.15	25.0	
	0.69	2.53	0.27	30.0	
	0.95	5.02	0.19	16.8	Ohtake et al. (2020b)
	1.76	7.12	0.25	15.0	
	0.33	4.68	0.07	15.5	
	0.61	7.84	0.08	19.4	
	0.24	7.45	0.03	21.7	
	0.24	7.86	0.03	23.3	
	0.15	7.02	0.02	26.9	
	0.32	10.50	0.03	28.6	
	0.85	9.45	0.09	23.9	
	1.05	6.45	0.16	22.7	
	0.80	7.61	0.11	19.2	
	1.40	6.16	0.23	18.2	
	1.73	10.26	0.17	15.5	
Scytosiphon lomentaria	6.59	0.77	8.50	6.0	Wallentinus (1984)
Xiphophora chondrophylla	0.31	8.11	0.04	17.5	Dougals et al. (2014)
Zonaria turneriana	0.17	9.90	0.02	17.5	